# CT Technology
## Detectors, Acquisition, Prefilters and TCM

**Marc Kachelrieß**

**German Cancer Research Center (DKFZ)**
**Heidelberg, Germany**
**www.dkfz.de/ct**

DEUTSCHES
KREBSFORSCHUNGSZENTRUM
IN DER HELMHOLTZ-GEMEINSCHAFT

**Canon Aquilion ONE Vision**

**GE Revolution CT**

**Philips IQon Spectral CT**

**Siemens Naeotom Alpha**

**In-plane resolution: 0.2 … 0.7 mm**

**Nominal slice thickness: $S$ = 0.2 … 1.5 mm**

**Tube (max. values): 120 kW, 150 kV, 1300 mA**

**Effective tube current: $\text{mAs}_{\text{eff}}$ = 10 mAs … 1000 mAs**

**Rotation time: $T_{\text{rot}}$ = 0.25 … 0.5 s**

**Simultaneously acquired slices: $M$ = 16 … 320**

**Table increment per rotation: $d$ = 1 … 183 mm**

**Scan speed: up to 73 cm/s**

**Temporal resolution: 50 … 250 ms**

**Canon Megacool Vi**

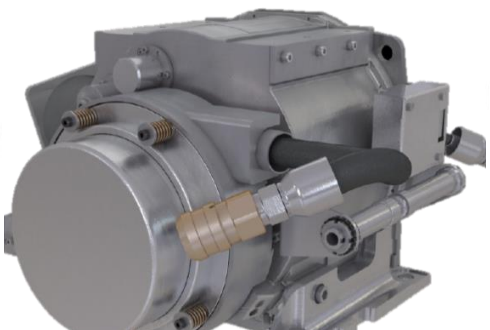

**GE Performix HDw**

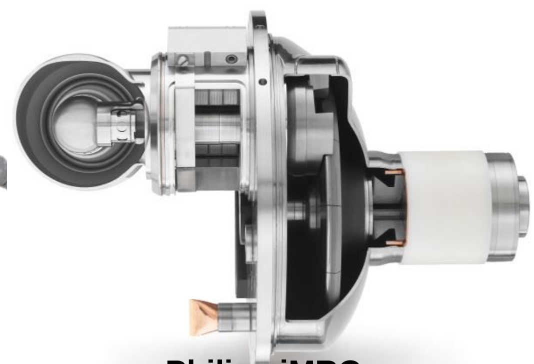

**Philips iMRC**

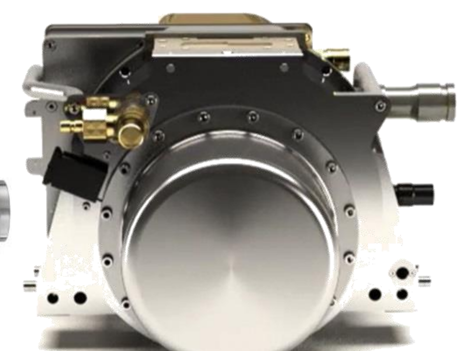

**Siemens Vectron**

# What does CT Measure?

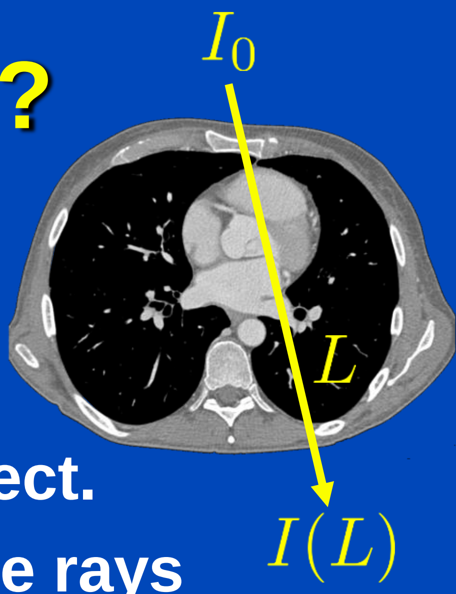


- X-rays are generated in an x-ray tube.
- The polychromatic radiation is attenuated in the patient. X-ray photon attenuation is dominated by the photo and the Compton effect.
- Detectors measure the x-ray intensity after the rays have passed through the patient along several lines *L*.
- The log intensity is the so-called x-ray transform:

$$q(L) = -\ln \frac{I(L)}{I_0} = -\ln \int dE\, w(E) e^{-\int dL \mu(\boldsymbol{r}, E)}$$

- Often, the follwing monochromatic approximation is used:

$$q(L) \approx p(L) = \int dL \mu(\boldsymbol{r}, E_{\mathrm{eff}})$$

# Demands on the Mechanical Design

- Continuous data acquisition (spiral, fluoro, dynamic, …)
- Able to withstand very fast rotation
  - Centrifugal acceleration at 550 mm with 0.5 s: $a = 9\ g$
  - with 0.4 s: $a = 14\ g$
  - with 0.3 s: $a = 25\ g$
  - with 0.2 s: $a = 55\ g$
- Mechanical accuracy better than 0.1 mm
- Compact and robust design
- Short installation times
- Long service intervals
- Low cost

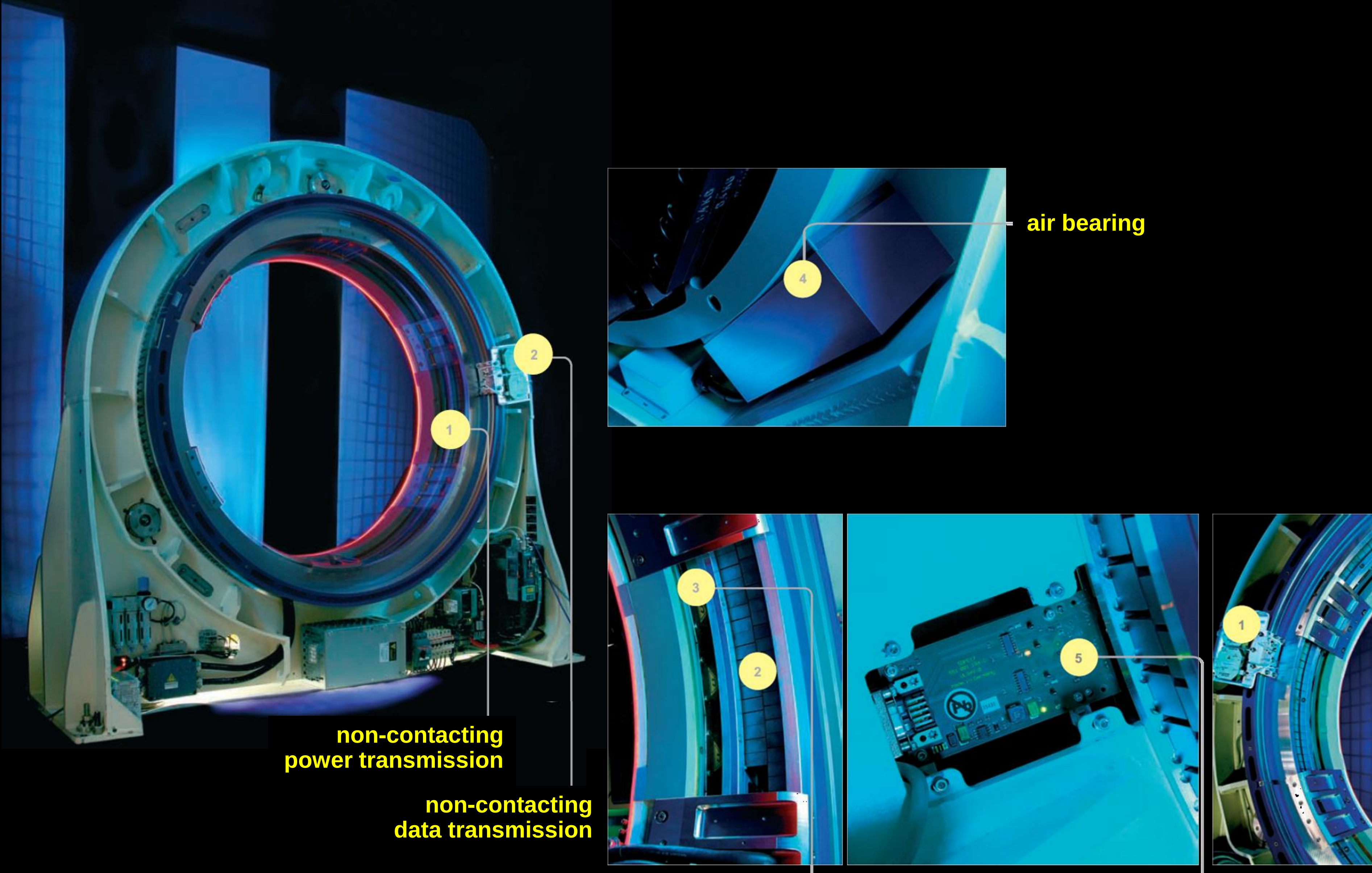


Data courtesy of Schleifring GmbH, Fürstenfeldbruck, Germany
and of rsna2011.rsna.org/exbData/1678/docs/Gantry_Subsystem.pdf

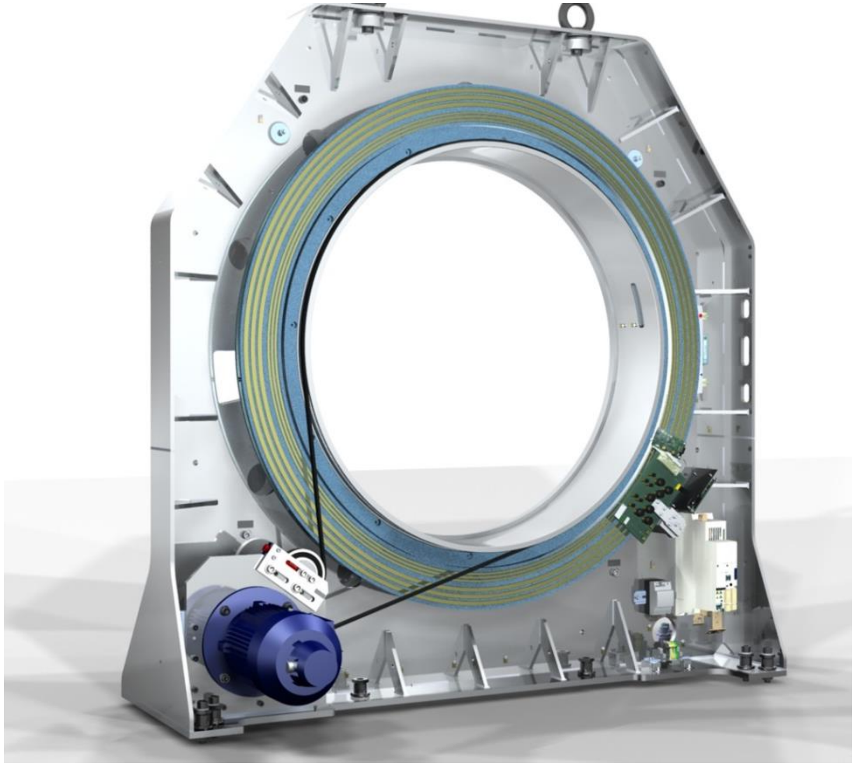

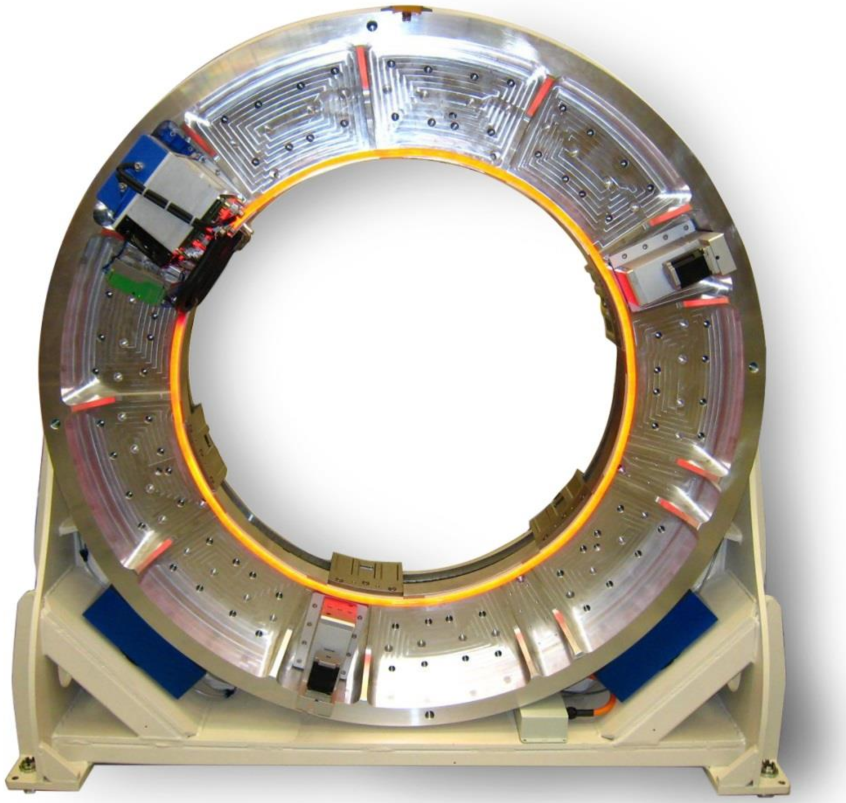

# Demands on X-Ray Sources

- Tube voltages from 70 to 150 kV in steps of 10 kV
- High instantaneous power levels (typ. 50 to 120 kW)
- High tube currents at low kV (good for Iodine contrast)
- High continuous power levels (typ. > 5 kW)
- High cooling rates (typ. about 25 kW ≈ 1 MHU/min*)
- High tube current variation (low inertia)
- Must withstand centrifugal forces
  - Centrifugal acceleration at 550 mm with 0.5 s: $a = 9\,g$
  - with 0.4 s: $a = 14\,g$
  - with 0.3 s: $a = 25\,g$
  - with 0.2 s: $a = 55\,g$
- Compact and robust design
- Long service intervals
  - Ball bearings cannot be lubricated and wear out early
  - Liquid bearings to be preferred (also due to good heat conduction)

* 1 MHU = √2 MJ

# Tube Technology

**conventional tube**
(rotating anode, helical wire emitter)

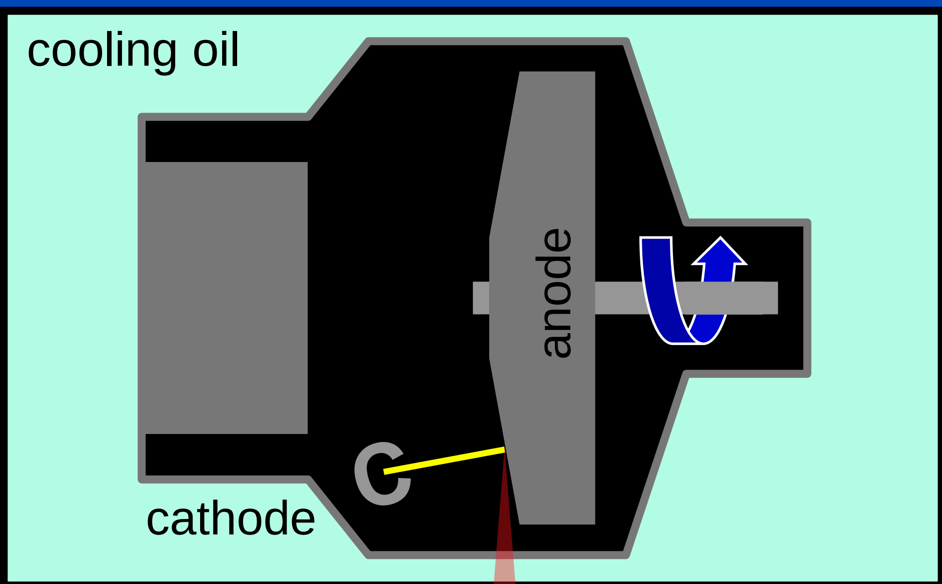


Photo courtesy of GE

Anode at high temperature (>> 1000 °C)

Radiative cooling ( $\propto T^4$ ) is dominant

**high performance tube**
(rotating cathode, anode + envelope, flat emitter)

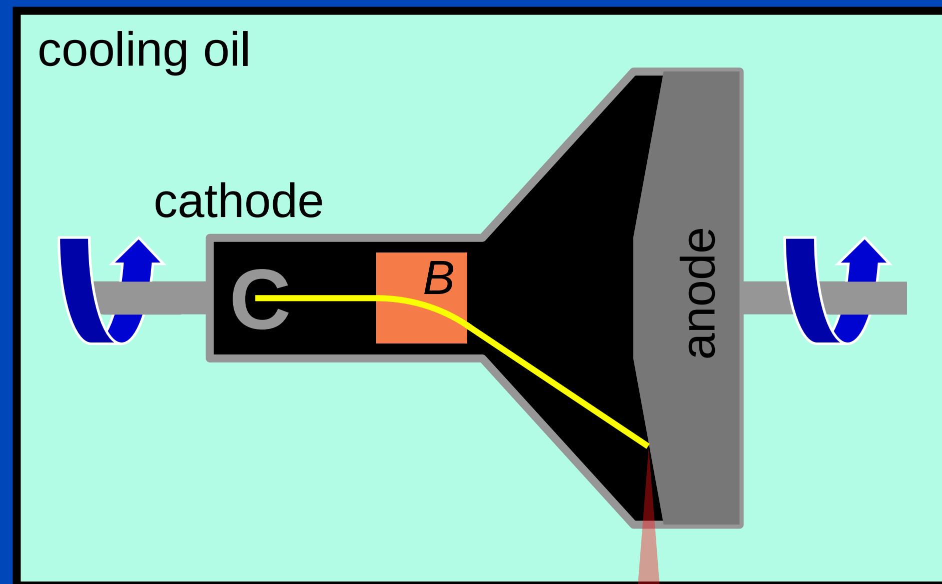


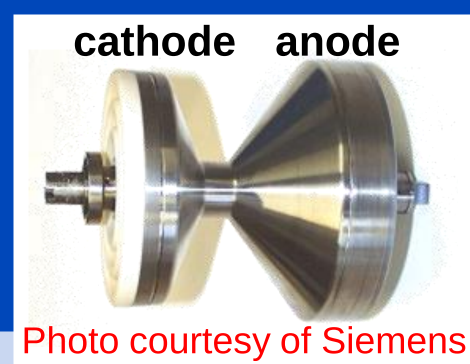

Photo courtesy of Siemens

Anode at low temperature (<< 1000 °C)

Conductive cooling ( $\propto T$ ) is dominant

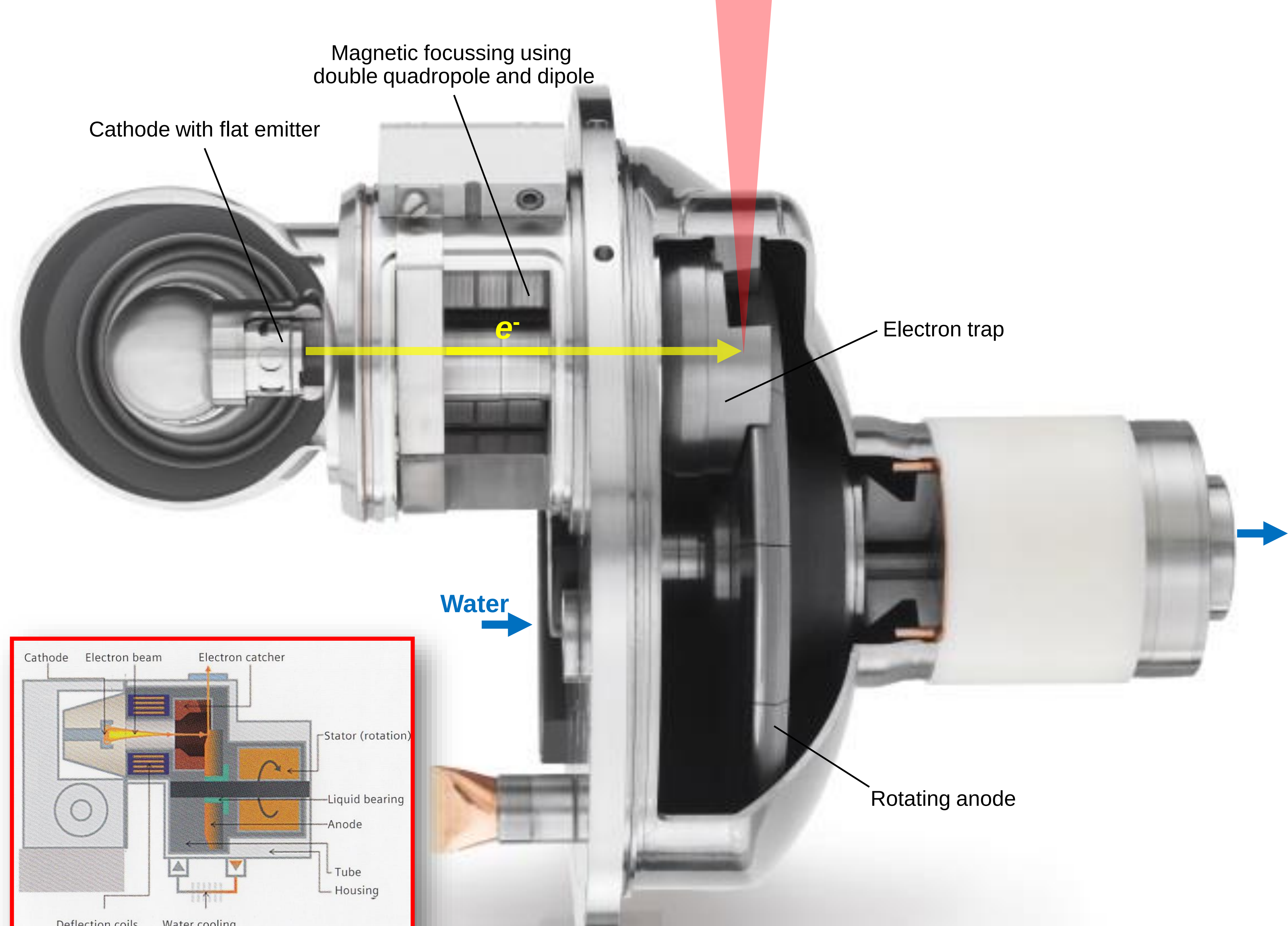


iMRC photo courtesy of Philips Medical Systems GmbH, Hamburg, Germany

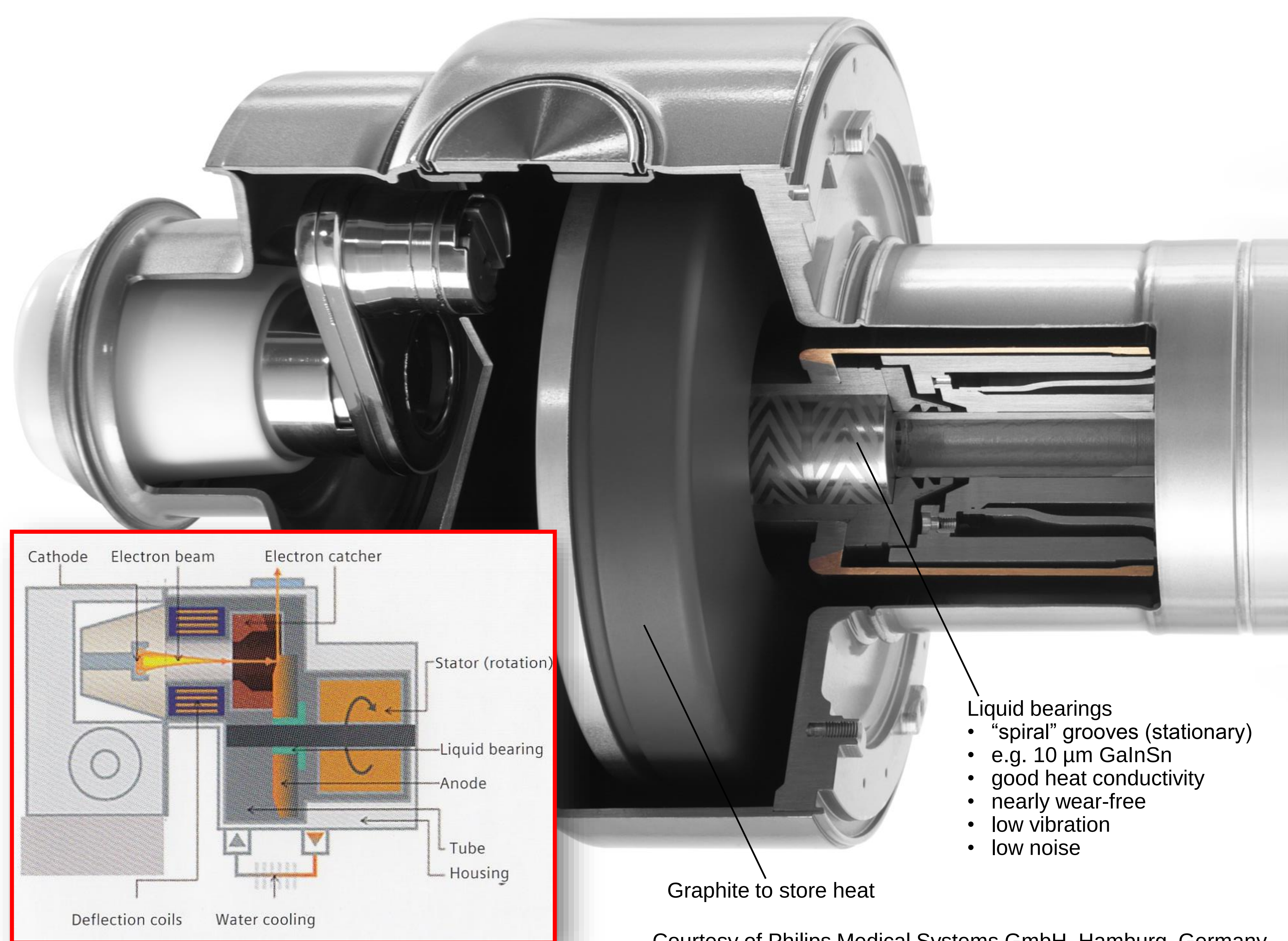


Courtesy of Philips Medical Systems GmbH, Hamburg, Germany

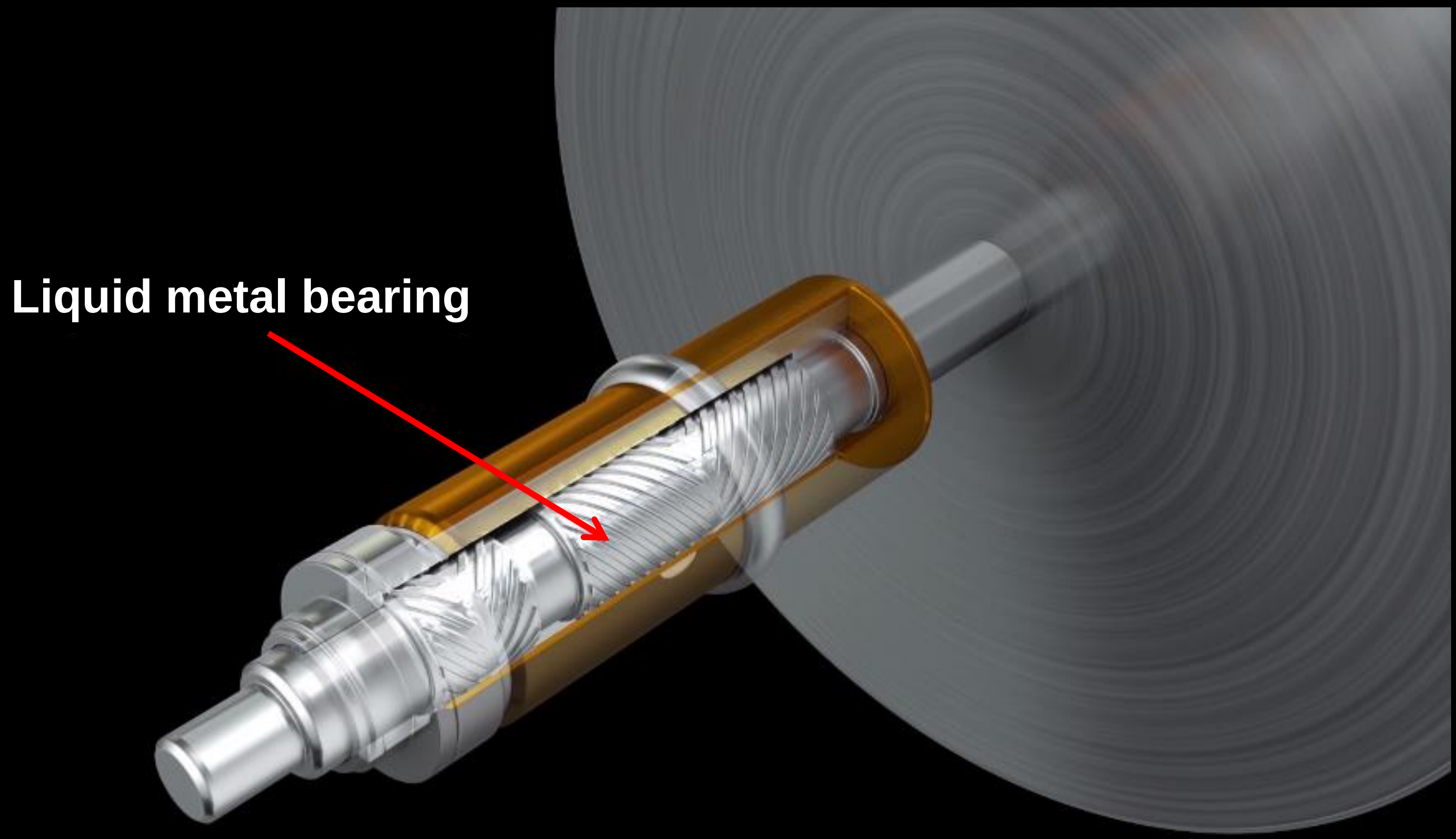


Courtesy of Canon Medical Systems, USA

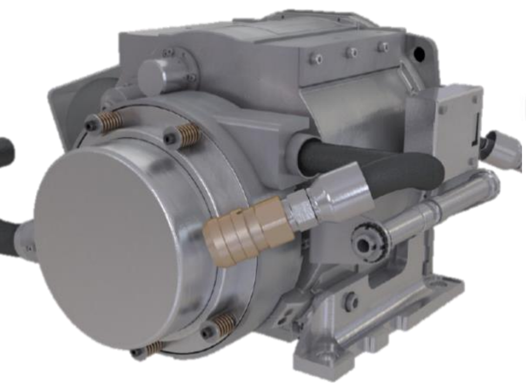

**Performix HDw (GE)**

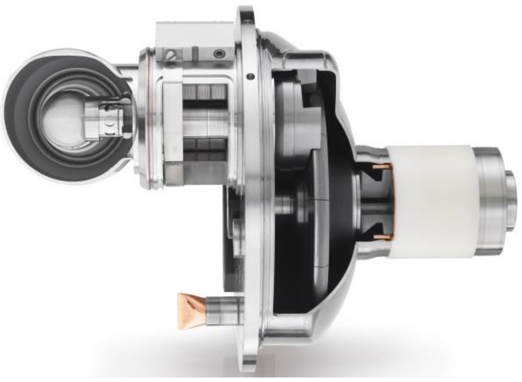

**iMRC (Philips)**

**Straton (Siemens)**

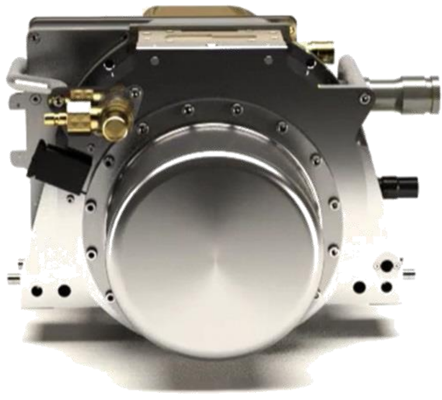

**Vectron (Siemens)**

# Straton vs. Vectron at all kV

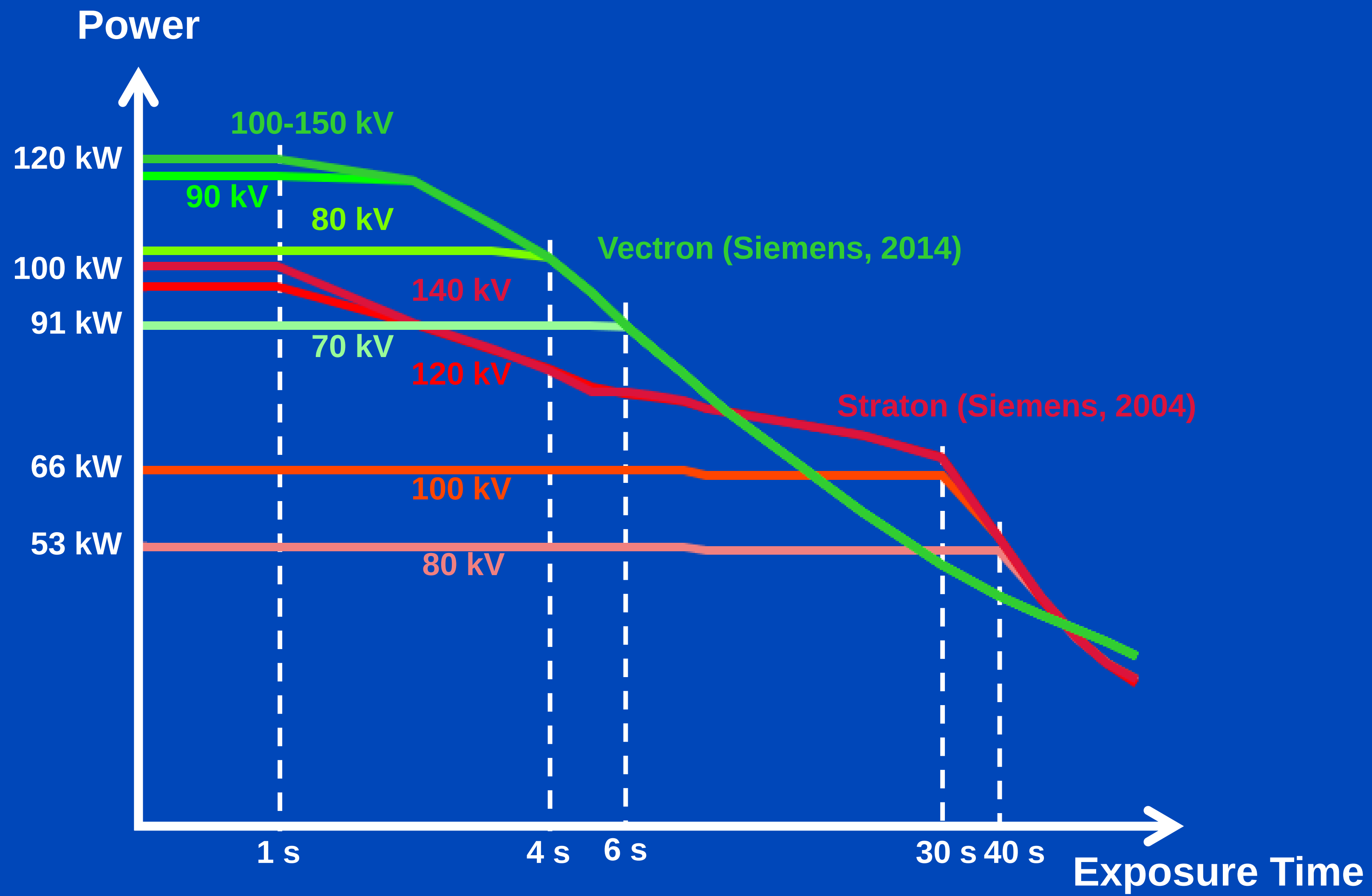

# Tube Voltage 80 kV

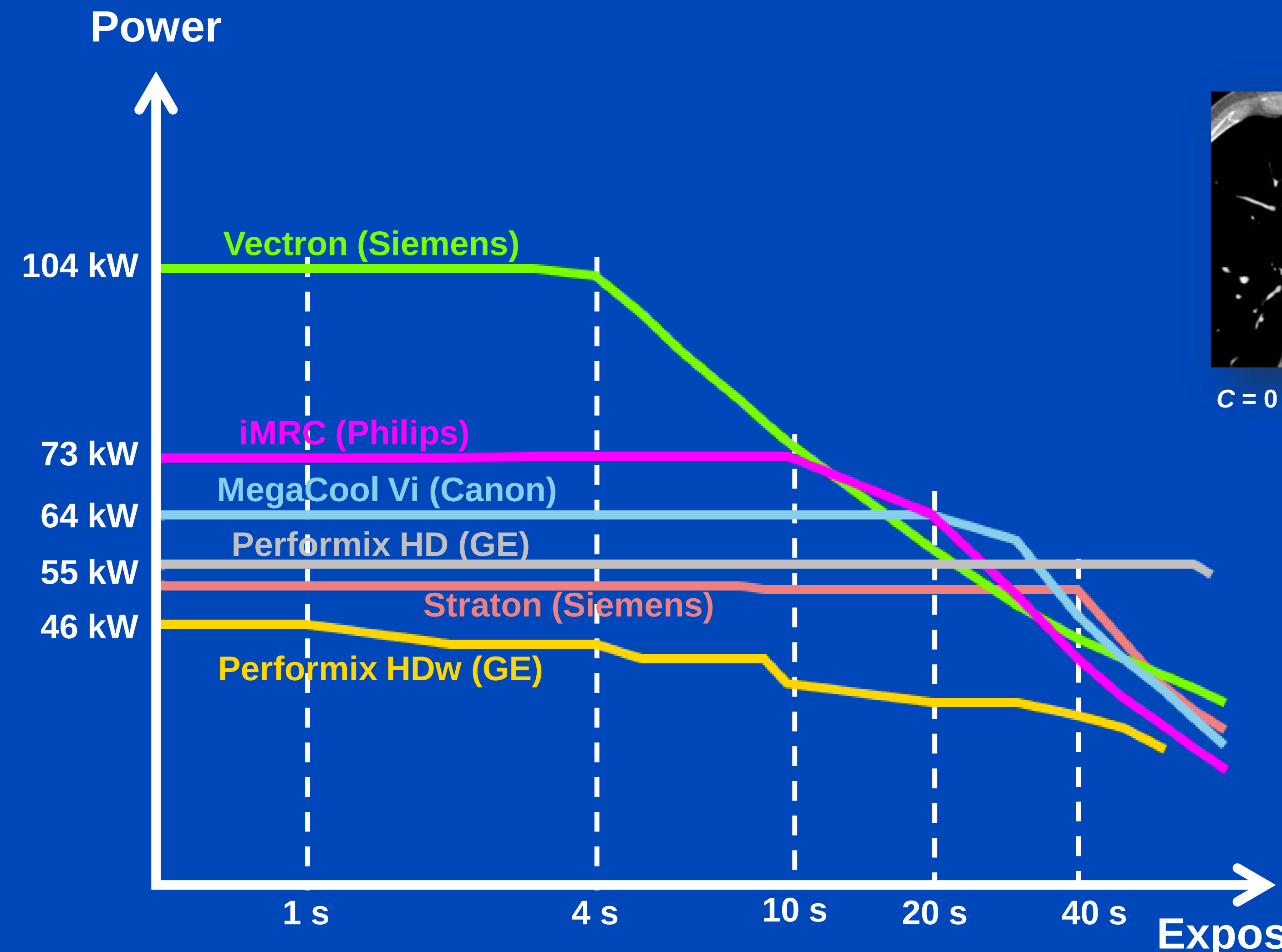


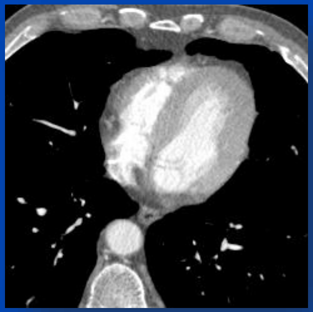

*C* = 0 HU, *W* = 700 HU

# Tube Voltage 120 kV

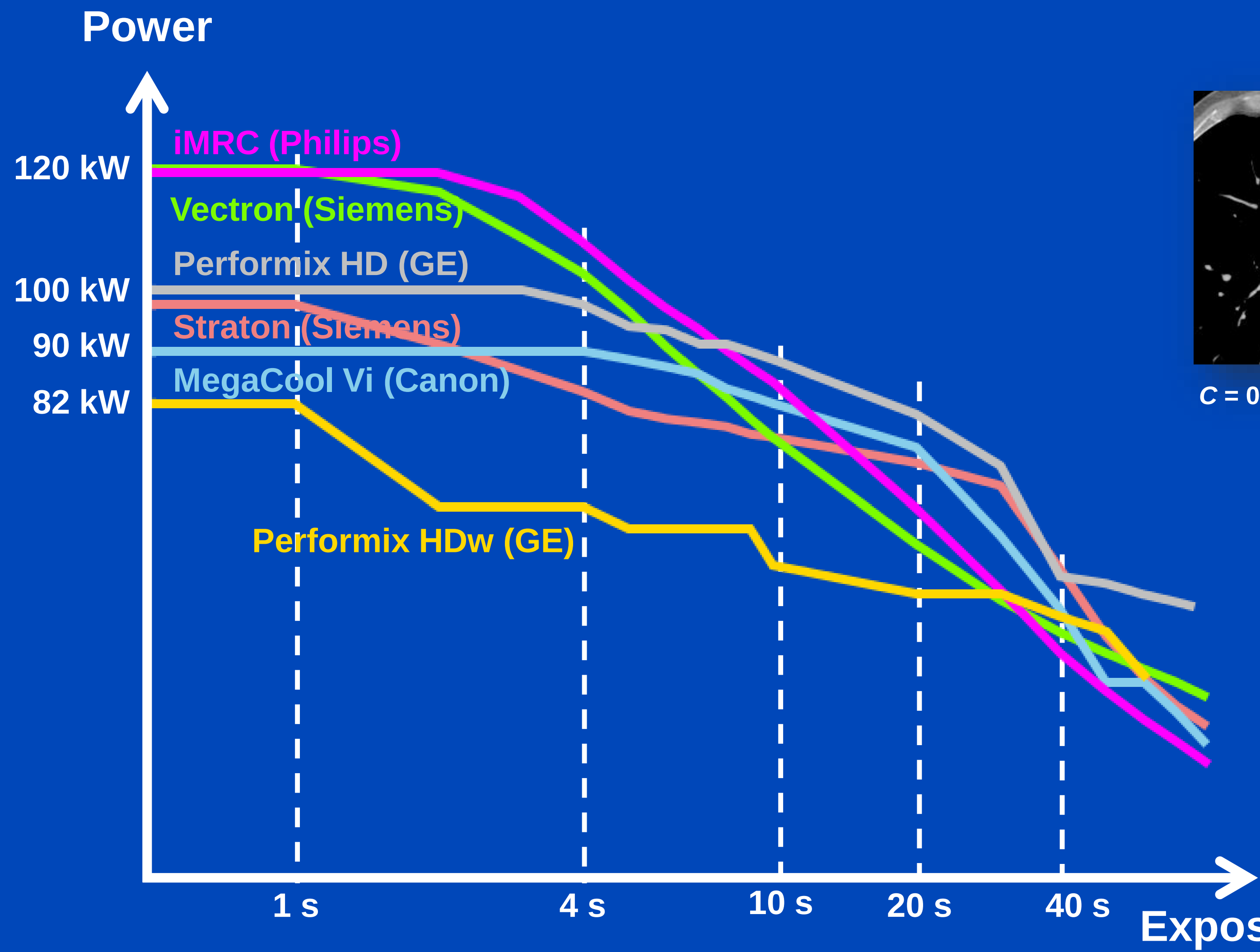


*C* = 0 HU, *W* = 700 HU

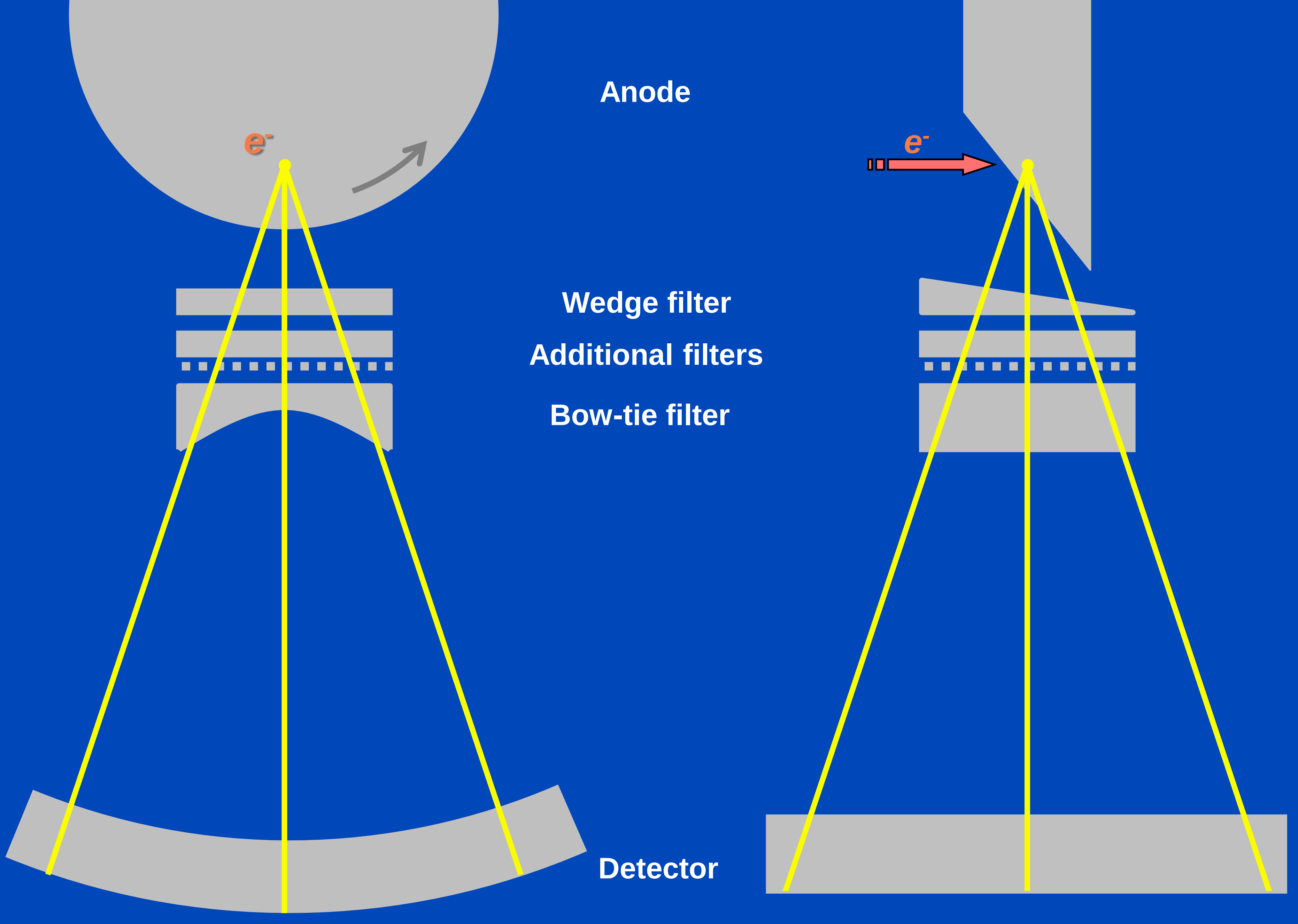


Figure not drawn to scale. Type and order of prefiltration may differ from scanner to scanner.
Depending on the selected protocol filters are changed automatically (e.g. small bowtie for pediatric scans).

# 120 kV + 0 mm water with and without prefilter

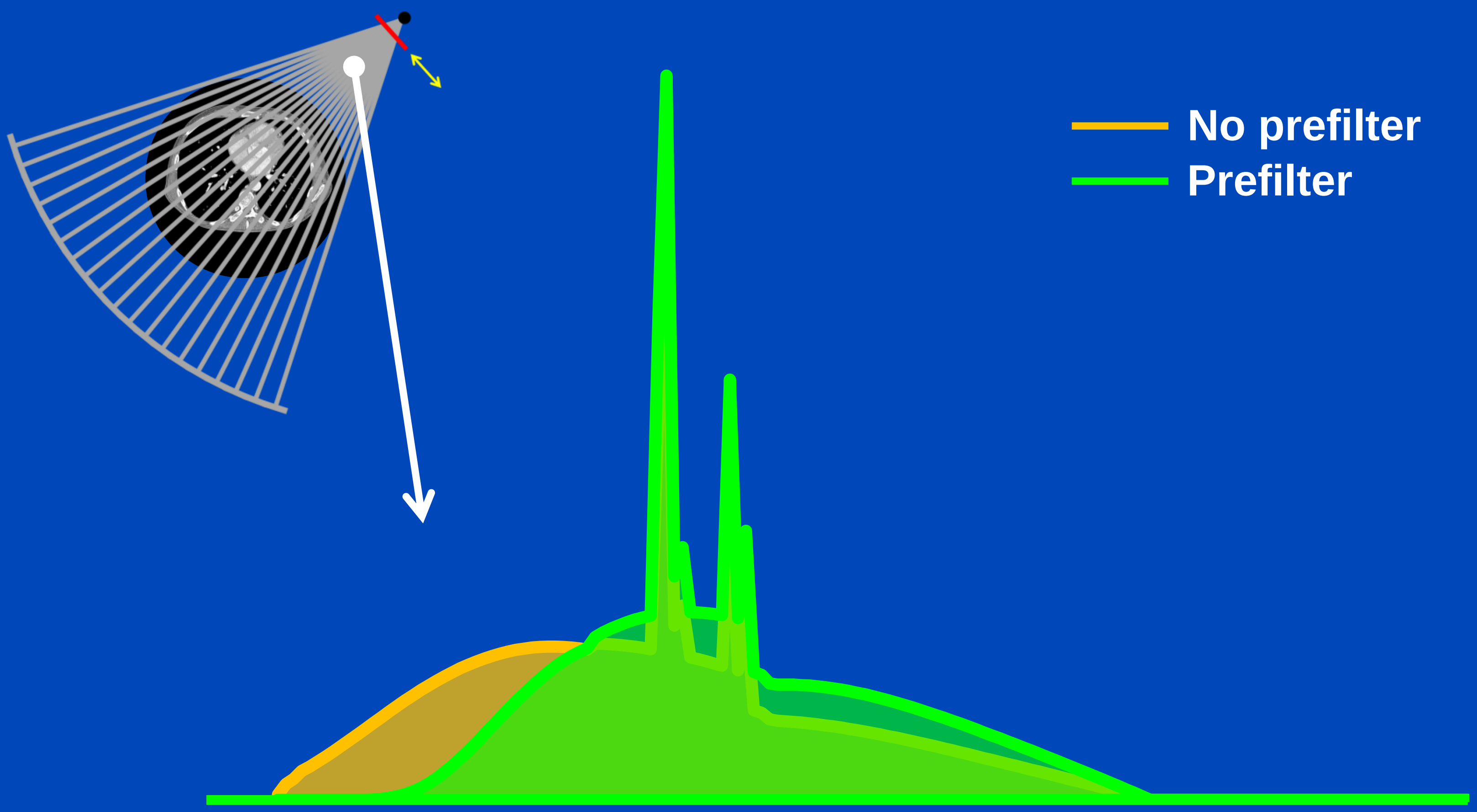

# 120 kV + 320 mm water with and without prefilter

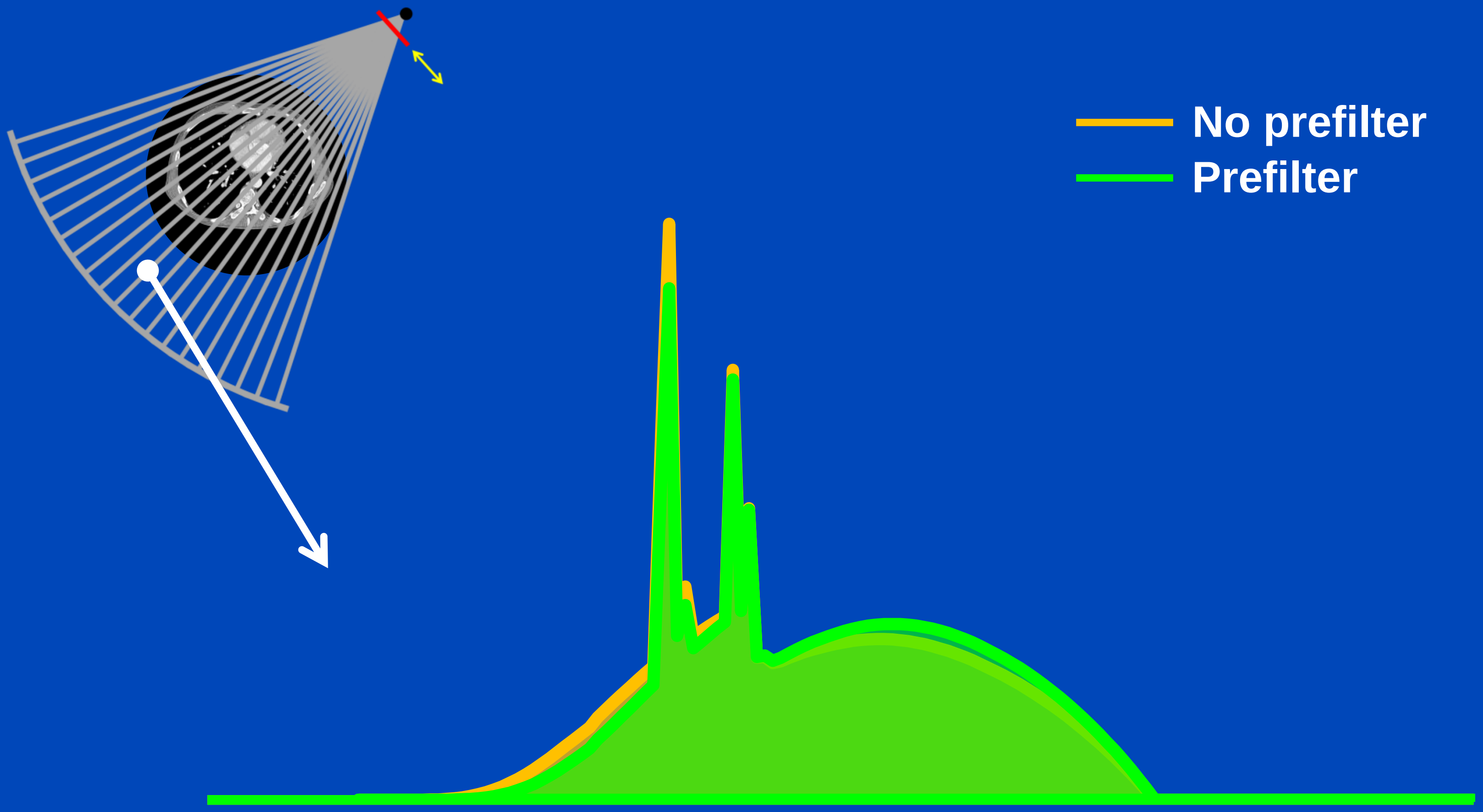

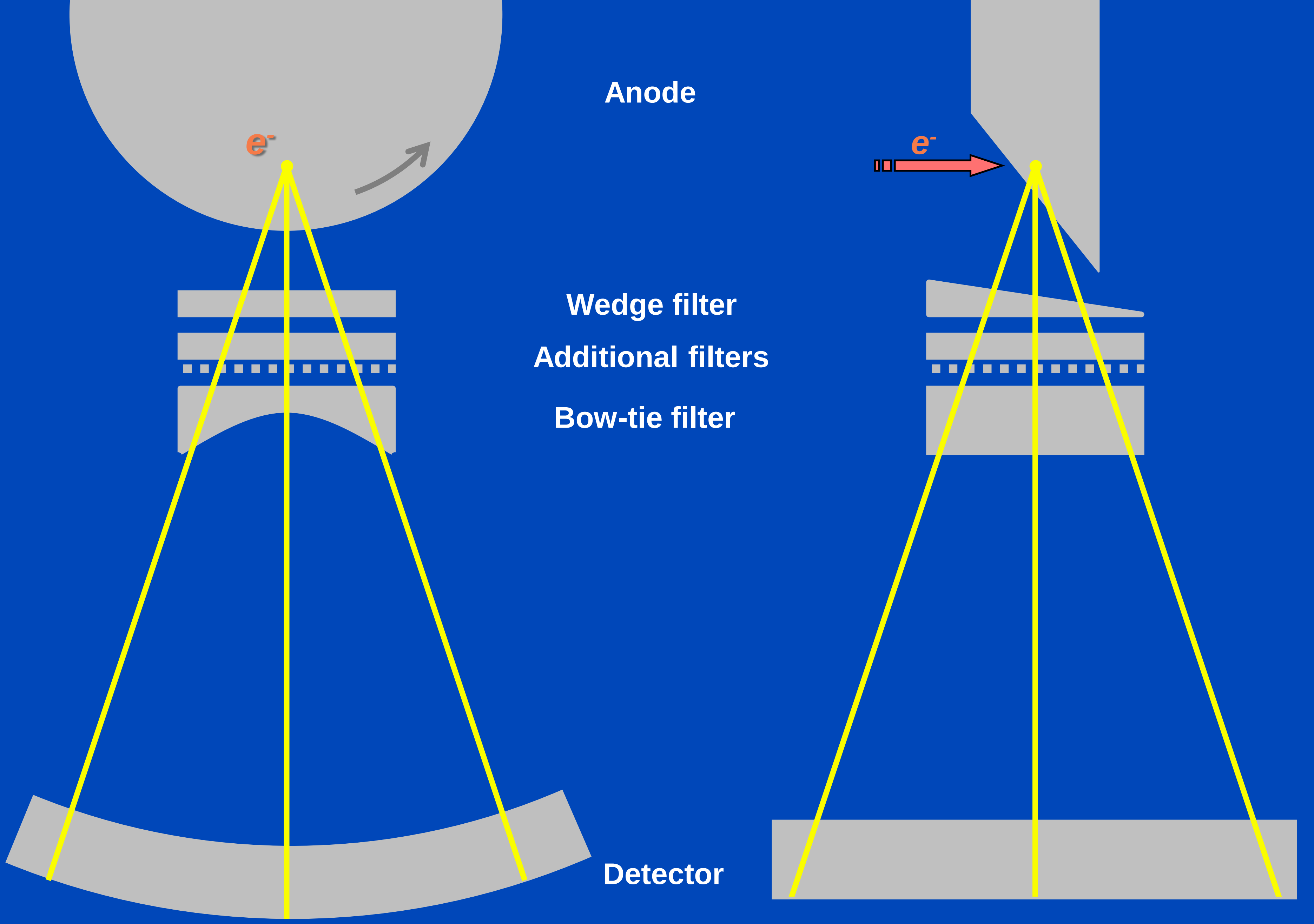


Figure not drawn to scale. Type and order of prefiltration may differ from scanner to scanner.
Depending on the selected protocol filters are changed automatically (e.g. small bowtie for pediatric scans).

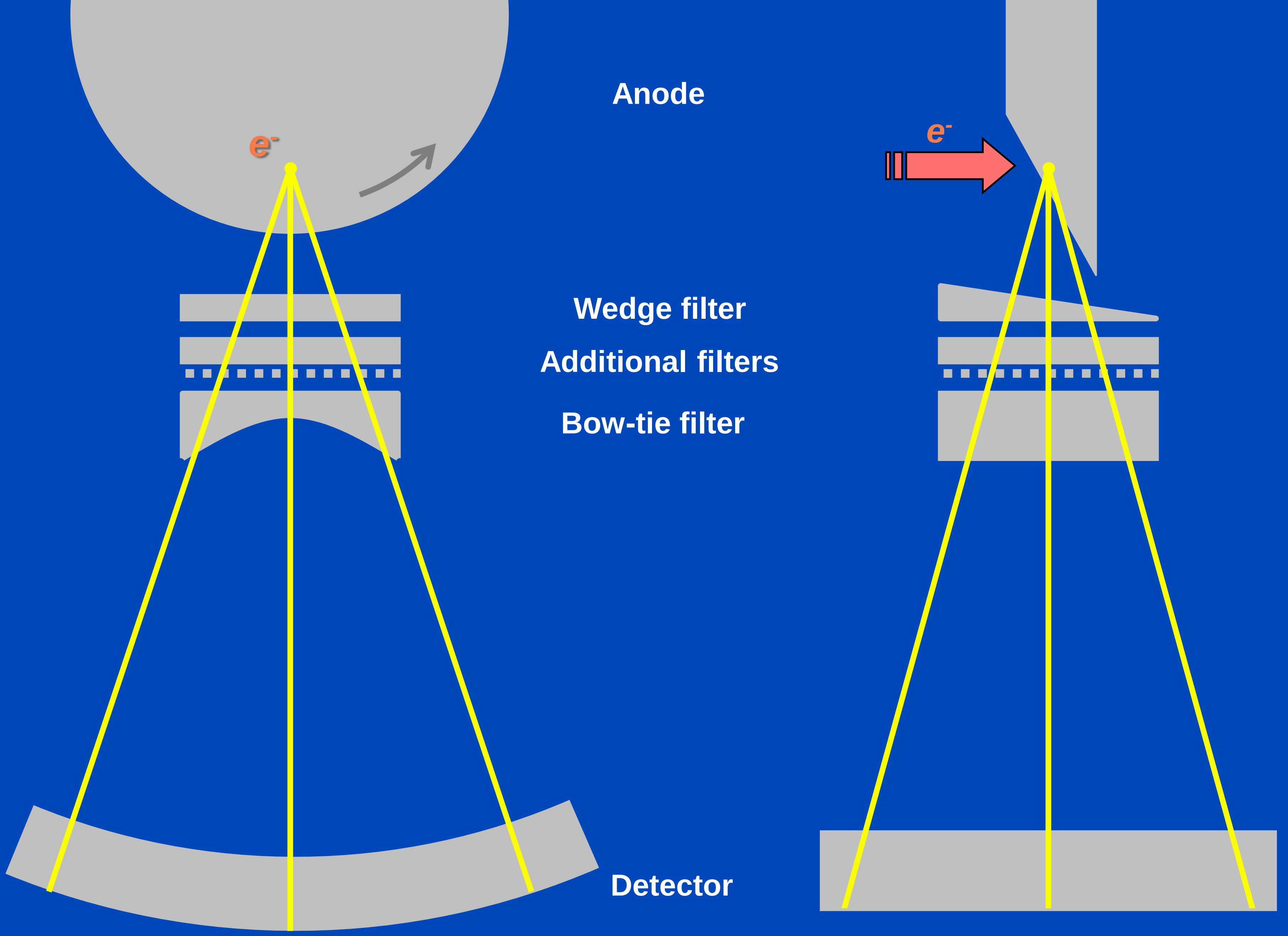


Figure not drawn to scale. Type and order of prefiltration may differ from scanner to scanner.
Depending on the selected protocol filters are changed automatically (e.g. small bowtie for pediatric scans).

dkfz.

## Narrow Cone = High Tube Power

## Wide Cone = Low Tube Power

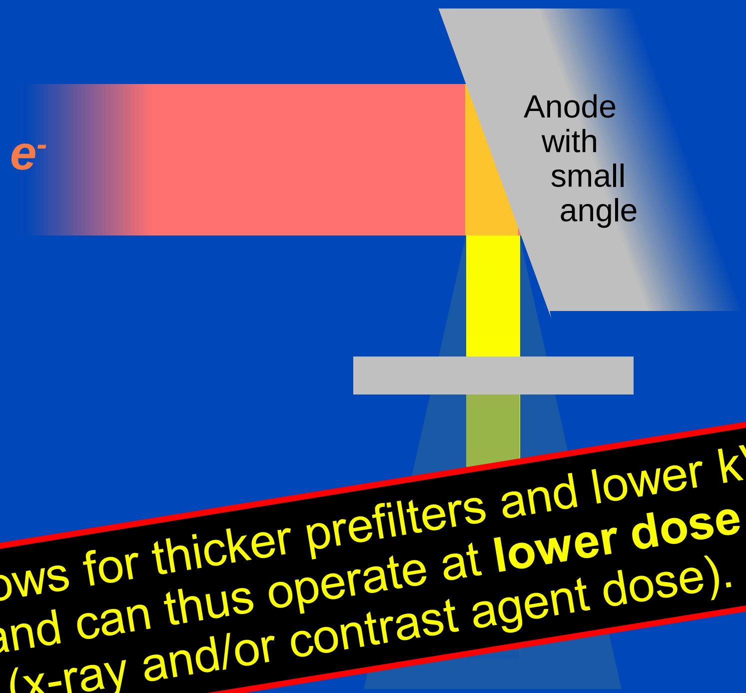


Allows for thicker prefilters and lower kV and can thus operate at **lower dose** (x-ray and/or contrast agent dose).

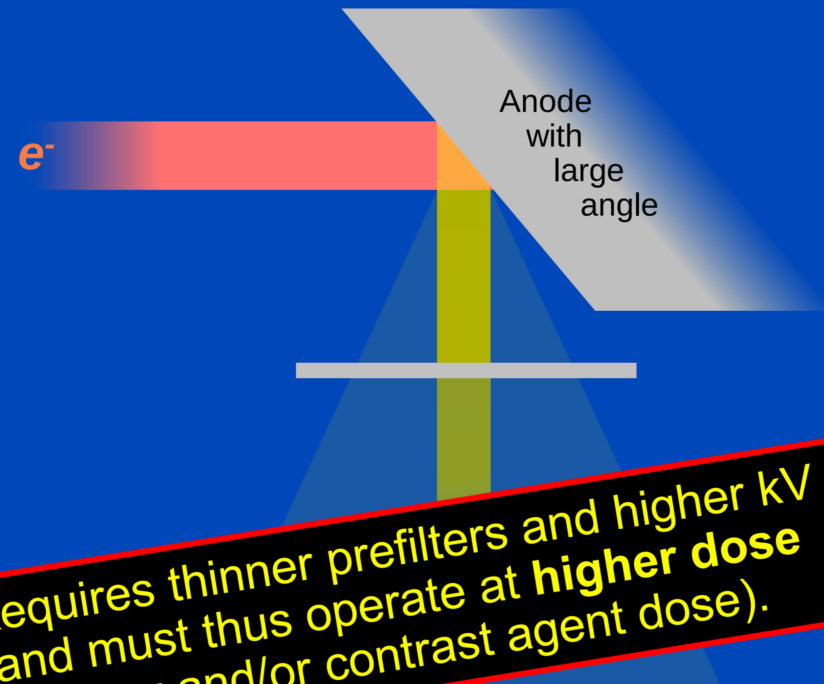


Requires thinner prefilters and higher kV and must thus operate at **higher dose** (x-ray and/or contrast agent dose).

# … at the same spatial resolution

**Onset of target melting (rule of thumb)[1]: 1 W/µm**

[1] D.E. Grider, A. Writh, and P.K. Ausburn. Electron Beam Melting in Microfocus X-Ray Tubes. J. Phys. D: Appl. Phys 19:2281-2292, 1986

# Data Completeness

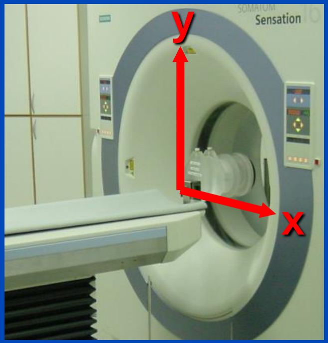


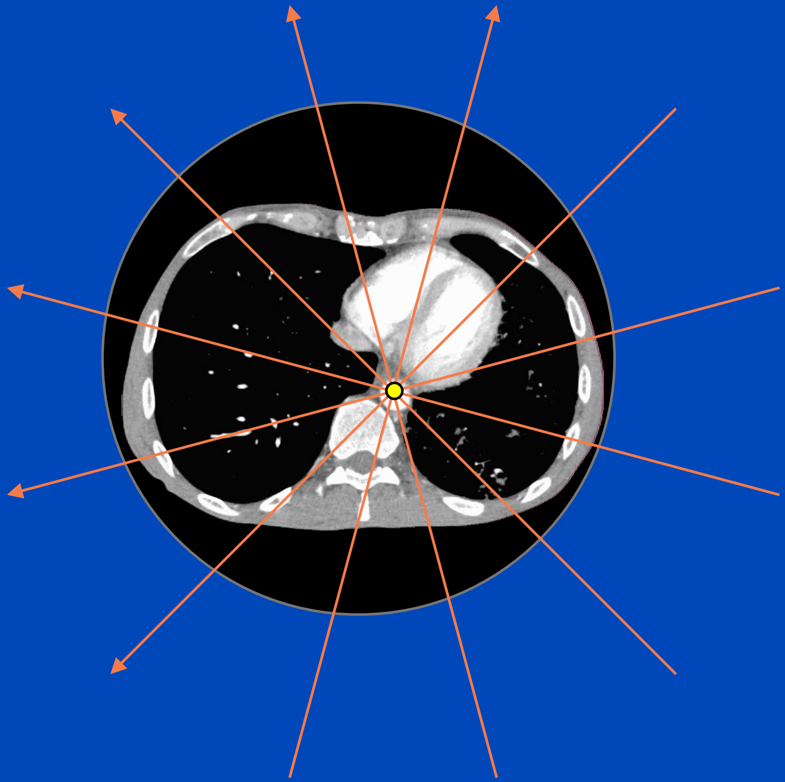

**Each object point must be viewed by an angular interval of 180° or more. Otherwise image reconstruction is not possible.**

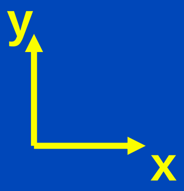


dkfz.

# Axial Geometry (z-Direction)

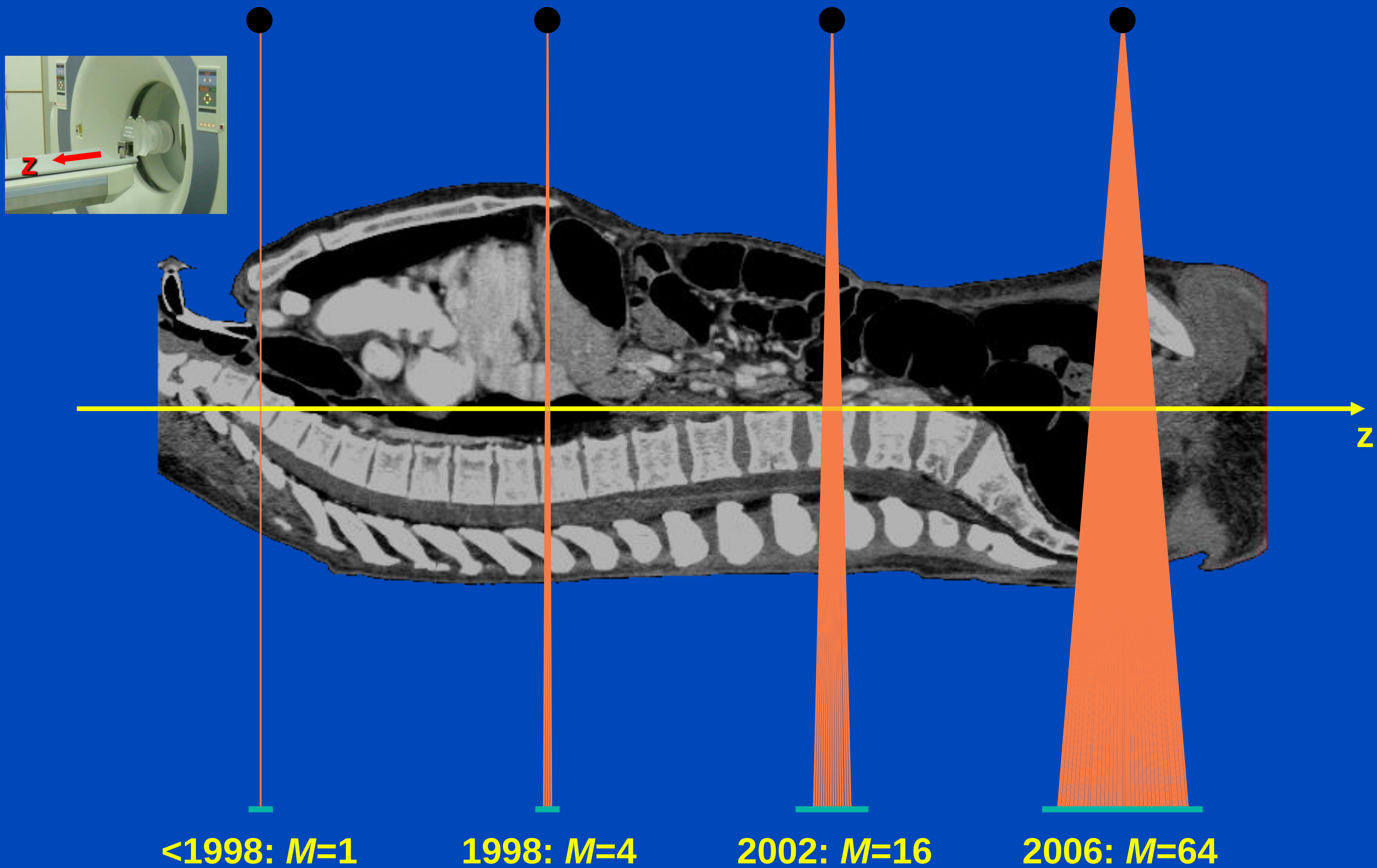

# Axial Geometry (z-Direction)


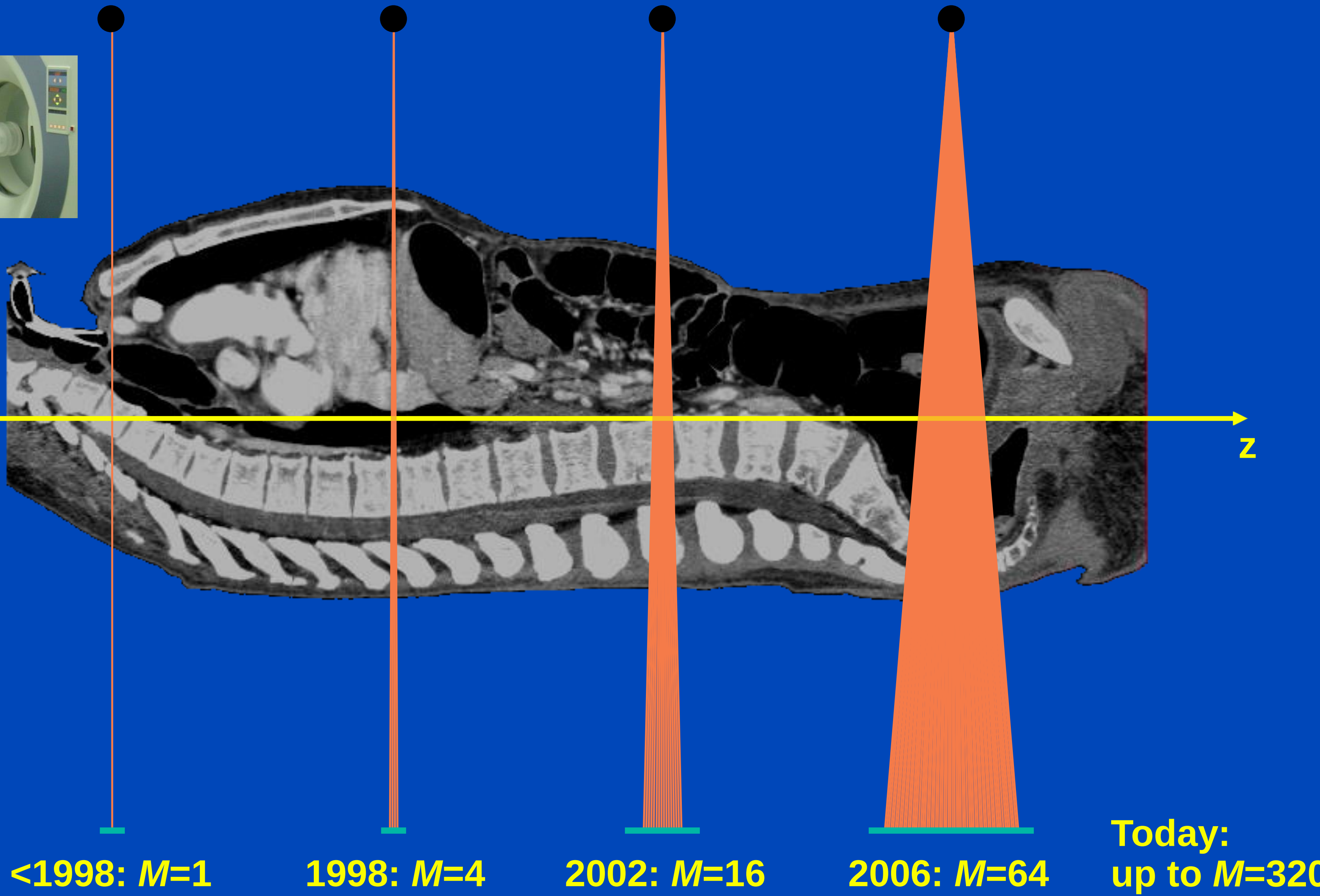

# Somatom Force: Ultra Low Dose Lung Imaging

- Atypical pneumonia in inspiration and expiration
- Turbo Flash mode, 737 mm/s, 100 kV Sn
- DLP = 7 mGy·cm ≈ 0.1 mSv per scan

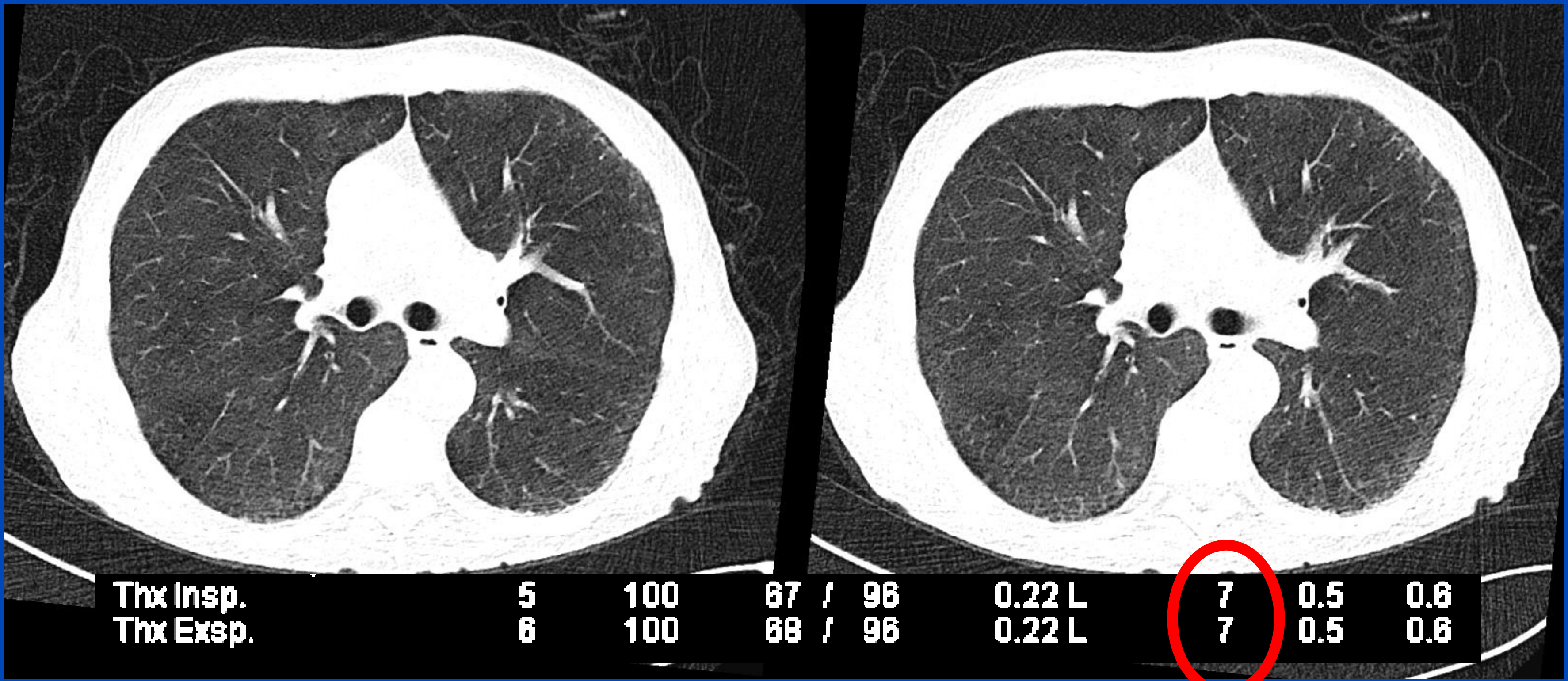


Courtesy of University Hospital Mannheim

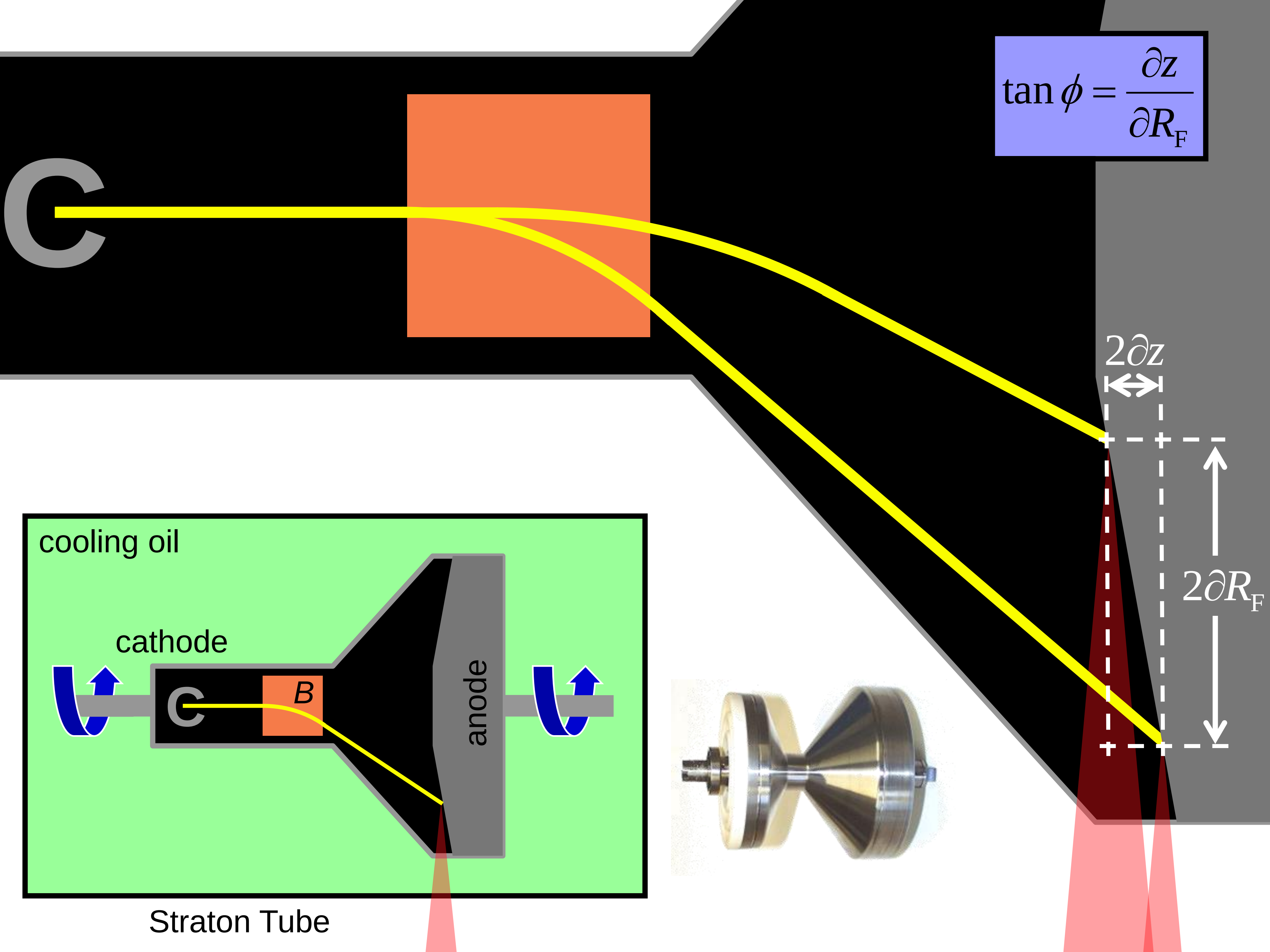

C
$\tan\phi = \frac{\partial z}{\partial R_F}$
$2\partial z$
$2\partial R_F$
cooling oil
cathode
C
B
anode
Straton Tube

# αFFS and zFFS

- The flying focal spot (FFS) can be used to improve the in-plane (lateral) sampling as well as the through-plane (longitudinal) sampling.

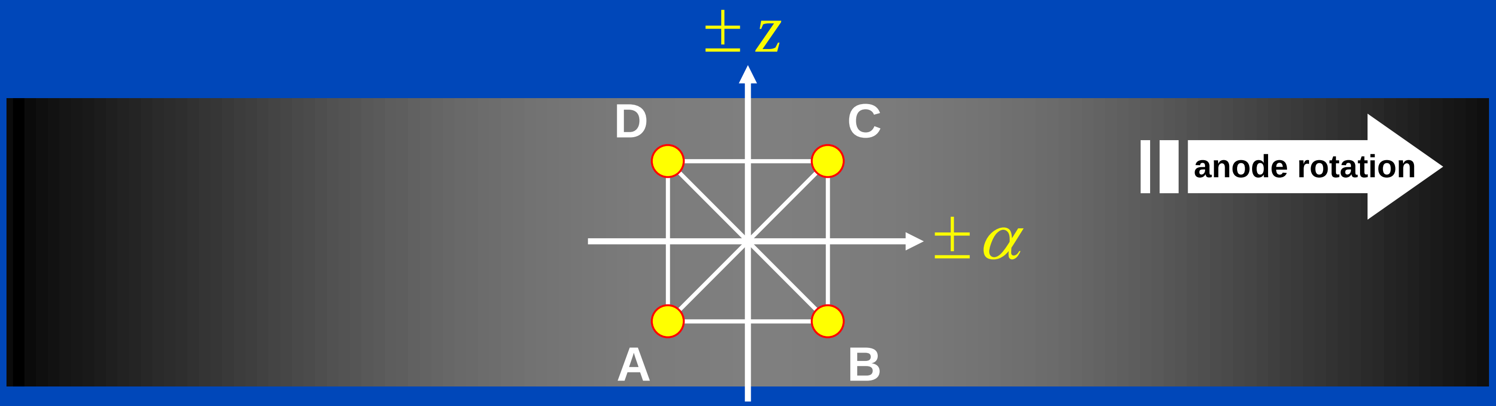


Anode as viewed from the isocenter

# αFFS

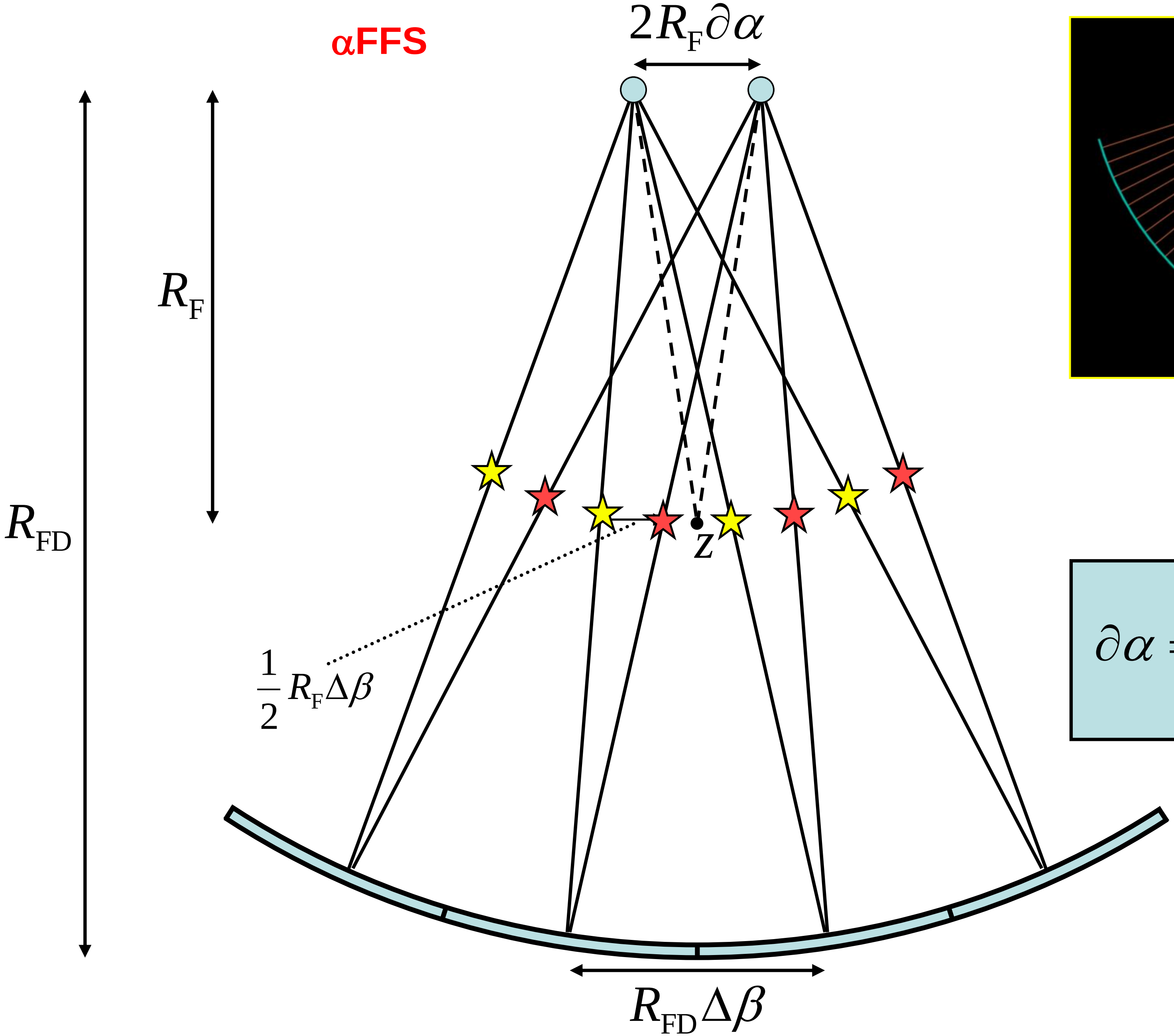


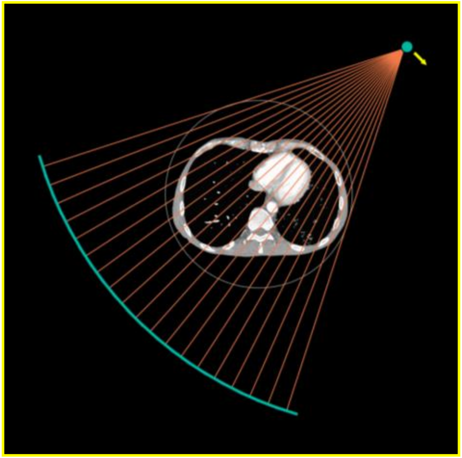

$$\partial\alpha = \frac{1}{4}\Delta\beta\frac{R_{FD}}{R_D}$$

# zFFS

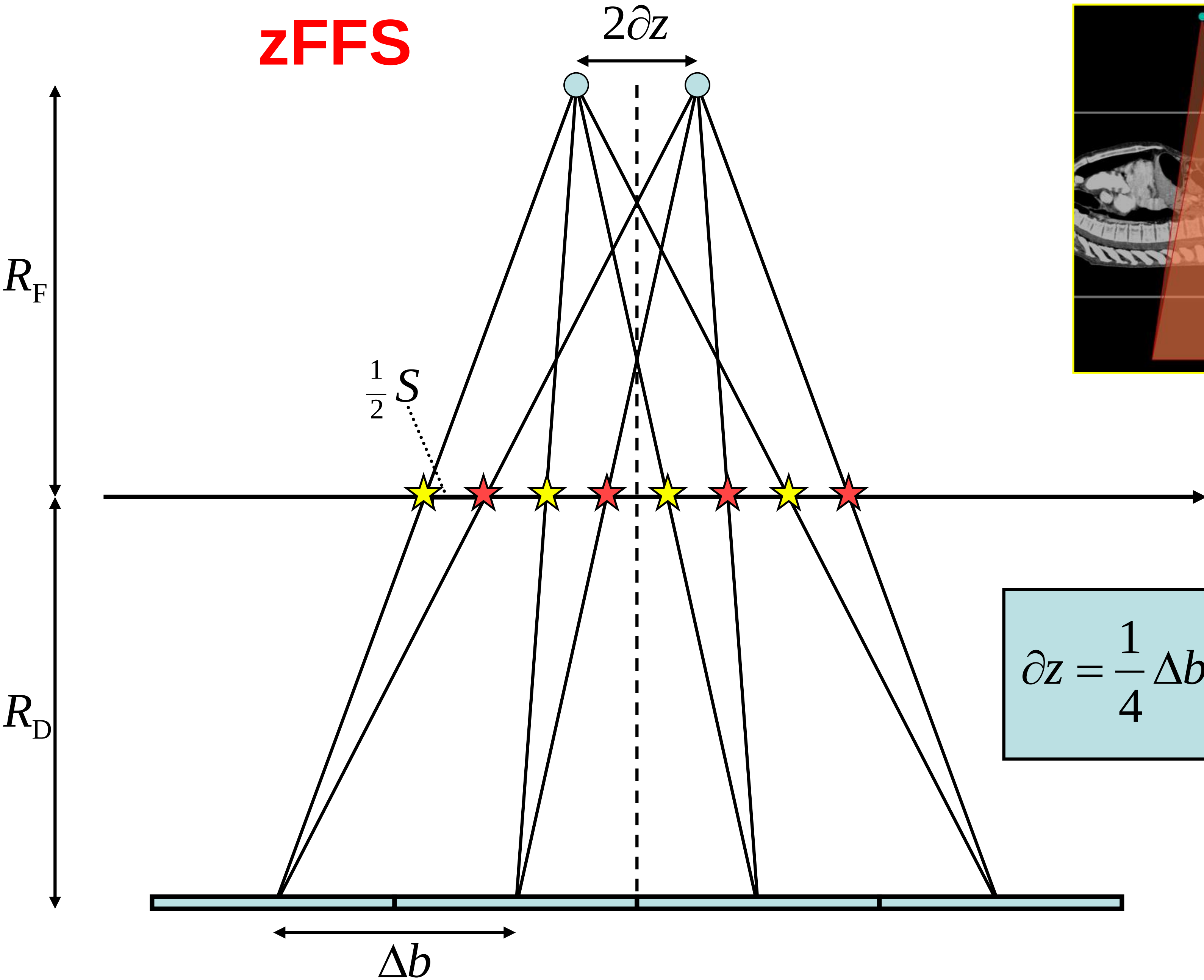


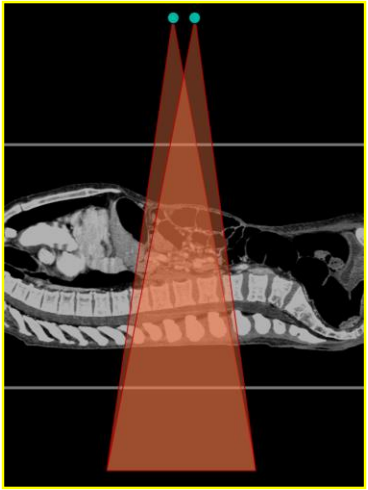

$$\partial z = \frac{1}{4} \Delta b \frac{R_\mathrm{F}}{R_\mathrm{D}}$$

# Demands on CT Detector Technology

- Available as multi-row arrays
- Very fast sampling (typ. 300 µs)
- Favourable temporal characteristics (decay time < 10 µs)
- High absorption efficiency
- High geometrical efficiency
- High count rate (up to $10^9$ cps*)
- Adequate dynamic range (18 to 22 bit)
- Signal stability (better than 0.1%)

* in the order of $10^5$ counts per reading and $10^4$ readings per second

# Detector Technology

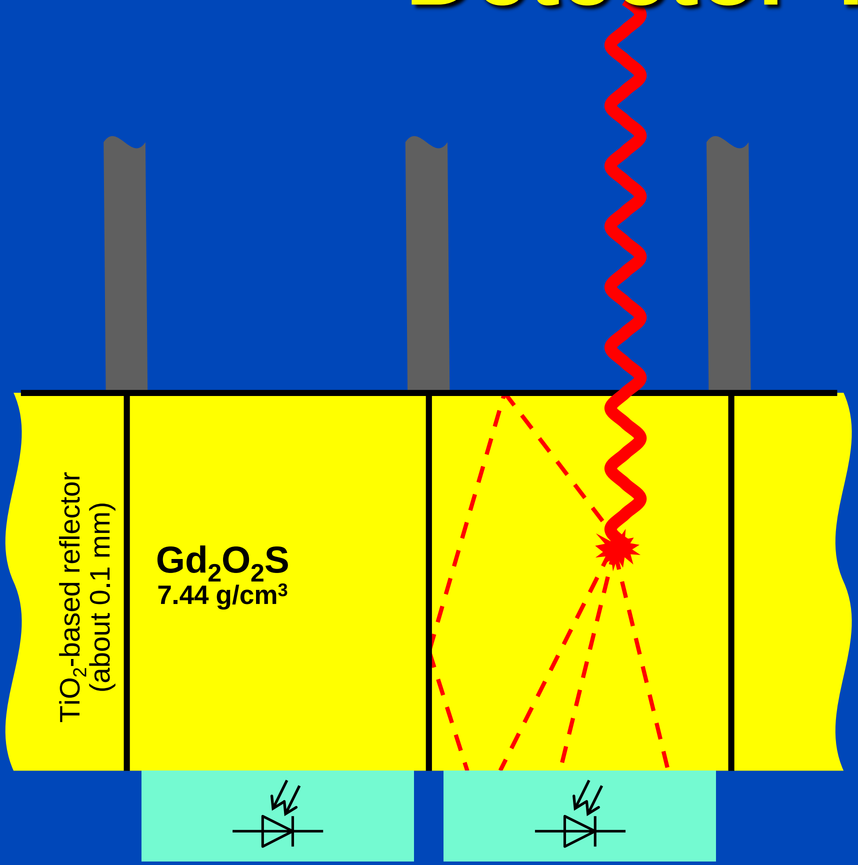


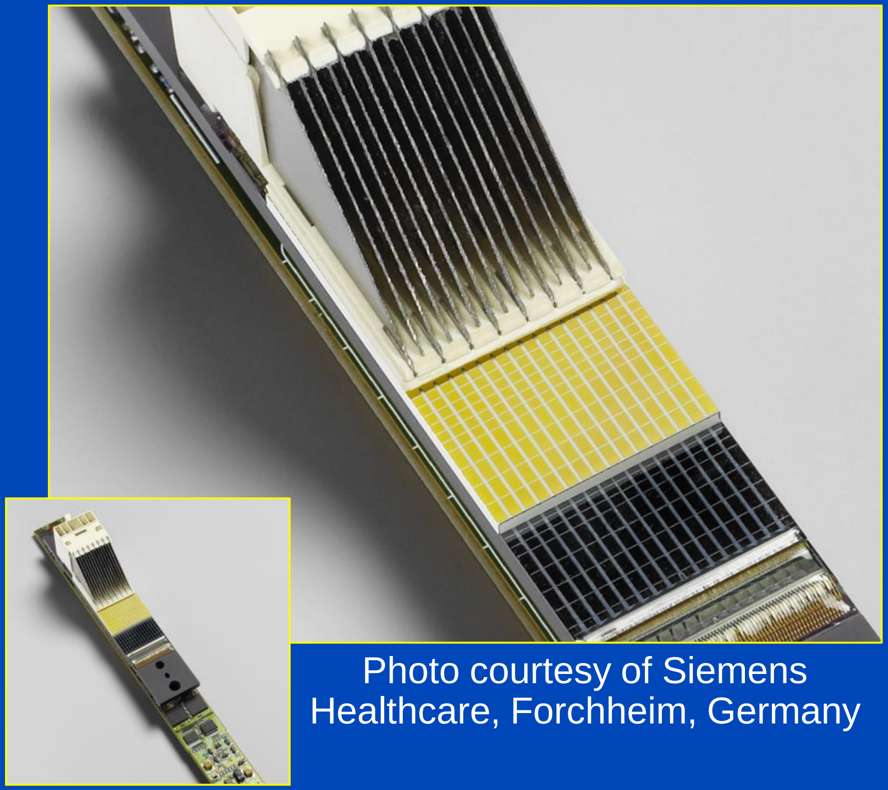

Photo courtesy of Siemens Healthcare, Forchheim, Germany

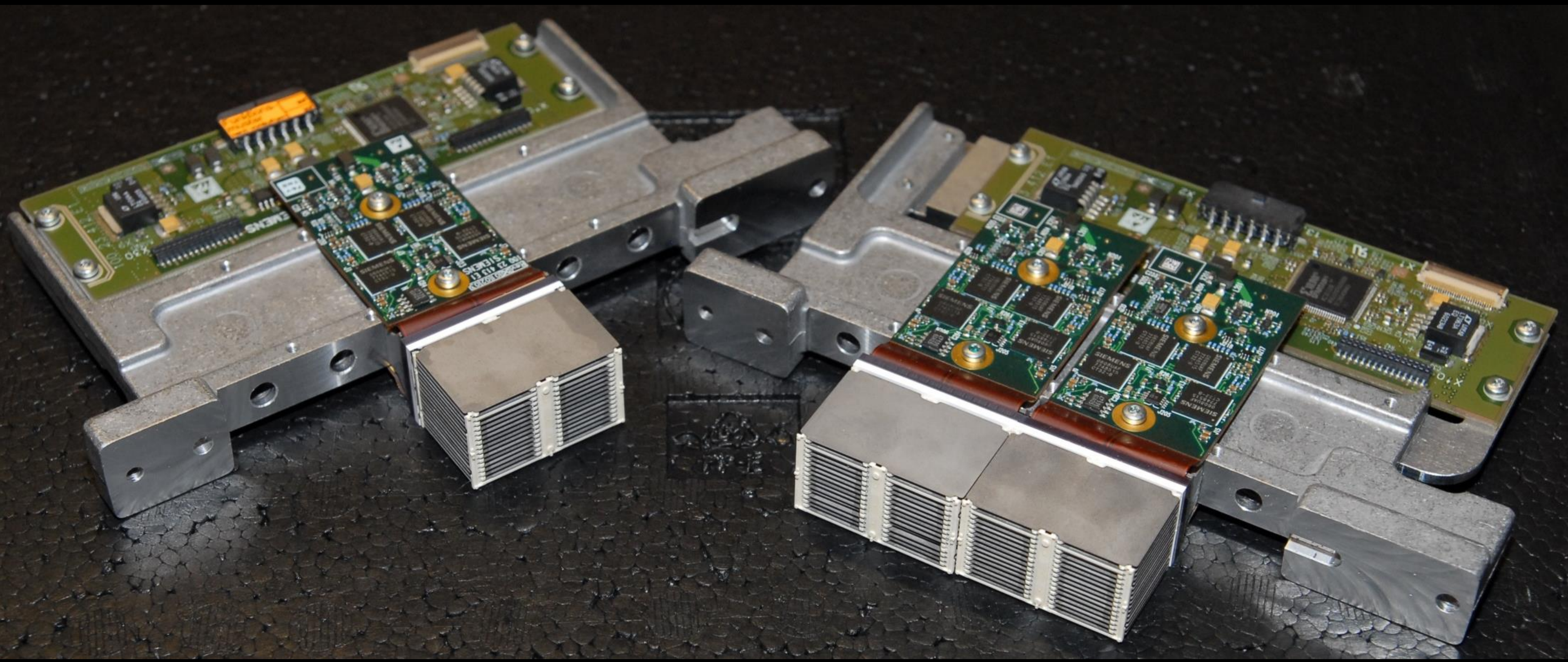

**modular and 2D tileable, 1D anti-scatter grid,**
**modules arranged on the surface of a cylinder segment**
**(Photo courtesy by Siemens)**

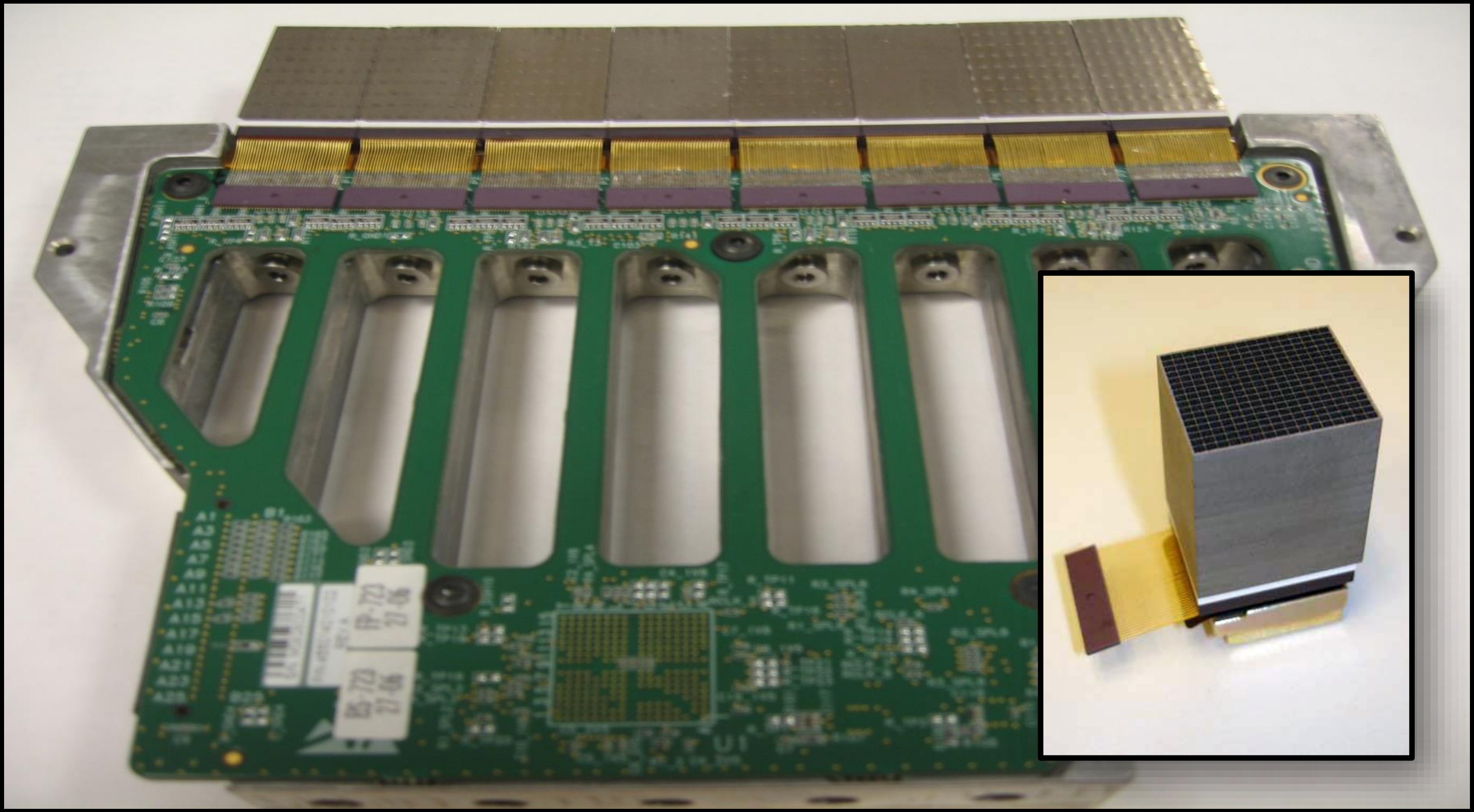

**“Nano-panel detectors”, modular and 2D tileable, focussed 2D anti scatter grid (Photo courtesy by Philips)**

# Fully Integrated Detector Electronics

- Electronics fully integrated into detector
- Very low electronic noise
- Less dose for infants, better images for obese

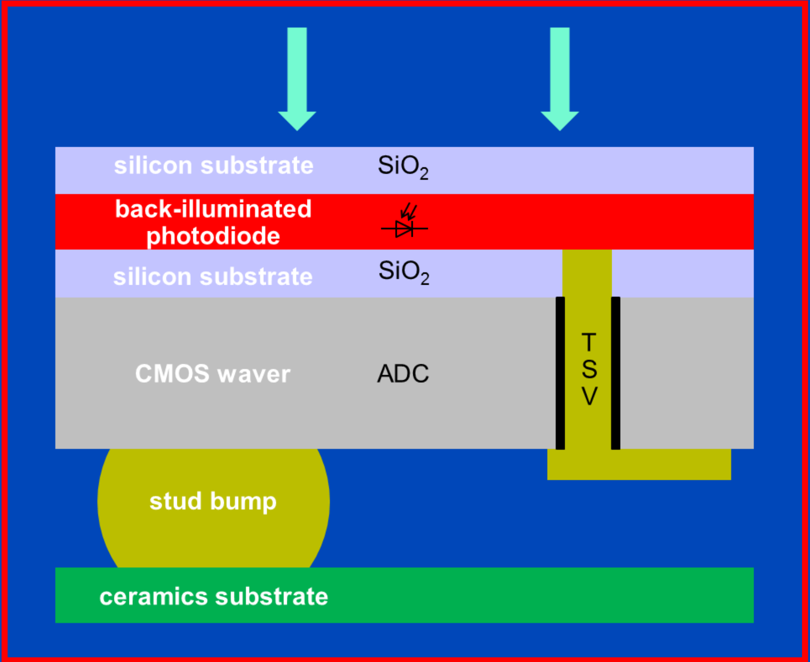


“Stellar detector”, modular and 2D tileable, focussed 2D anti scatter grid. Photo courtesy by Siemens.

dkfz.

“Stellar detector”, modular and 2D tileable, focussed 2D anti scatter grid. Photo courtesy by Siemens.

# Ultra High Resolution Scans

- With energy integrating detectors UHR requires[1,2]
  - detector comb or detector grid
  - αFFS and/or zFFS
- Realizations
  - Somatom Flash and Force comb (0.61 mm → 0.33 mm)
  - Somatom Flash grid (0.61 mm → 0.33 mm and 0.56 mm → 0.53 mm)
- Dose loss
  - about 50% with comb (46% + penumbra for Flash or Force)
  - about 75% with grid (66% + penumbra for Flash)
- Dose penalty
  - about two-fold dose needed with comb
  - about three-fold dose needed with grid

Flash (0.7 mm × 0.8 mm focus)
- UHR: 1D comb
- zUHR: 2D grid

Force (0.4 mm × 0.5 mm focus)
- UHR: 1D comb
- sUHR: 1D comb + z-deconv

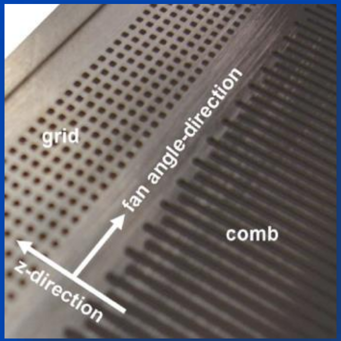


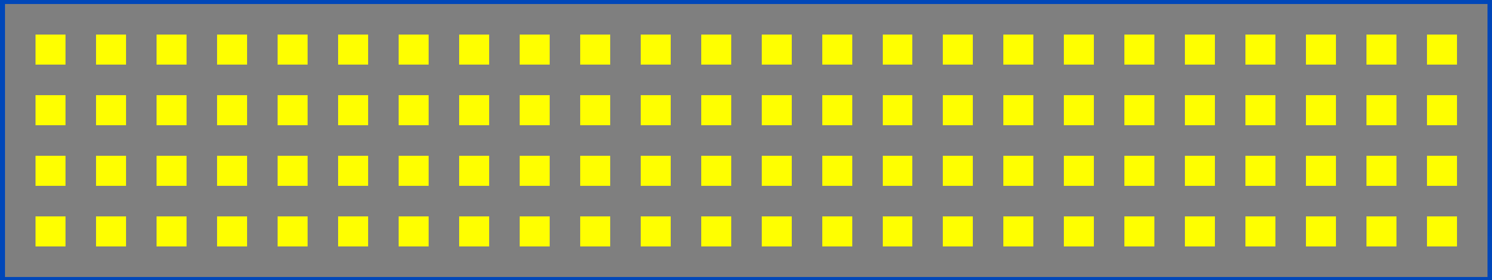

[1]Flohr et al. Novel ultrahigh resolution data acquisition and image reconstruction for multi-detector row CT. Med. Phys. 34(5):1712-1723, May 2007.
[2]Meyer et al. Initial results of a new generation DSCT system using only an in-plane comb filter for UHR temporal bone imaging. Eur Radiol 25:178-185, 2015.

# Ultra High Resolution Scans

- **Canon offers the Aquilion Precision, a system with dedicated ultra high resolution pixels**
  - **0.25 mm pixel size at iso**
  - **50% less septa thickness**
  - **1792 channels**
  - **160 detector rows**
  - **1D anti scatter grid**
  - **0.4 × 0.5 mm focal spot**
  - **10800 rpm anode, liquid metal bearing**
  - **512, 1024 or 2048 pixels per image**
  - **No need for post patient grid or comb: no dose penalty, small pixel effect can be utilized.**

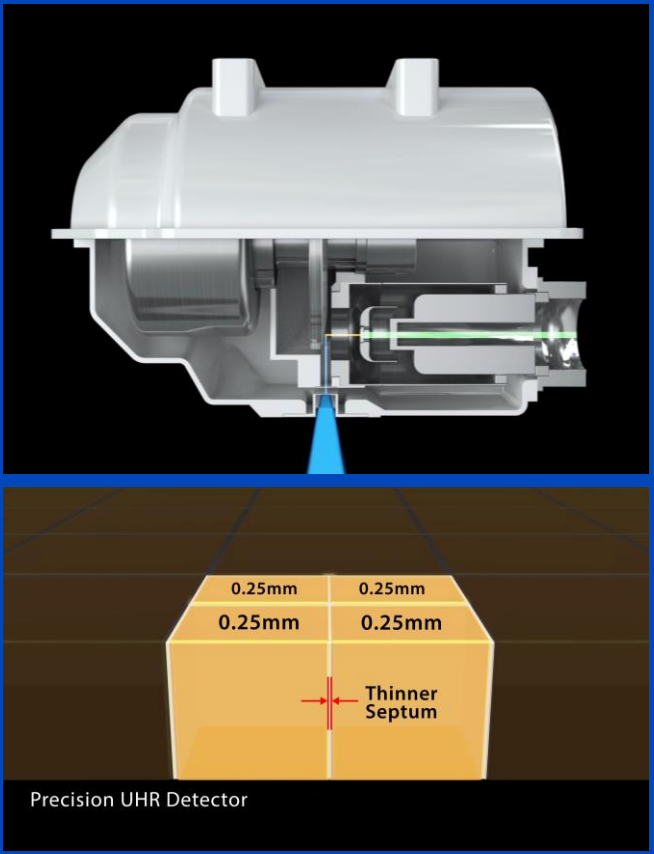

# Photon Counting CT (since 2021)


Alpha PCCT at University Medical Center Mannheim (UMM), Heidelberg University, Germany

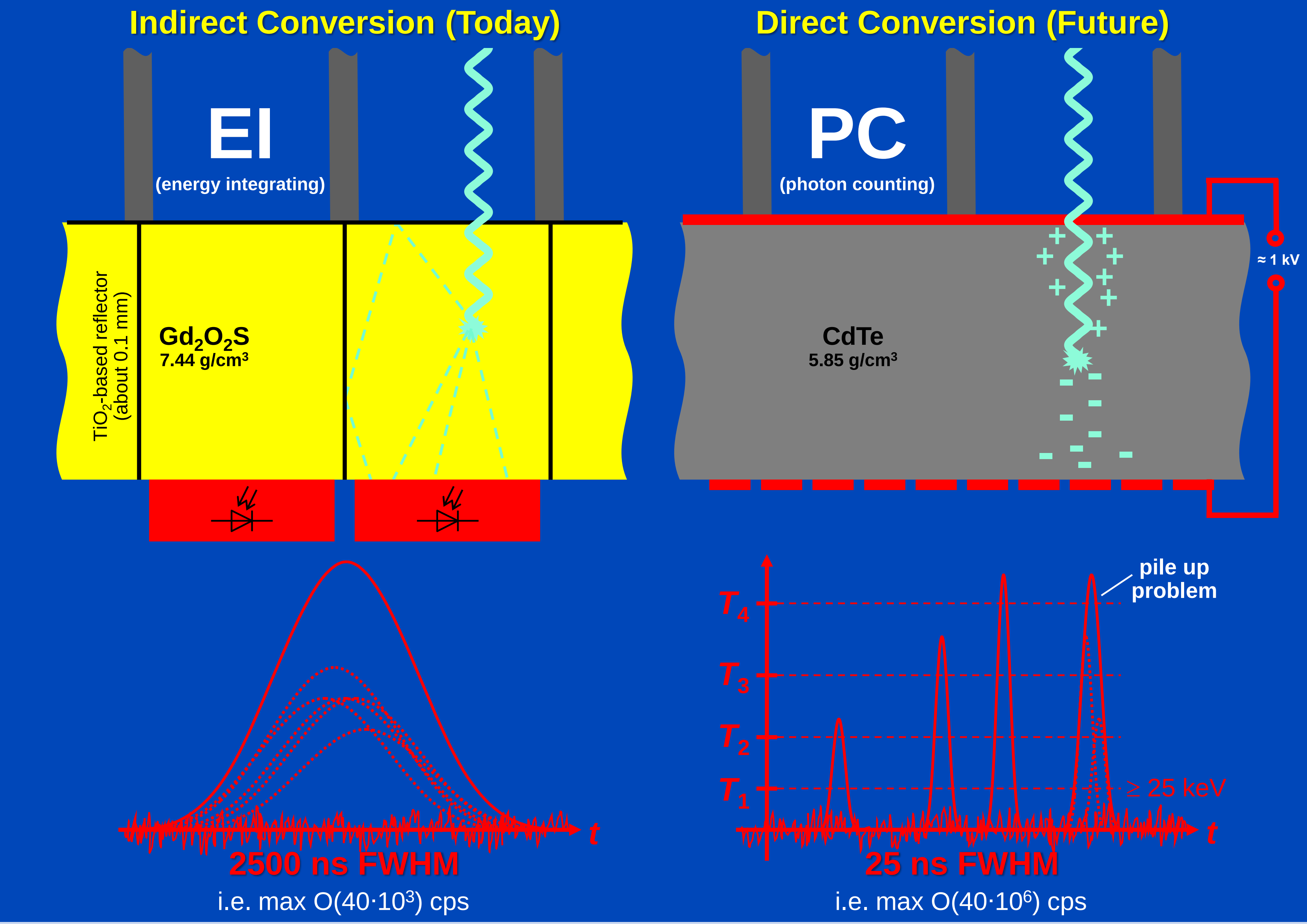


Requirements for CT: up to $10^9$ x-ray photon counts per second per $mm^2$.
Hence, photon counting only achievable for direct converters.

dkfz.

# Evolution of Spatial Resolution

**2005: Somatom Flash (B70)** | **2014: Somatom CounT (U70)** | **2021: Naeotom Alpha (Br98u)**

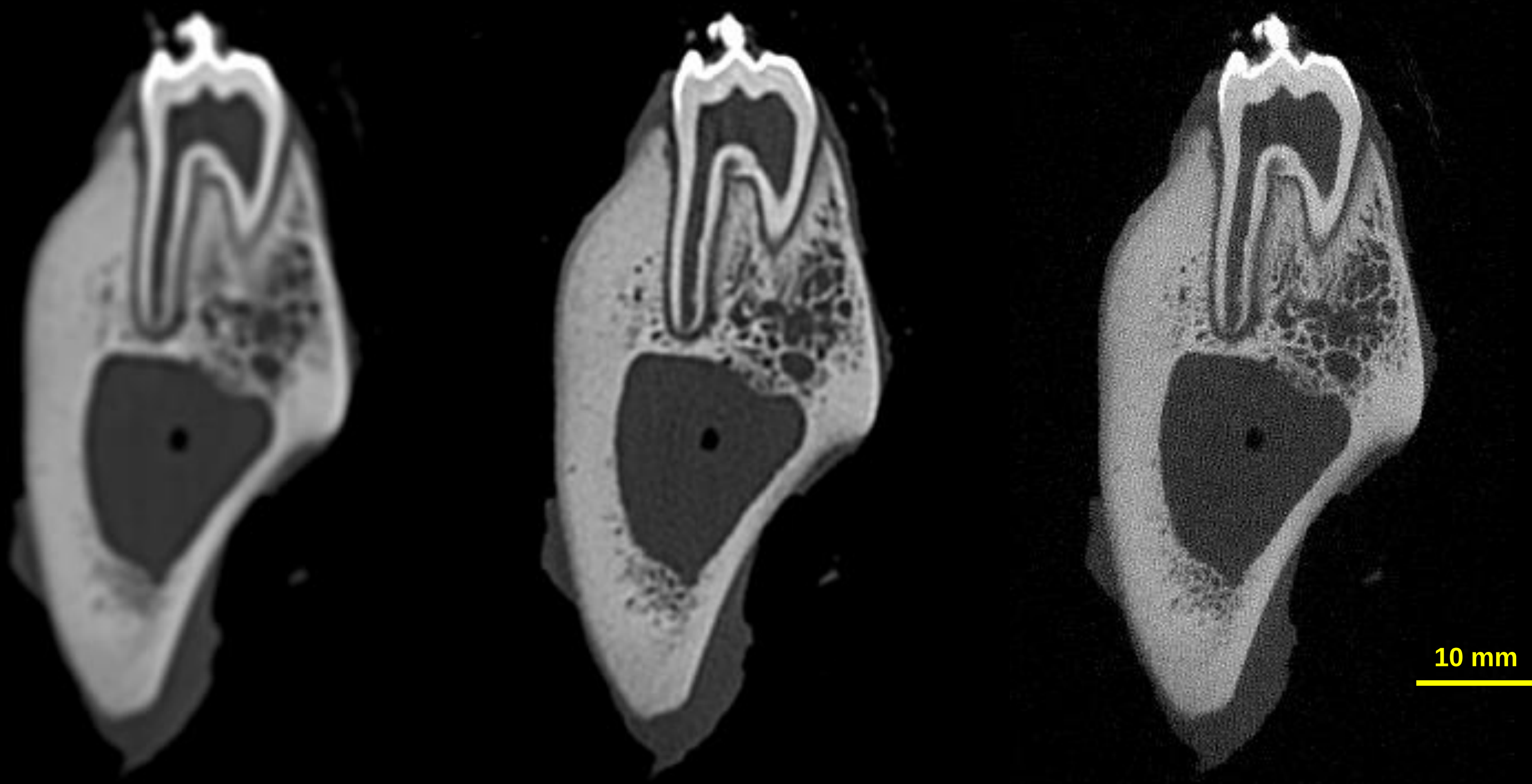


| 2005: Somatom Flash (B70) | 2014: Somatom CounT (U70) | 2021: Naeotom Alpha (Br98u) |
|---|---|---|
| Pixel size 0.181 mm | Pixel size 0.181 mm | Pixel size 0.181 mm |
| Slice Thickness 0.60 mm | Slice Thickness 0.20 mm | Slice Thickness 0.20 mm |
| Slice Increment 0.30 mm | Slice Increment 0.10 mm | Slice Increment 0.10 mm |
| $MTF_{50\%}$ = 8.0 lp/cm | $MTF_{50\%}$ = 12.1 lp/cm | $MTF_{50\%}$ = 39.0 lp/cm |
| $MTF_{10\%}$ = 9.2 lp/cm | $MTF_{10\%}$ = 16.0 lp/cm | $MTF_{10\%}$ = 42.9 lp/cm |

All measurements at Naeotom Alpha, Siemens Healthineers. QIR Reconstructions such that the maximum spatial resolution of Flash, CounT and Alpha is demonstrated on the same sample. *C* = 1200 HU, *W* = 4000 HU

dkfz.

# To Bin or not to Bin?
## (the continuous view)

*This nice phrase was coined by Norbert Pelc.*

- We have $\mathrm{PSF}(x) = s(x) * a(x)$ and $\mathrm{MTF}(u) = S(u)A(u)$.
- From Rayleigh's theorem we find noise is

$$\sigma^2 = \int dx\, a^2(x) = \int du\, A^2(u) = \int du\, \frac{\mathrm{MTF}^2(u)}{S^2(u)}$$

- Compare Small (A) with la … pixels:

**Avoid binning, if possible!**

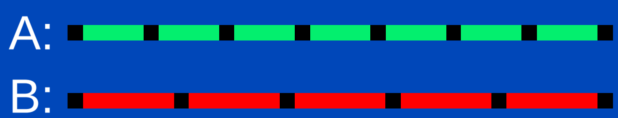


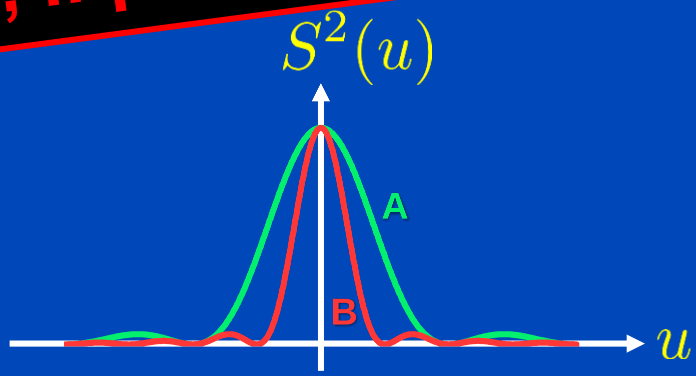


- We have $S_\mathrm{A}(u) > S_\mathrm{B}(u)$ and thus $\sigma_\mathrm{A}^2 < \sigma_\mathrm{B}^2$.
- This means that a desired PSF/MTF is often best achieved with smaller detectors.

Kachelrieß, Kalender. Med. Phys. 32(5):1321-1334, May 2005
Baek, Pineda, and Pelc. PMB 58:1433-1446, 2013

# The “Small Pixel Effect”

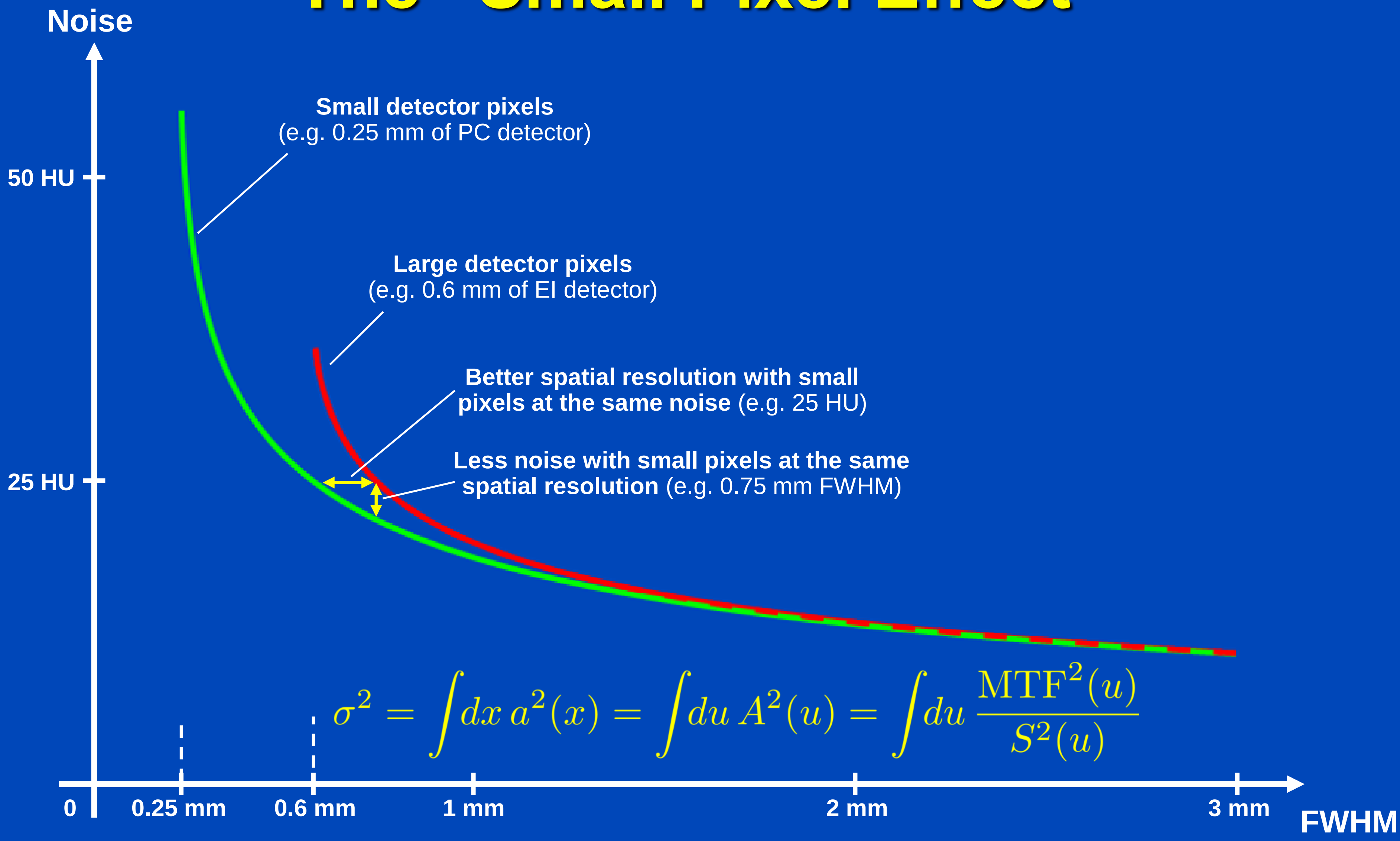


$$\sigma^2 = \int dx\, a^2(x) = \int du\, A^2(u) = \int du\, \frac{\mathrm{MTF}^2(u)}{S^2(u)}$$

Kachelrieß, Kalender. Med. Phys. 32(5):1321-1334, May 2005

dkfz.

# The “Small Pixel Effect”

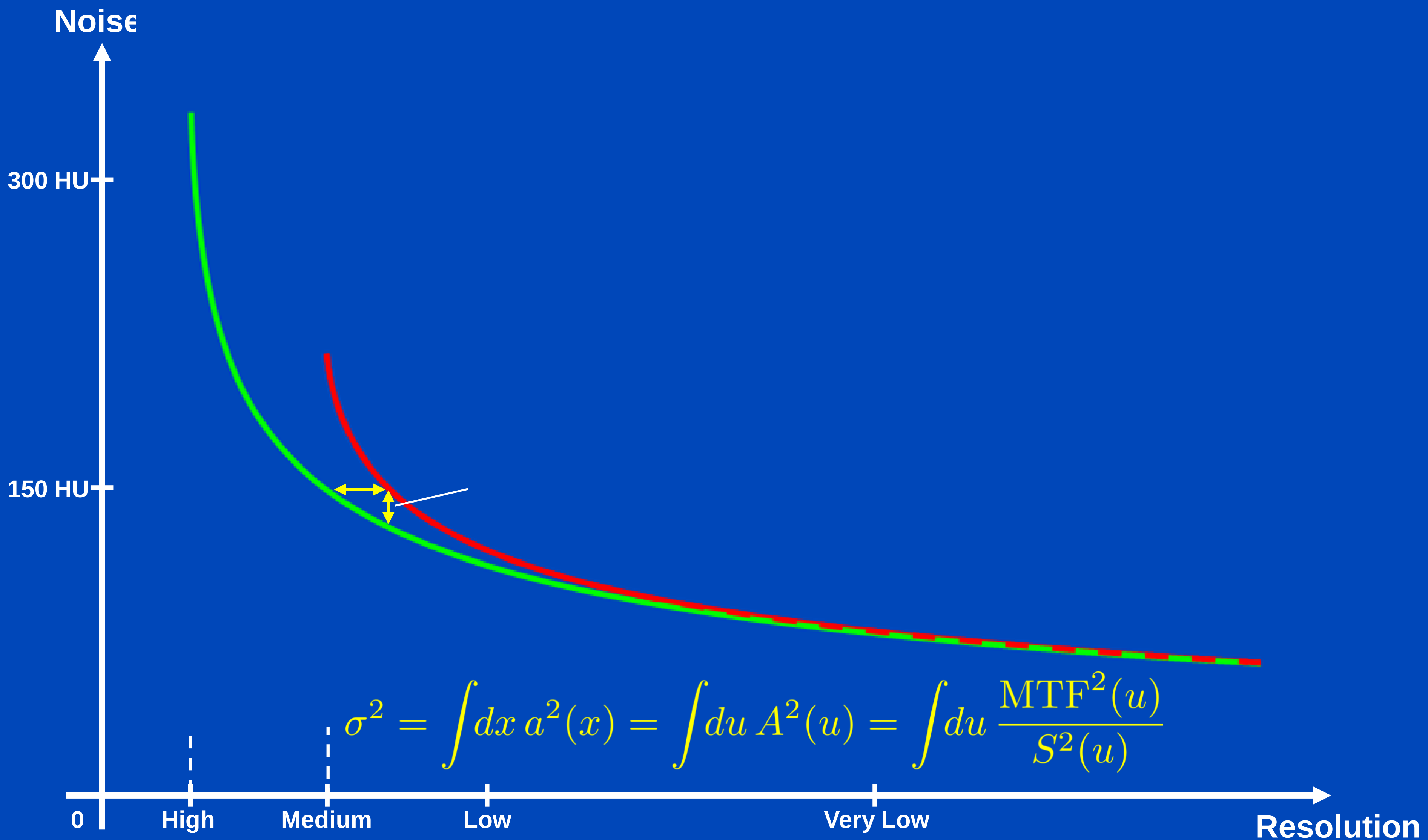


$$\sigma^2 = \int dx\, a^2(x) = \int du\, A^2(u) = \int du\, \frac{\mathrm{MTF}^2(u)}{S^2(u)}$$

Kachelrieß, Kalender. Med. Phys. 32(5):1321-1334, May 2005

# To Bin or not to Bin?

## (the discrete view, LI)

- Let detector B be the 2-binned version of detector A:

$$B_{2n} = \tfrac{1}{2}(A_{2n} + A_{2n+1}) \qquad \mathrm{Var}\,B = \tfrac{1}{2}\mathrm{Var}\,A$$

- Assume LI to be used to find in-between pixel values. Wlog we may then consider B to be upsampled with mid-point interpolati… …r A:

$$\hat{B} \ldots \ldots)$$

- To ol… …etector we n…

$$a = \tfrac{1}{2}\left(1,\ 1\right) * \tfrac{1}{4}\left(1,\ 2,\ 1\right) = \tfrac{1}{8}\left(1,\ 3,\ 3,\ 1\right)$$

- Noise propagation yields 20% more noise (variance) for the binned detector:

$$\mathrm{Var}\,\hat{A} = \tfrac{20}{64}\mathrm{Var}\,A = \tfrac{5}{16}\mathrm{Var}\,A$$

$$\mathrm{Var}\,\hat{B} = \tfrac{3}{8}\,\mathrm{Var}\,A = \tfrac{6}{5}\,\mathrm{Var}\,\hat{A} = 1.2\,\mathrm{Var}\,\hat{A}$$

20% more noise variance may be compensated by
20% more x-ray dose. Any alternative? Yes:

**Avoid binning, if possible!**

In 2D binning implies 44% more noise variance or dose.
Again, the answer is: „not to bin“.

# To Bin or not to Bin?

## (the discrete view, NN)

- Let detector B be the 2-binned version of detector A:

$$B_{2n} = \tfrac{1}{2}(A_{2n} + A_{2n+1}) \qquad \operatorname{Var} B = \tfrac{1}{2}\operatorname{Var} A$$

- Let us now do an upsampling of the detector B such that each of B´s pixels becomes two pixels with the same value and with th

30% more noise variance may be compensated by 30% more x-ray dose. Any alternative? Yes:

**Avoid binning, if possible!**

In 2D binning implies 69% more noise variance or dose. Again, the answer is: „not to bin“.

- To o … etector we n

$$\boldsymbol{a} = \tfrac{1}{4}\left(1,\ 2,\ 1\right)$$

- Noise propagation yields 20% more noise (variance) for the binned detector:

$$\operatorname{Var}\hat{A} = \tfrac{6}{16}\operatorname{Var} A = \tfrac{3}{8}\operatorname{Var} A$$

$$\operatorname{Var}\hat{B} = \tfrac{1}{2}\operatorname{Var} A = \tfrac{4}{3}\operatorname{Var}\hat{A} = 1.3\operatorname{Var}\hat{A}$$

All images reconstructed with $1024^2$ matrix and 0.15 mm slice increment.
*C* = 1000 HU
*W* = 3500 HU

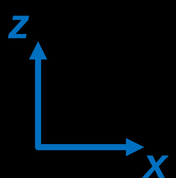


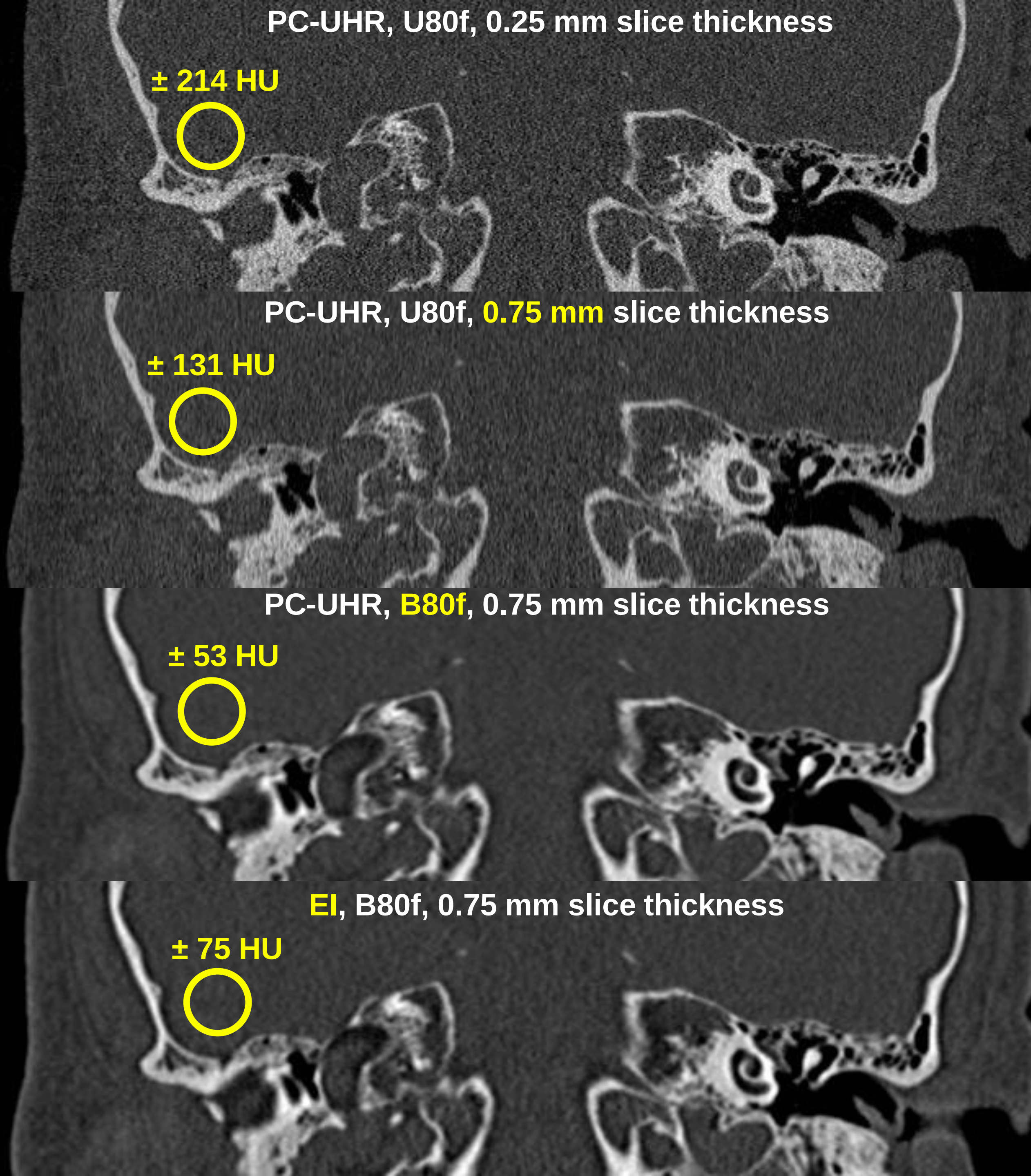


10% MTF: 19.1 lp/cm
10% MTF:17.2 lp/cm
xy FWHM: 0.48 mm
z FWHM: 0.40 mm
$CTDI_{vol}$: 16.0 mGy

10% MTF: 19.1 lp/cm
10% MTF:17.2 lp/cm
xy FWHM: 0.48 mm
z FWHM: 0.67 mm
$CTDI_{vol}$: 16.0 mGy

10% MTF: 9.3 lp/cm
10% MTF:10.5 lp/cm
xy FWHM: 0.71 mm
z FWHM: 0.67 mm
$CTDI_{vol}$: 16.0 mGy

10% MTF: 9.3 lp/cm
10% MTF:10.5 lp/cm
xy FWHM: 0.71 mm
z FWHM: 0.67 mm
$CTDI_{vol}$: 16.0 mGy

Data courtesy of the Institute of Forensic Medicine of the University of Heidelberg and of the Division of Radiology of the German Cancer Research Center (DKFZ)

L. Klein, C. Amato, S. Heinze, M. Uhrig, H.-P. Schlemmer, M. Kachelrieß, and S. Sawall. **Effects of Detector Sampling on Noise Reduction in a Clinical Photon Counting Whole-Body CT**. Investigative Radiology, vol. 55(2):111-119, February 2020.

**Energy Integrating Detector (B70f)**

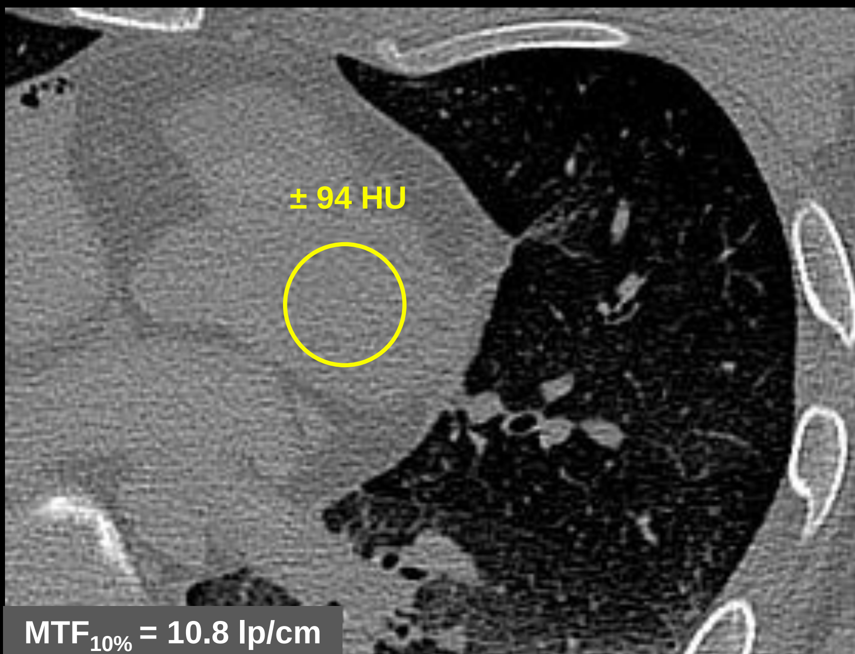


**Photon Counting Detector (B70f)**

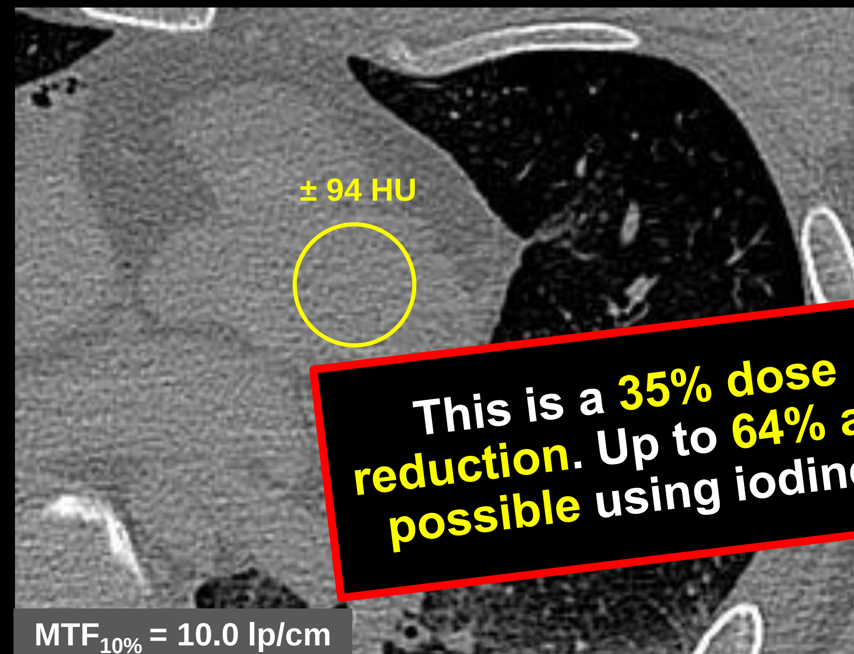


**This is a 35% dose reduction. Up to 64% are possible using iodine.**

**Acquisition with EI:**

- **Tube voltage of 120 kV**
- **Tube current of 300 mAs**
- **Resulting dose of $CTDI_{vol\ 32\ cm}$ = 22.6 mGy**

**Acquisition with UHR:**

- **Tube voltage of 120 kV**
- **Tube current of 180 mAs**
- **Resulting dose of $CTDI_{vol\ 32\ cm}$ = 14.6 mGy**

***C* = 50 HU, *W* = 1500 HU**

dkfz.

# Premium CT Systems 2021/2022

| Vendor | CT-System | Configuration | Collim, Cone | Rotation, FOM | Max. Power, Anode Angle | Max. mA @ low kV, patient-specific filters | Matrix | DECT |
|---|---|---|---|---|---|---|---|---|
| Canon | Aquilion ONE Genesis | 320 × 0.5 mm PUREViSION | 160 mm 15° | 0.275 s 50 cm | 100 kW, 10° MegaCool Vi | 600 mA @ 80 kV, none | 512 | 2 scans |
| Canon | Aquilion Precision | 160 × 0.25 mm PUREViSION | 40 mm 3.9° | 0.35 s 50 cm | 72 kW, 7° MegaCool | 600 mA @ 80 kV, none | 512, 1024, 2048 | 2 scans |
| GE | Revolution Apex | 256 × 0.625 mm GemStone Clarity | 160 mm 15° | 0.28 s 50 cm | 108 kW, 10° Quantix 160 | 1300 mA @ 70+80 kV, none | 512 | fast TVS or 2 scans |
| GE | Cardio-Graphe | 192 × 0.73 mm (focused FOM) | 140 mm 17° | 0.24 s 25 cm | 72 kW, 13° Dual MCS-2093 | 600 mA @ 80 kV, none | 512 | 2 scans |
| Philips | Brilliance iCT | 2 · 128 × 0.625 mm NanoPanel 3D | 80 mm 7.7° | 0.27 s 50 cm | 120 kW, 8° iMRC | 925 mA @ 80 kV, none | 512, 768, 1024 | 2 scans |
| Philips | Spectral CT 7500 | 2 · 128 × 0.625 mm NanoPanel Prism | 80 mm 7.7° | 0.27 s 50 cm | 120 kW, 8° iMRC | 925 mA @ 80 kV, none | 512, 768, 1024 | sandwich |
| Siemens | Somatom X.cite | 2 · 64 × 0.6 mm Stellar | 38.4 mm 3.7° | 0.3 s 50 cm | 105 kW, 8° Vectron | 1200 mA @ 70+80+90 kV, {0, 0.4, 0.7} mm Sn | 512, 768, 1024 | split filter or 2 scans |
| Siemens | Somatom Force | 2 · 2 · 96 × 0.6 mm Stellar | 57.6 mm 5.5° | 0.25 s 50/35 cm | 2 · 120 kW, 8° Vectron | 2 · 1300 mA @ 70+80+90 kV, {0, 0.6} mm Sn | 512, 768, 1024 | DSCT |
| **Siemens** | **Naeotom Alpha** | **2 · 144×0.4/120×0.2 mm Photon Counting!** | **57.6 mm 5.5°** | **0.25 s 50/36 cm** | **2 · 120 kW, 8° Vectron** | **2 · 1300 mA @ 90 kV, {0, 0.4} mm Sn** | **512, 768, 1024** | **DSPCCT** |

# Scan Trajectories

**Circle**

**Sequence**

$$p = \frac{d}{MS} \leq 0.9$$

**Spiral**

$$p = \frac{d}{MS} \leq 1.5$$

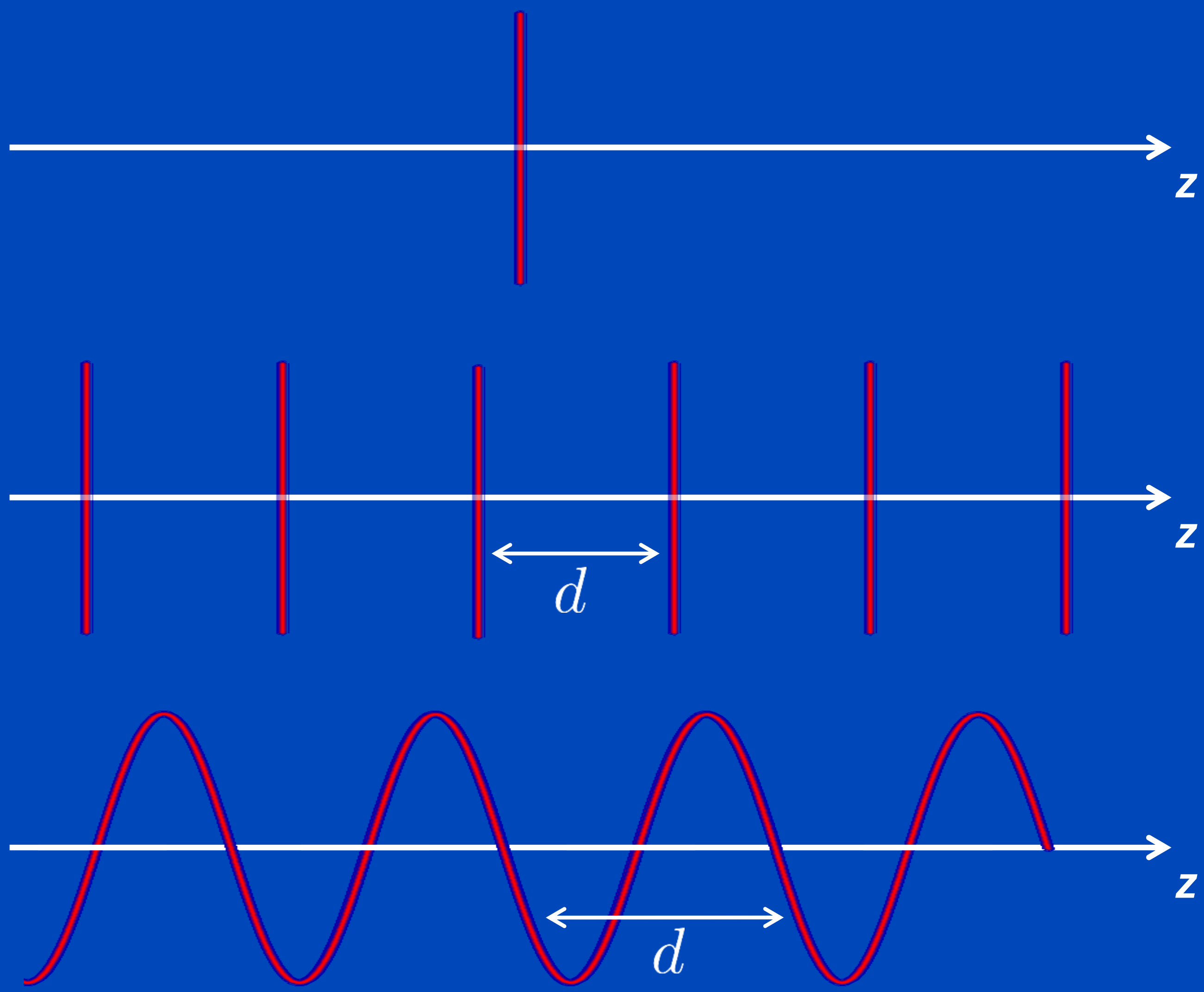

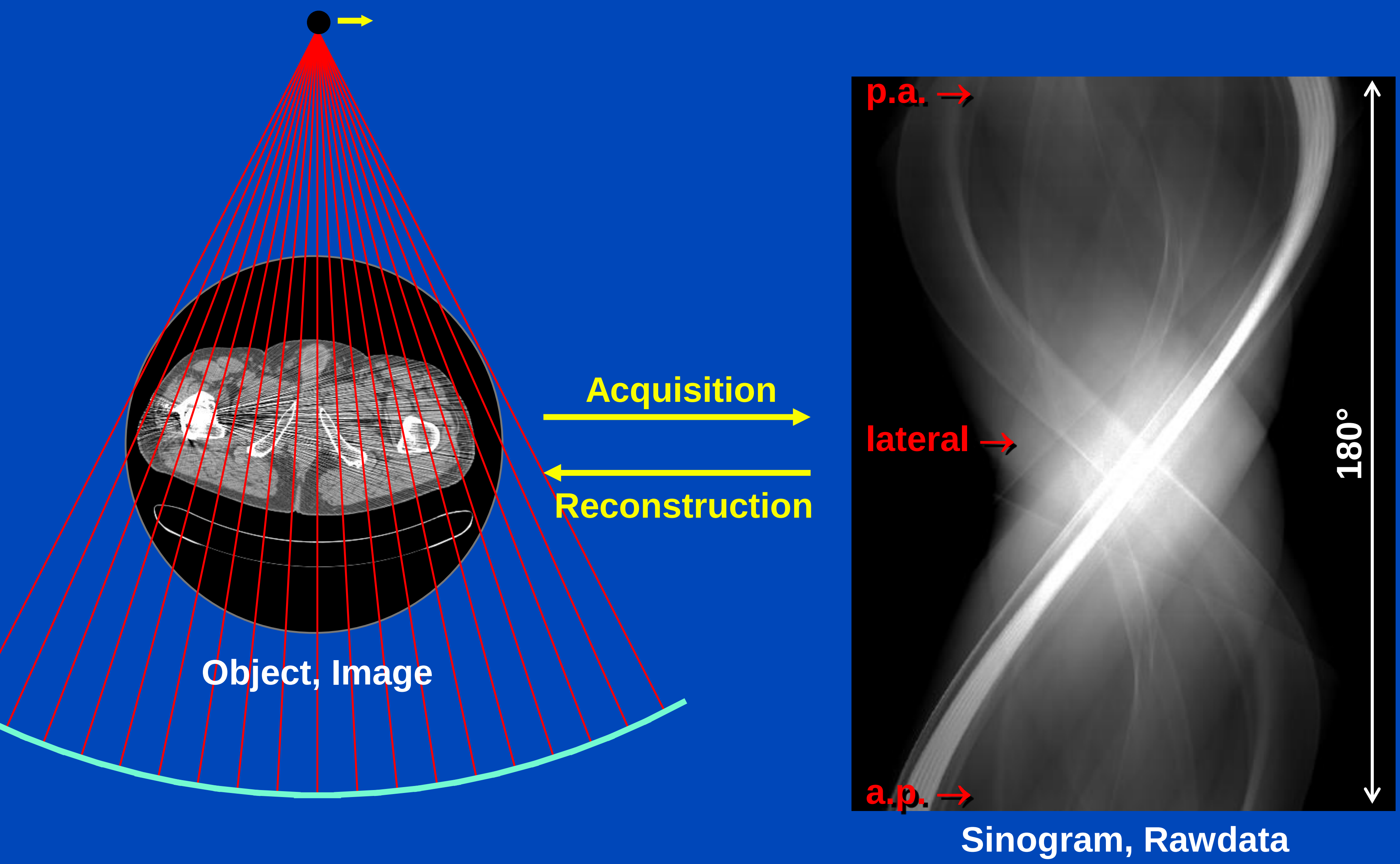

Acquisition
Reconstruction
Object, Image
p.a.
lateral
a.p.
180°
Sinogram, Rawdata

# Filtered Backprojection (FBP)

1. Filter projection data with the reconstruction kernel.
2. Backproject the filtered data into the image:

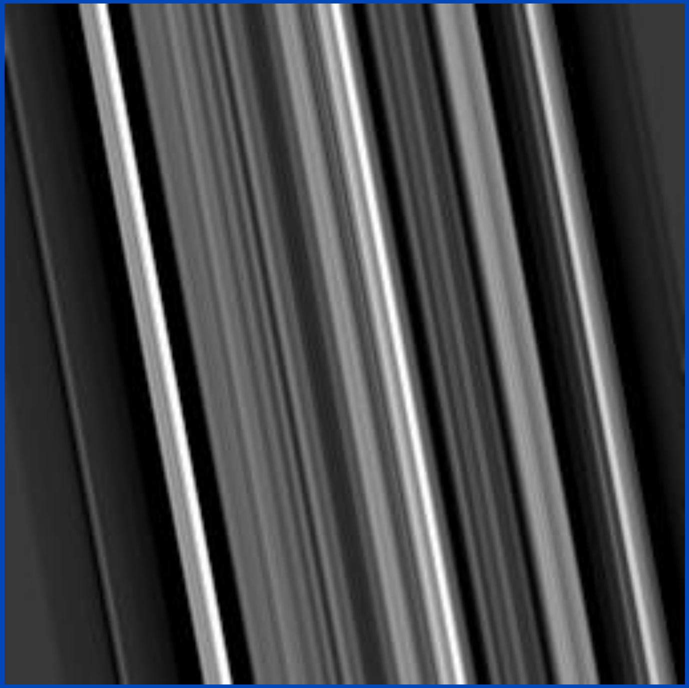

Smooth kernel (e.g. B30)

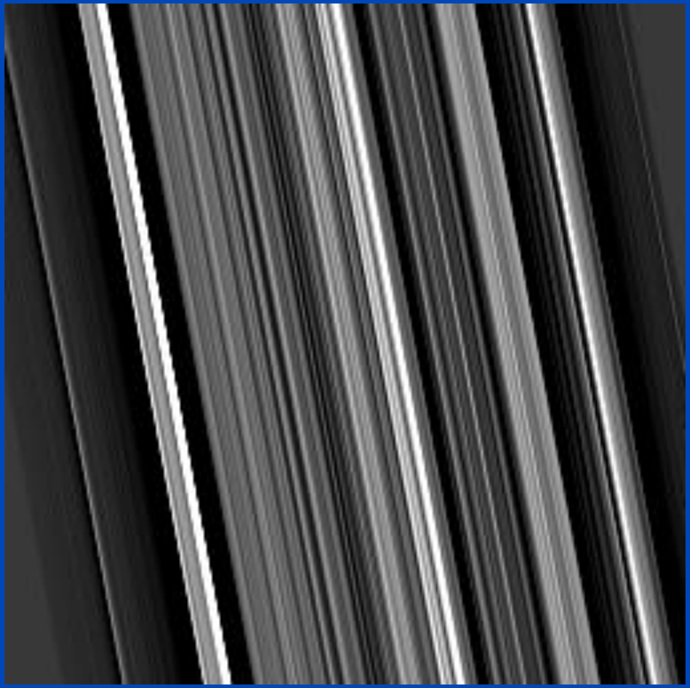

Sharp kernel (e.g. B70)

**Reconstruction kernels balance between spatial resolution and image noise.**

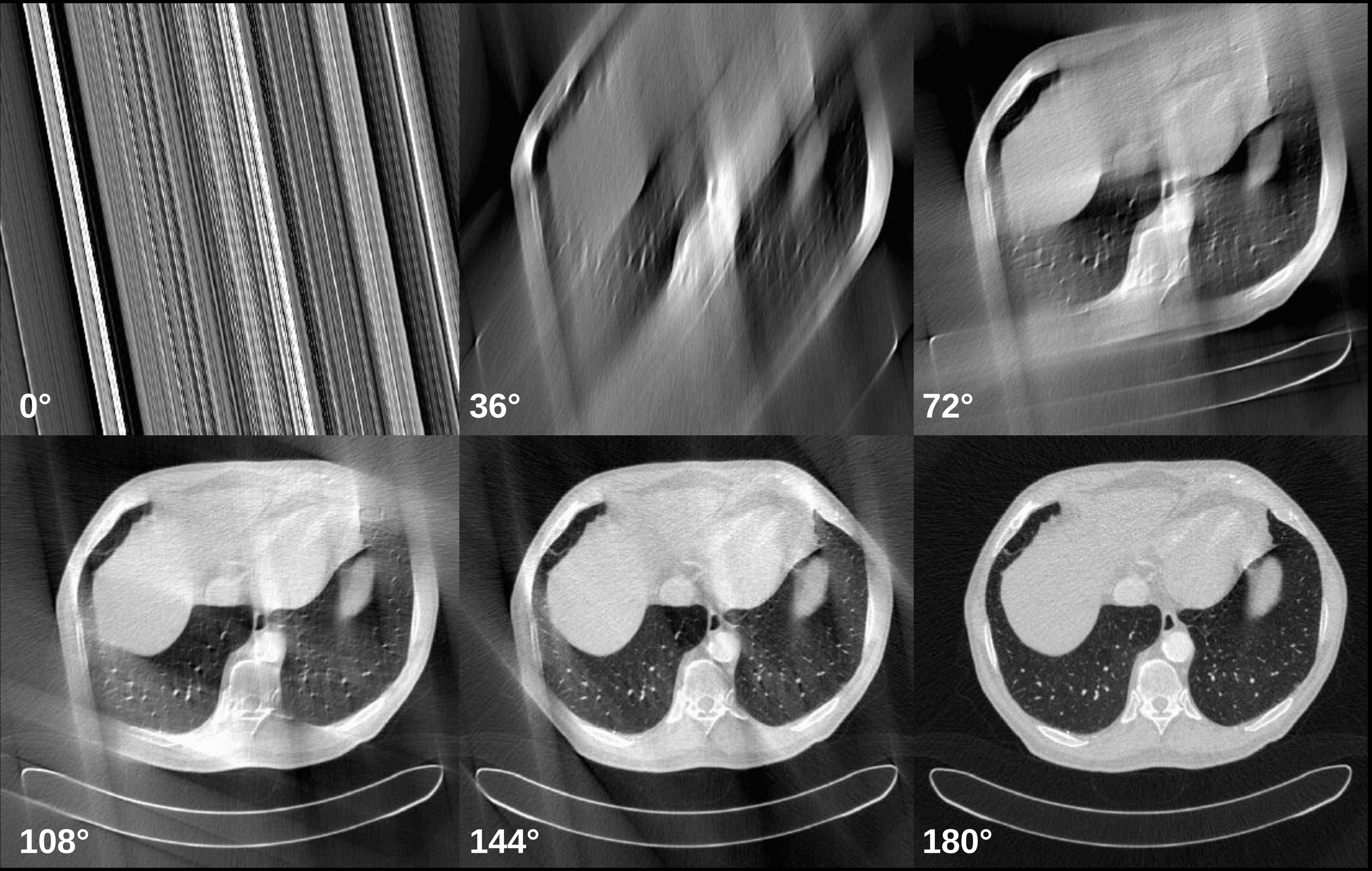


dkfz.

normalized

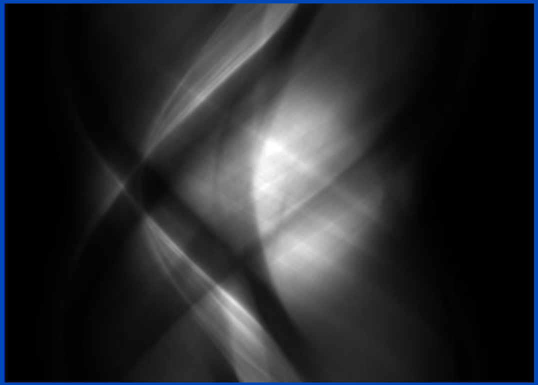

log normalized

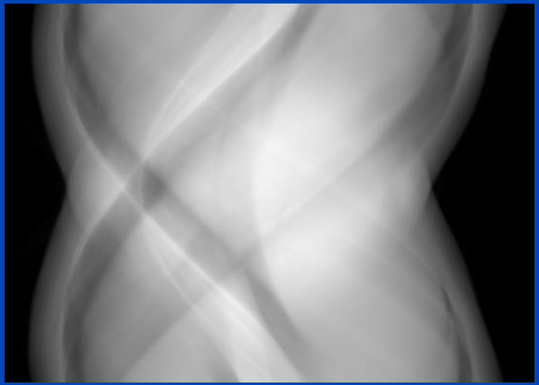

log normalized and convolved

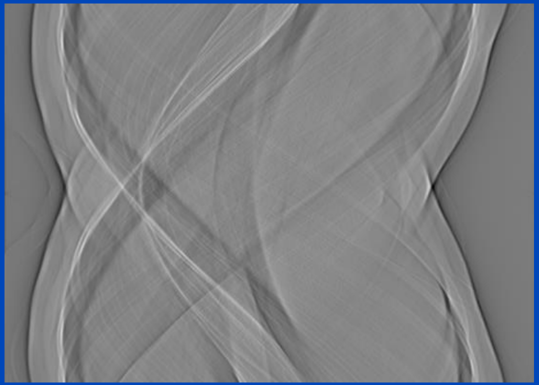

after 36°

after 72°

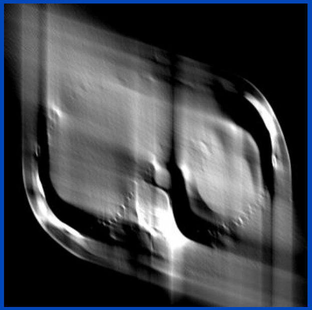

after 108°

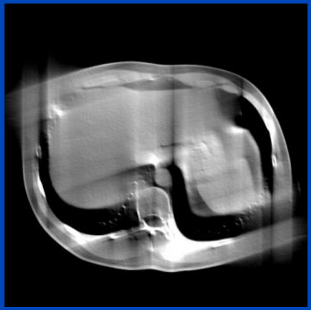

after 144°

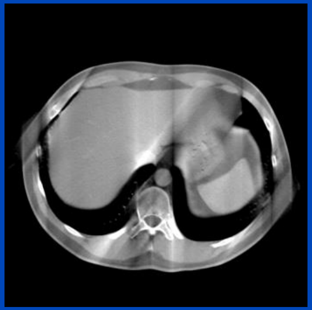

after 180°

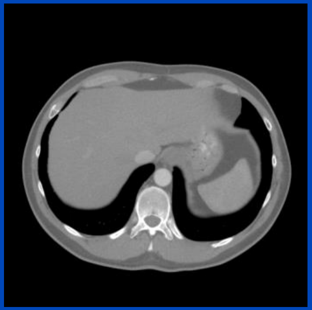

1 projection

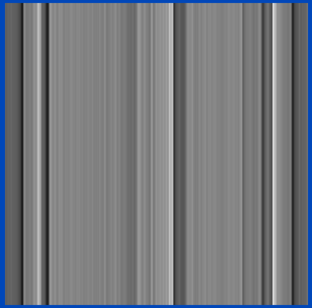

2 projections

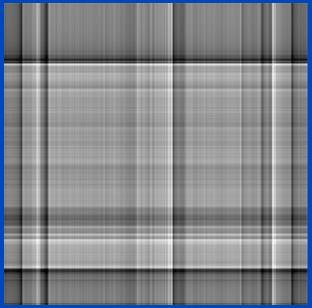

4 projections

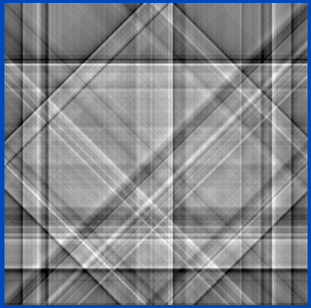

8 projections

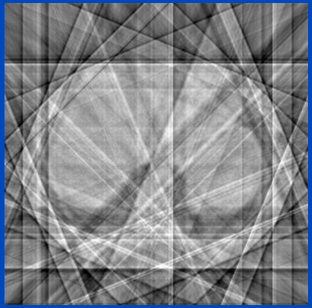

all projections

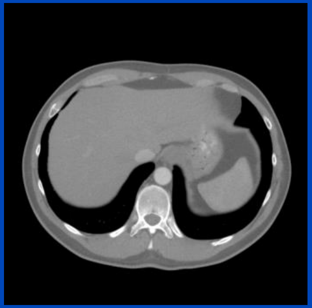

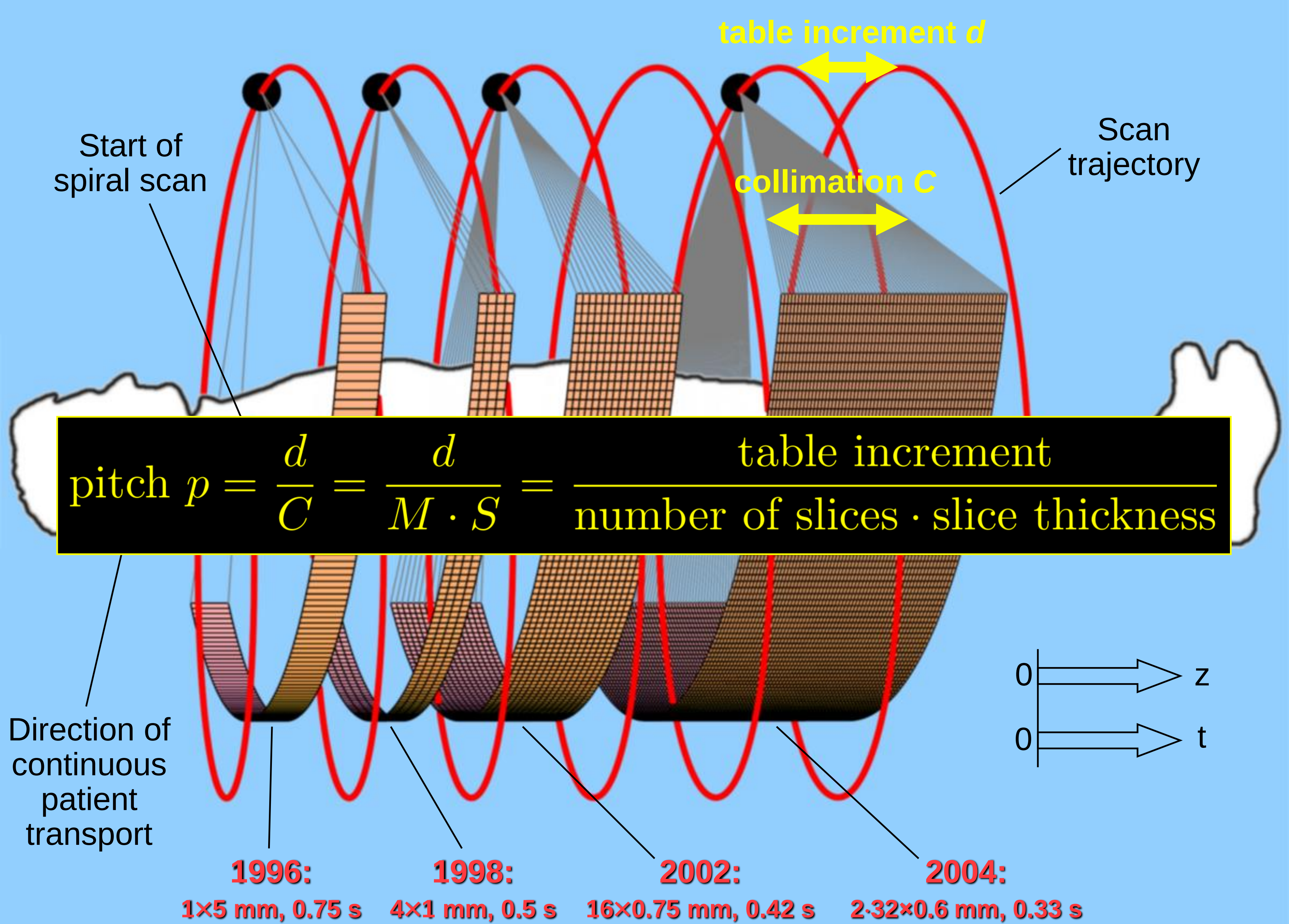


$$\text{pitch } p = \frac{d}{C} = \frac{d}{M \cdot S} = \frac{\text{table increment}}{\text{number of slices} \cdot \text{slice thickness}}$$

Kalender et al., Radiology 173(P):414 (1989) and 176:181-183 (1990)

# 360° LI Spiral z-Interpolation for Single-Slice CT ($M$=1)

$$p = \frac{d}{MS} \leq 2$$

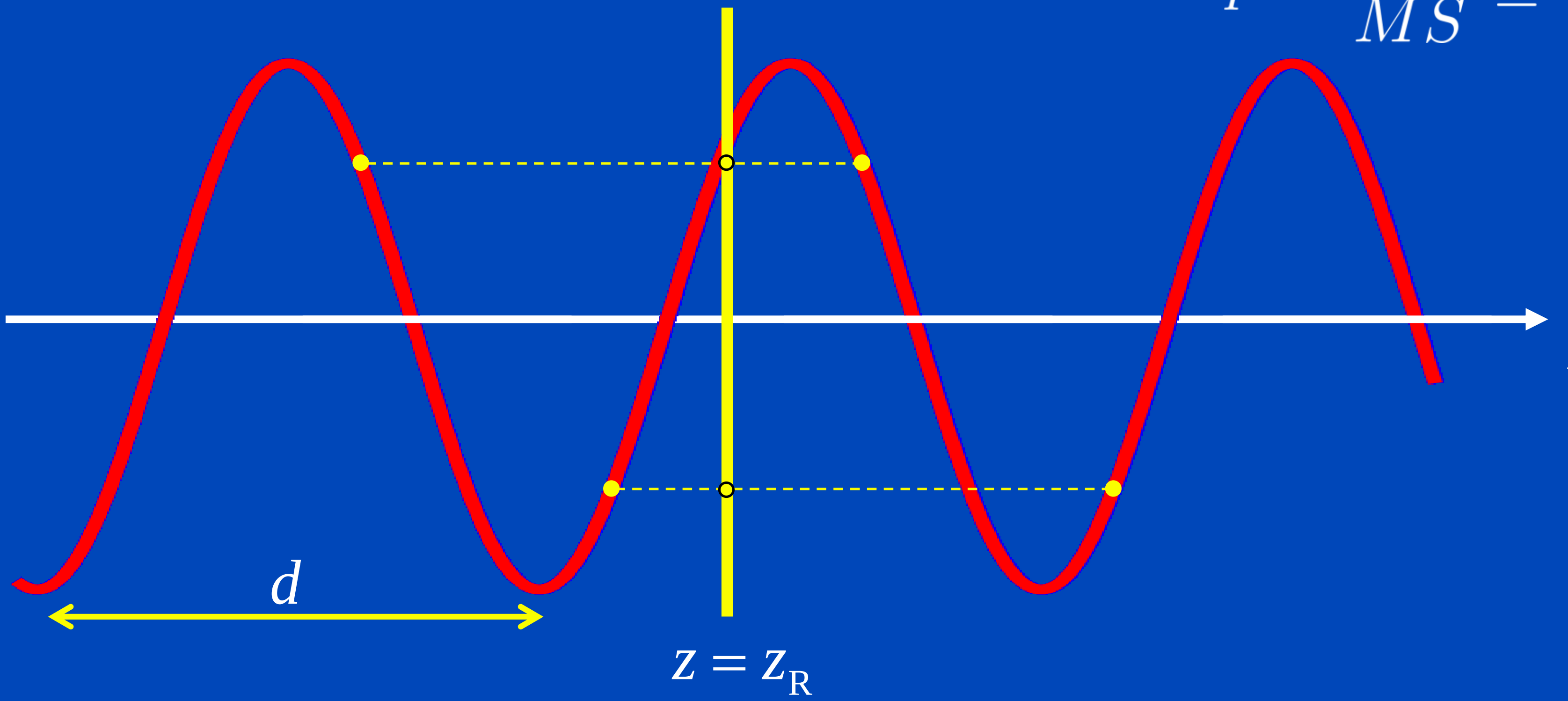


**Spiral z-interpolation is typically a linear interpolation between points adjacent to the reconstruction position to obtain circular scan data.**

**without *z*-interpolation**

**with *z*-interpolation**

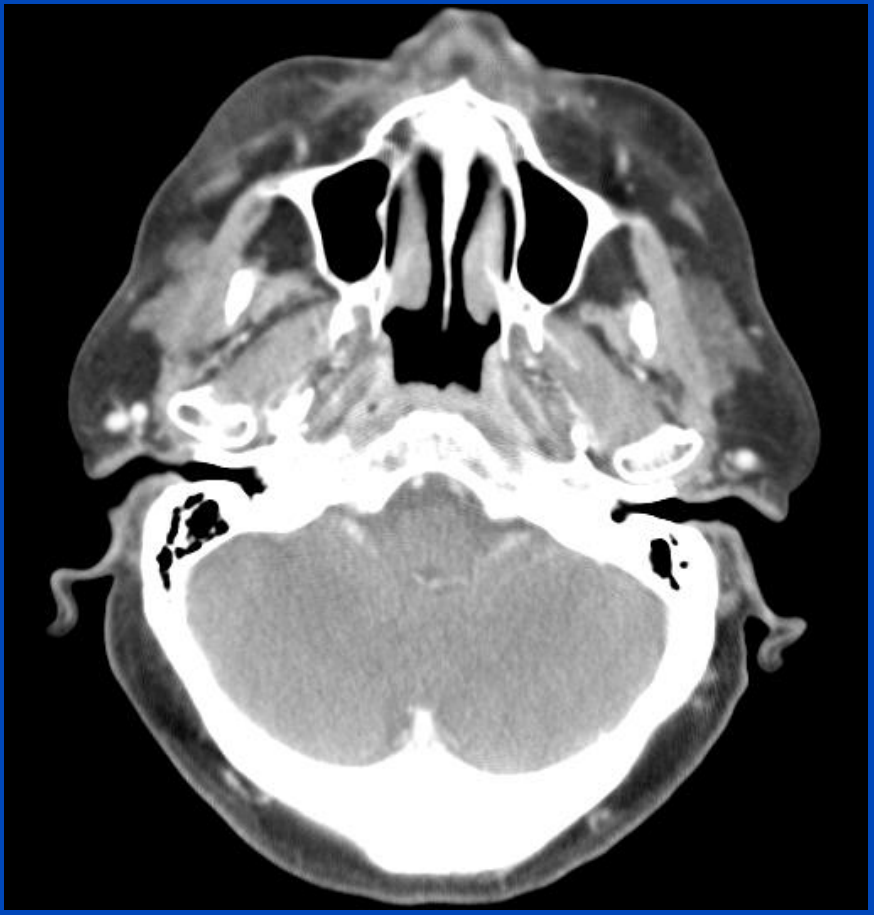

# What’s so Nice about Spiral CT?

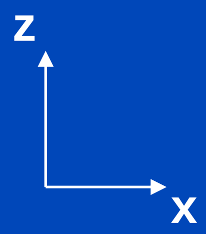


*S* = 3 mm, *RI* = 3 mm

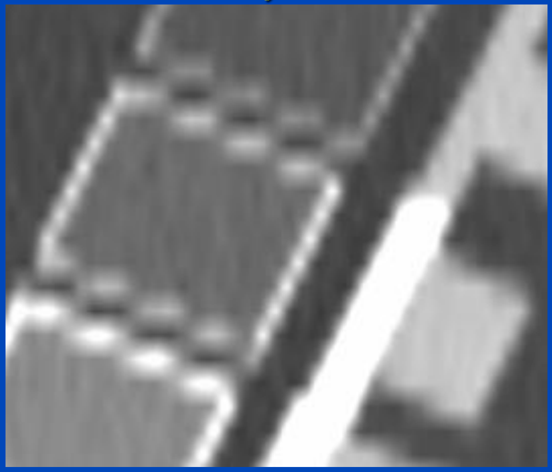

*S* = 3 mm, *RI* = 1 mm

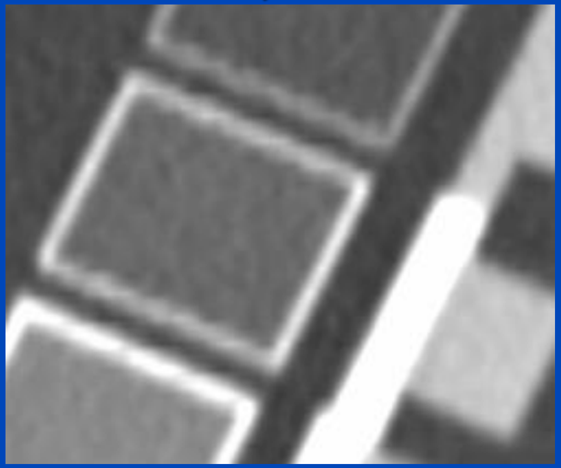

MPR images of the European Spine Phantom (inclined at 25°).

Kalender WA, Polacin A, Süß C. Radiology 1994; 193:170-171

# Sampling Artifact

$S_{eff}$ = 3 mm, $RI$ = 3 mm

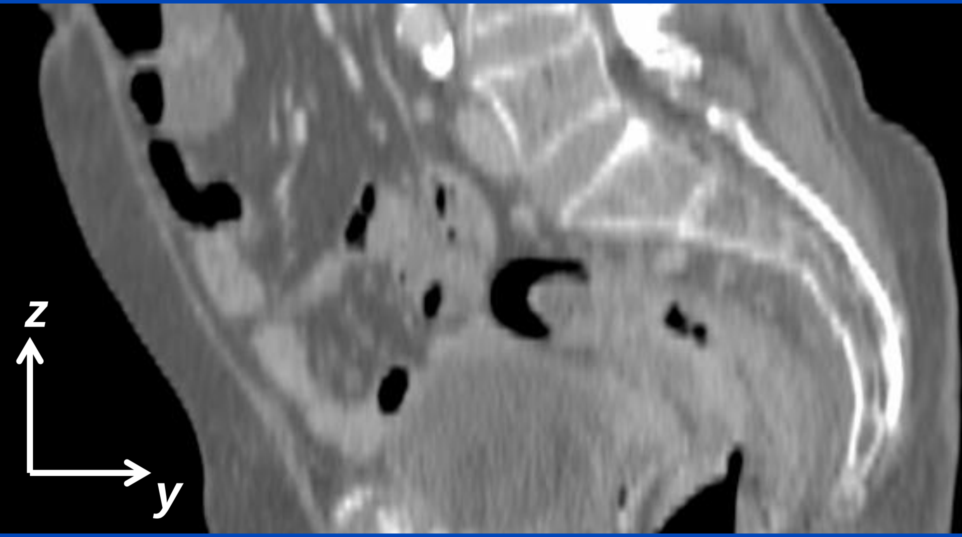


$S_{eff}$ = 3 mm, $RI$ = 1 mm

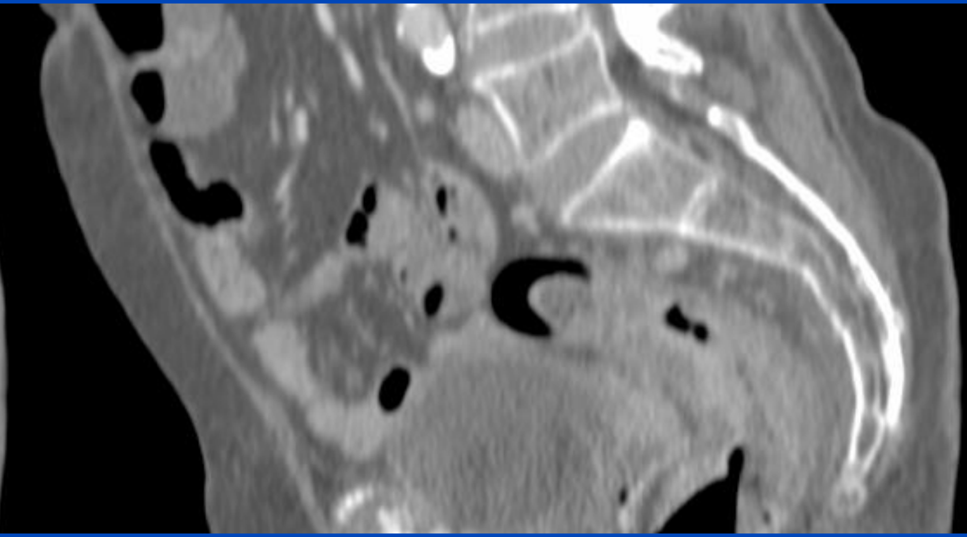

**Always perform overlapping recons!**

$C$ = 0 HU, $W$ = 800 HU

# The Pitch Value is the Measure for Scan Overlap

**The pitch is defined as the ratio of the table increment per full rotation to the *total* collimation width in the center of rotation:**

$$p = \frac{d}{M \cdot S}$$

Recommended by and in:

***IEC, International Electrotechnical Commision: Medical electrical equipment – 60601 Part 2-44: Particular requirements for the safety of x-ray equipment for computed tomography. Geneva, Switzerland, 1999.***

**Examples:**

- $p$=1/3=0.333 means that each z-position is covered by 3 rotations (3-fold overlap)
- $p$=1 means that the acquisition is not overlapping
- $p=p_{max}$ means that each z-position is covered by half a rotation

# Multi-Threaded CT Scanners and Dual-Source-CT

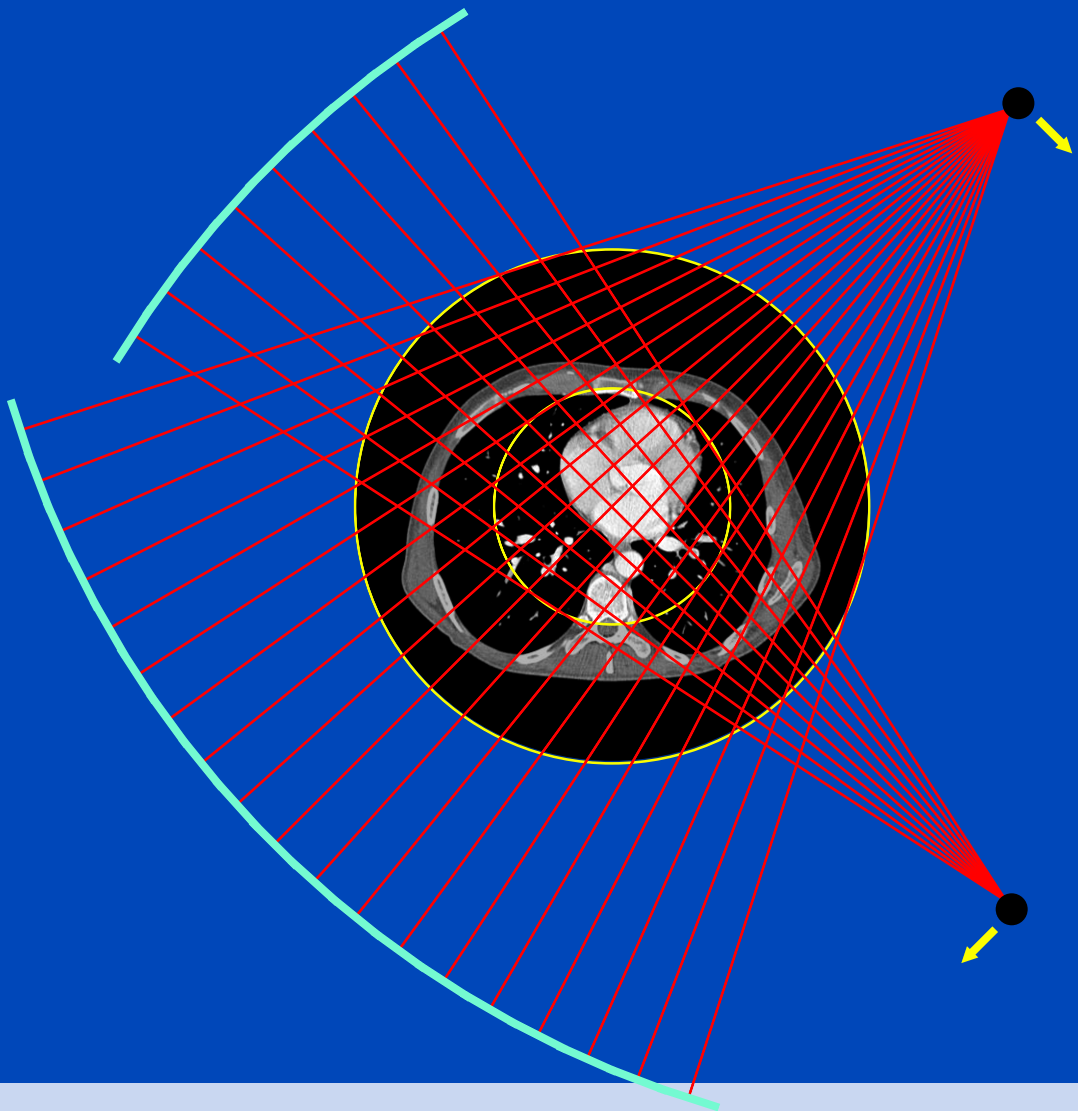


**Siemens SOMATOM Force**
**dual source cone-beam spiral CT**

# Dual Source CT =
# Best Possible Cardiac CT

- **Extremely high temporal resolution**
- **Nearly free of motion artifacts**

dual source CT, 330 ms rotation,
partial scan reconstruction, 83 ms temporal resolution

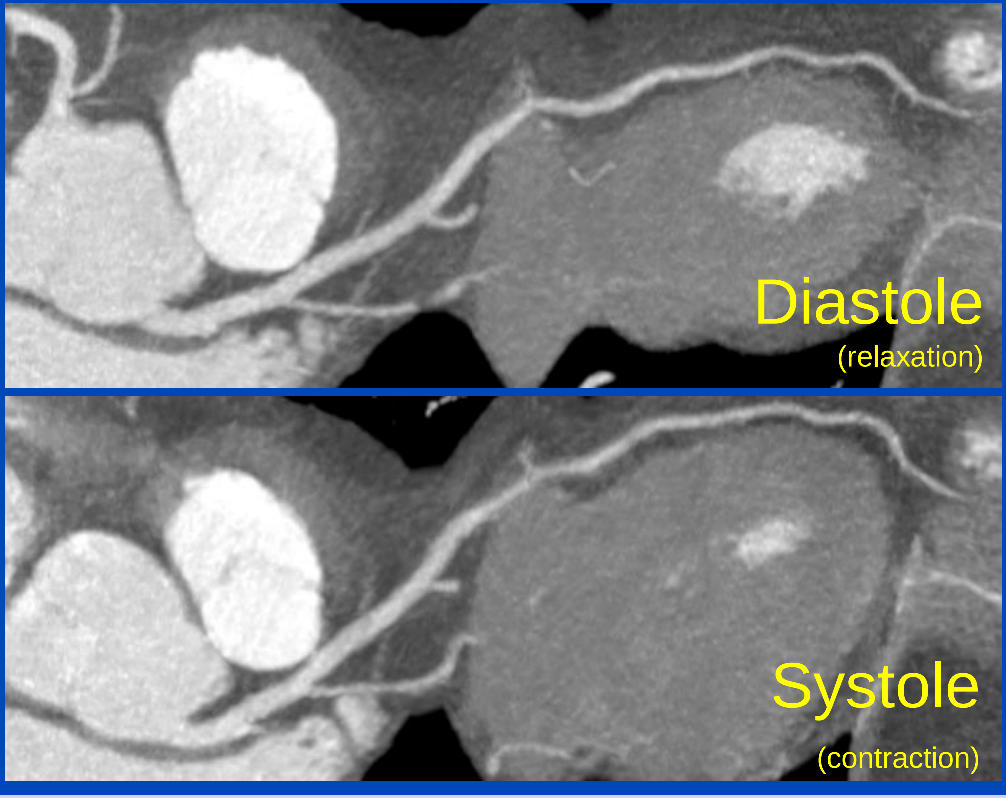


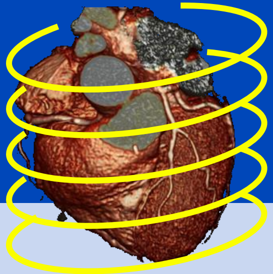

Data courtesy of Stephan Achenbach

# Dual Source CT =
# Best Possible Dual Energy CT

- Tube currents can be selected and modulated for each thread independently
- Prefiltration can be optimized for each thread independently
- Optimal sampling

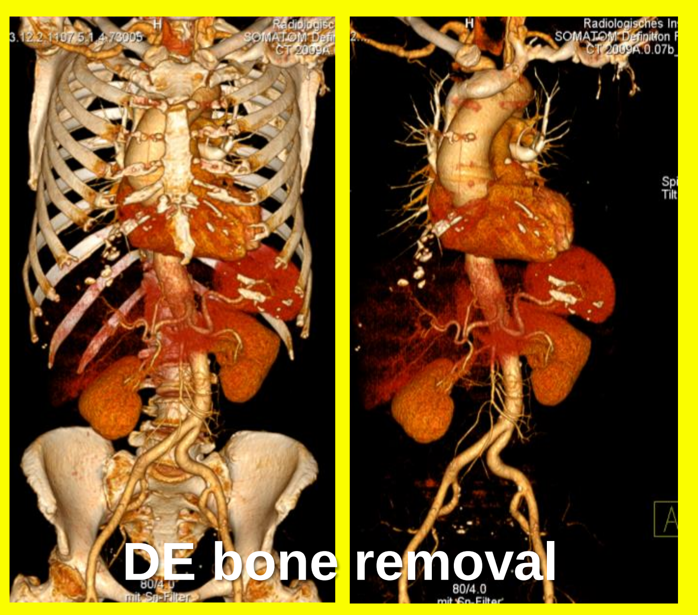


Single DECT Scan

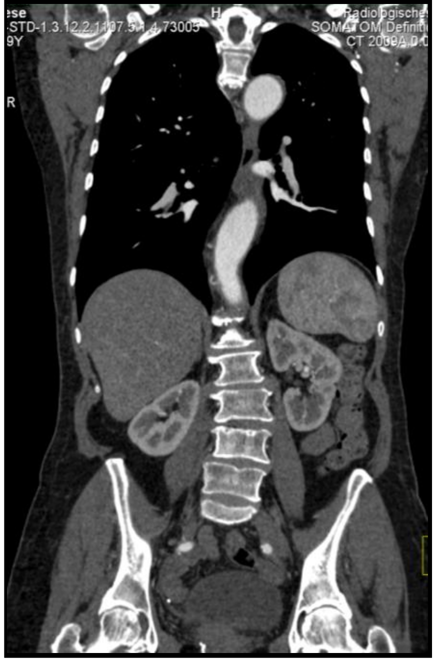

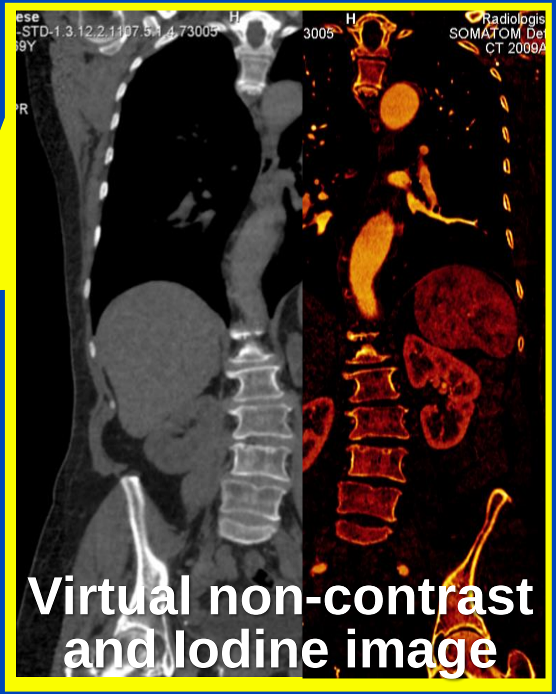


**Dual Energy whole body CTA: 100/140 Sn kV @ 0.6mm**

# Prefilters

## Narrow Cone = High Tube Power

## Wide Cone = Low Tube Power

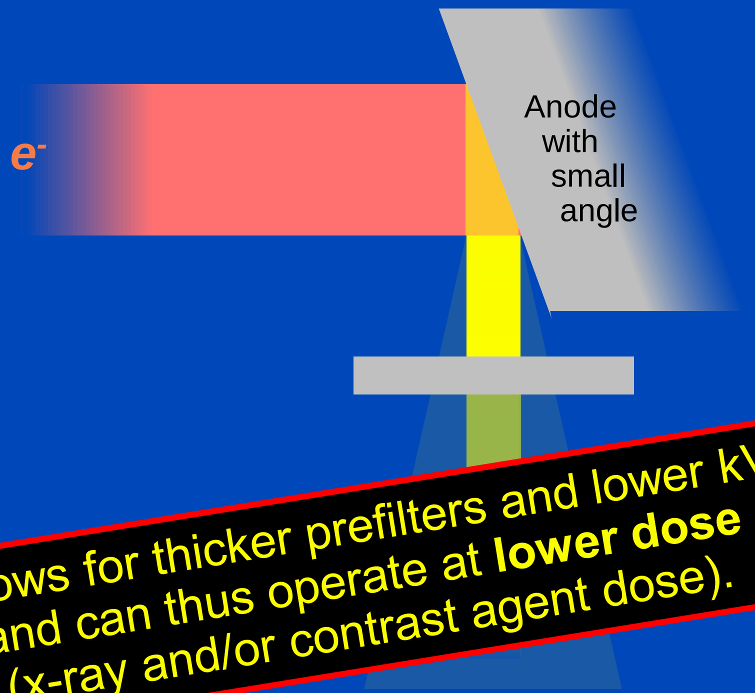


Allows for thicker prefilters and lower kV and can thus operate at **lower dose** (x-ray and/or contrast agent dose).

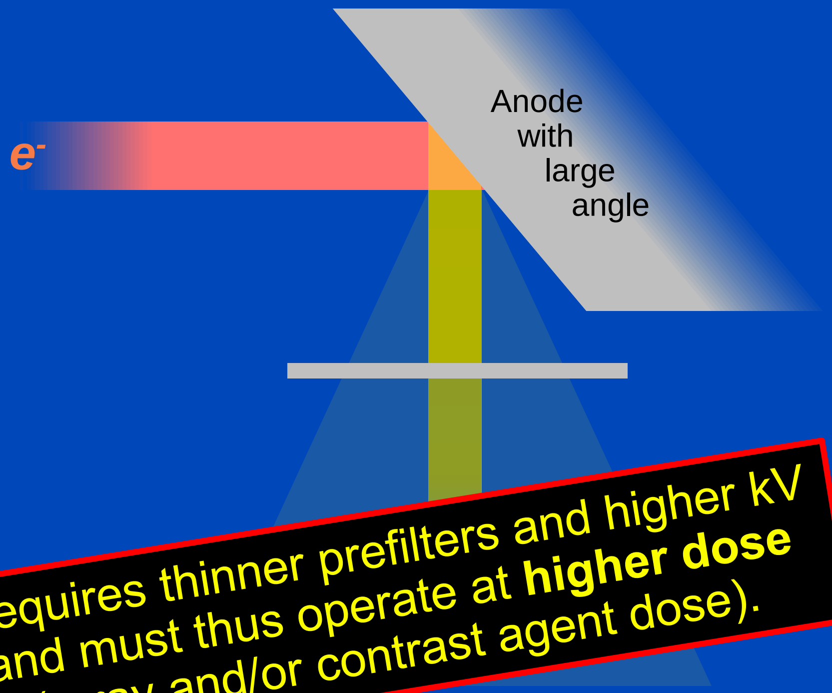


Requires thinner prefilters and higher kV and must thus operate at **higher dose** (x-ray and/or contrast agent dose).

## … at the same spatial resolution

**Onset of target melting (rule of thumb)[1]: 1 W/µm**

[1] D.E. Grider, A. Writh, and P.K. Ausburn. Electron Beam Melting in Microfocus X-Ray Tubes. J. Phys. D: Appl. Phys 19:2281-2292, 1986

dkfz.

## LUNG CANCER SCREENING CT (selected SIEMENS scanners, continued)

(Back to INDEX)

**TOPOGRAM:** PA; scan from top of shoulder through mid-liver.

| SIEMENS | Definition DS (Dual source 64-slice) | Somatom Drive (Dual source 128-slice) | Definition Flash (Dual source 128-slice) | Definition Force (Dual source 192-slice) |
|---|---|---|---|---|
| Software version | VA44 | VB10 | VB10 | VB10 |
| Scan Mode | Spiral | Spiral | Spiral | Spiral |
| Rotation Time (s) | 0.5 | 0.5 | 0.5 | 0.5 |
| Detector Configuration | *64 × 0.6 mm (32 x 0.6 mm =19.2 mm) | *128 × 0.6 mm (64 x 0.6 mm = 38.4 mm) | *128 × 0.6 mm (64 x 0.6 mm = 38.4 mm) | *192 × 0.6 mm (96 x 0.6 mm = 57.6 mm) |
| Pitch | 1.2 | 1.2 | 1.2 | 1.2 |
| kV | 120 | 100Sn (0.4 mm) | 120 | 100Sn (0.6 mm) |
| Quality ref. mAs | 20 | 81 | 20 | 101 |
| CARE Dose4D | ON | ON | ON | ON |
| CARE kV | ON | ON | ON | ON |
| CTDIvol*** | 1.4 mGy | 0.6mGy | 1.3 mGy | 0.4 mGy |

**RECON 1**

| | | | | |
|---|---|---|---|---|
| Type | Axial | Axial | Axial | Axial |
| Kernel | B31f | Bf37, strength = 3** | Bf37, strength = 3** | Br40, strength = 3** |
| Slice (mm) | 5.0 | 5.0 | 5.0 | 5.0 |
| Increment (mm) | 5.0 | 5.0 | 5.0 | 5.0 |

# → thicker prefilter means less dose

# Dose Reduction by Patient-Specific Tin or Copper Prefilters[1,2]
# 1000 mAs Limit, 70-150 kV, 10 kV steps

| | **Child**<br>(15 cm × 10 cm)  | **Adult**<br>(30 cm × 20 cm)  | **Obese**<br>(50 cm × 40 cm) 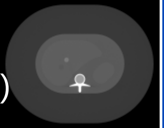 |
|---|---|---|---|
| **Soft tissue (basis)** | 30 mAs, 90 kV | 100 mAs, 130 kV | 600 mAs, 150 kV |
| **Soft tissue, Sn** | 0.6 mm, 1000 mAs, 80 kV<br>**14%** → 19% | 1.0 mm, 1000 mAs, 120 kV<br>**32%** → 36% | 0.2 mm, 870 mAs, 150 kV<br>**25%** → 57% |
| **Soft tissue, Cu** | 1.6 mm, 1000 mAs, 70 kV<br>**17%** → 19% | 3.1 mm, 1000 mAs, 120 kV<br>**31%** → 36% | 0.8 mm, 1000 mAs, 150 kV<br>**29%** → 57% |
| **Iodine (basis)** | 50 mAs, 70 kV | 120 mAs, 90 kV | 720 mAs, 120 kV |
| **Iodine, Sn** | 0 mm, 50 mAs, 70 kV<br>**0%** | 0.1 mm, 1000 mAs, 70 kV<br>**40%** | 0.0 mm, 1000 mAs, 110 kV<br>**26%** → 79% |
| **Iodine, Cu** | 0.1 mm, 58 mAs, 70 kV<br>**3%** | 0.4 mm, 1000 mAs, 70 kV<br>**44%** | 0.1 mm, 1000 mAs, 110 kV<br>**28%** → 80% |

[1]Steidel, Maier, Sawall, Kachelrieß. Tin or Copper Prefilters for Dose Reduction in Diagnostic Single Energy CT? RSNA 2020.
[2]Steidel, Maier, Sawall, Kachelrieß. Dose Reduction through Patient-Specific Prefilters in Diagnostic Single Energy CT. RSNA 2020.

dkfz.

# Dose Reduction by Patient-Specific Tin or Copper Prefilters 1000 mAs Limit

I: $Z = 53$, $E_K = 33$ keV
Hf: $Z = 72$, $E_K = 65$ keV
(same no. of atoms / voxel)

| | Child (15 cm × 10 cm)  | Adult (30 cm × 20 cm)  | Obese (50 cm × 40 cm)  |
|---|---|---|---|
| **Soft tissue (basis)** | 30 mAs, 90 kV | 100 mAs, 130 kV | 600 mAs, 150 kV |
| **Soft tissue, Sn** | 0.6 mm, 1000 mAs, 75 kV **15%** → 19% | 1.0 mm, 1000 mAs, 120 kV **32%** → 36% | 0.2 mm, 1000 mAs, 150 kV **25%** → 57% |
| **Soft tissue, Cu** | 1.6 mm, 1000 mAs, 70 kV **17%** → 19% | 3.4 mm, 1000 mAs, 125 kV **31%** → 36% | 0.8 mm, 1000 mAs, 150 kV **29%** → 57% |
| **Iodine (basis)** | 50 mAs, 70 kV | 120 mAs, 90 kV | 720 mAs, 120 kV |
| **Iodine, Sn** | 0 mm, 210 mAs, 50 kV **39%** | 0.1 mm, 1000 mAs, 70 kV **40%** → 53% | 0.0 mm, 1000 mAs, 105 kV **39%** → 81% |
| **Iodine, Cu** | 0.4 mm, 1000 mAs, 50 kV **57%** → 67% | 0.2 mm, 1000 mAs, 65 kV **49%** → 68% | 0.0 mm, 1000 mAs, 105 kV **39%** → 89% |
| **Hafnium, no filter** | 0.0 mm, 25 mAs, 100 kV **-29%** | 0.0 mm, 100 mAs, 100 kV **55%** | 0.0 mm, 860 mAs, 115 kV **80%** |
| **Hafnium, Sn** | 1.0 mm, 1000 mAs, 85 kV **48%** → 60% | 0.7 mm, 1000 mAs, 95 kV **82%** → 88% | 0.1 mm, 1000 mAs, 120 kV **85%** → 95% |
| **Hafnium, Cu** | 3.3 mm, 1000 mAs, 85 kV **43%** → 60% | 2.3 mm, 1000 mAs, 95 kV **79%** → 88% | 0.3 mm, 1000 mAs, 120 kV **83%** → 95% |

[1]Steidel, Maier, Sawall, Kachelrieß. Tin or Copper Prefilters for Dose Reduction in Diagnostic Single Energy CT? RSNA 2020.
[2]Steidel, Maier, Sawall, Kachelrieß. Dose Reduction through Patient-Specific Prefilters in Diagnostic Single Energy CT. RSNA 2020.

dkfz.

# Ag, Cu, Sn: X-ray Absorption Properties

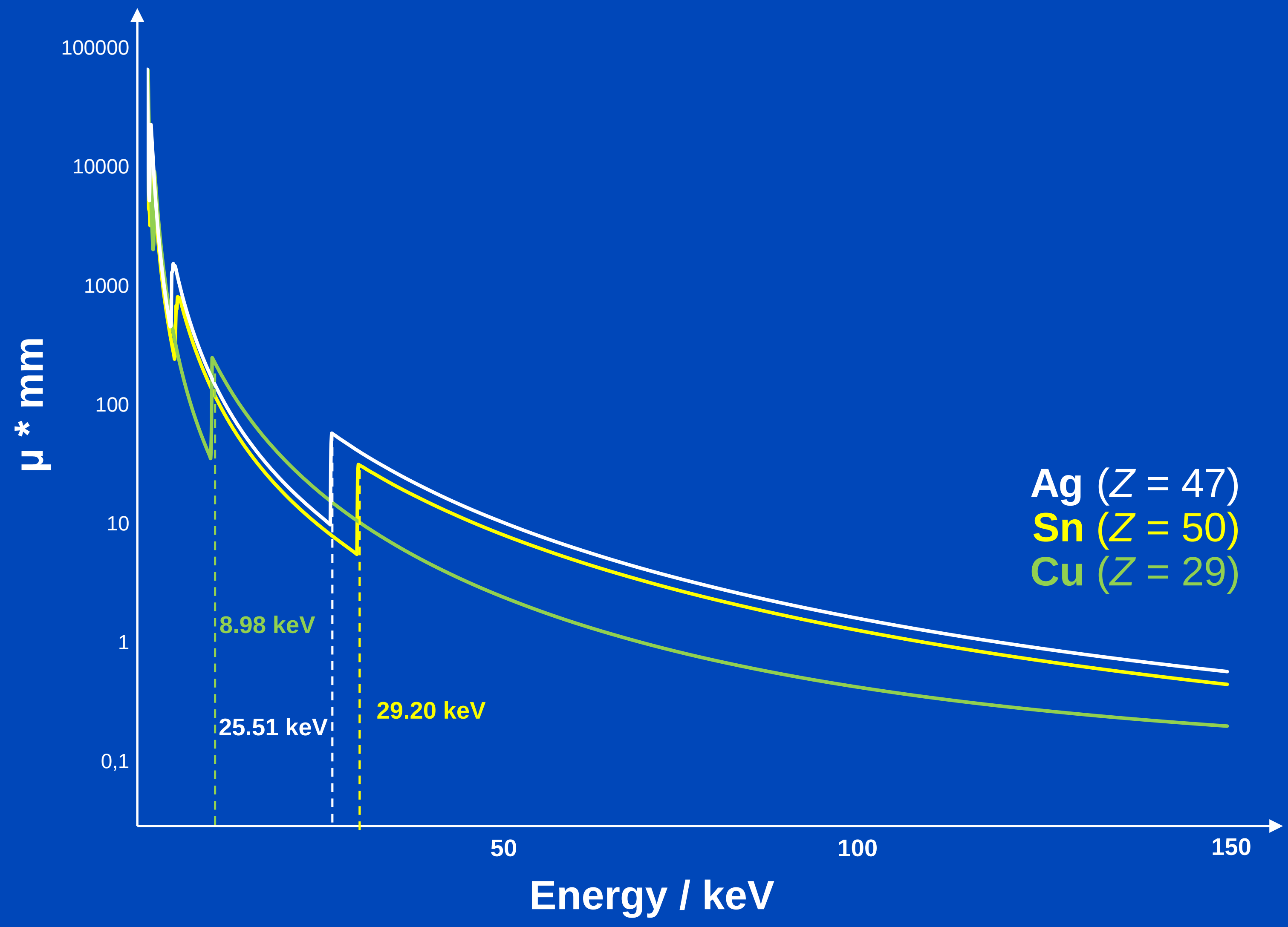

# Ag, Cu, Sn: Comparable Thicknesses?

- How do the thicknesses of Ag, Cu and Sn, if used as a prefilter, compare?
- Method
  - Tucker spectrum filtered by 6 mm Al + additional Ag/Cu/Sn prefilter passing through a 32 cm water layer
  - Determine filter thickness to match the signal in a 1.4 mm thick GOS energy integrating detector
- Results:
  - In the energy range of clinical CT and with objects similar to patients we find that 0.5 mm Ag ≈ 0.6 mm Sn ≈ 2.0 mm Cu
  - This assumes that the behaviour at energies close to the k-edges is irrelevant.
  - Thus, Ag and Sn cannot be used to reduce the dose for applications with iodine contrast enhancement (k-edge of iodine very close to the k-edge of Ag and Sn).

# Prefilters

- **We want**
  - a filter changer with, say, 10 different filters, or a sliding double wedge
  - tubes with much higher power and lower kV
  - to always operate the tube close to its power limit
  - to adjust the filter thickness and kV to the patient
  - automatic exposure control (AEC) to include such filter options

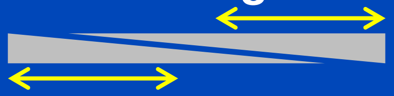

- **We get**
  - a significant dose reduction
  - improved image quality

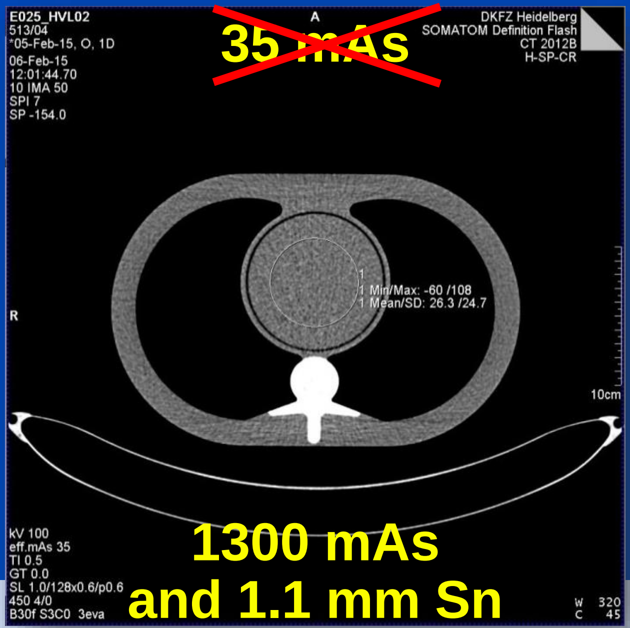


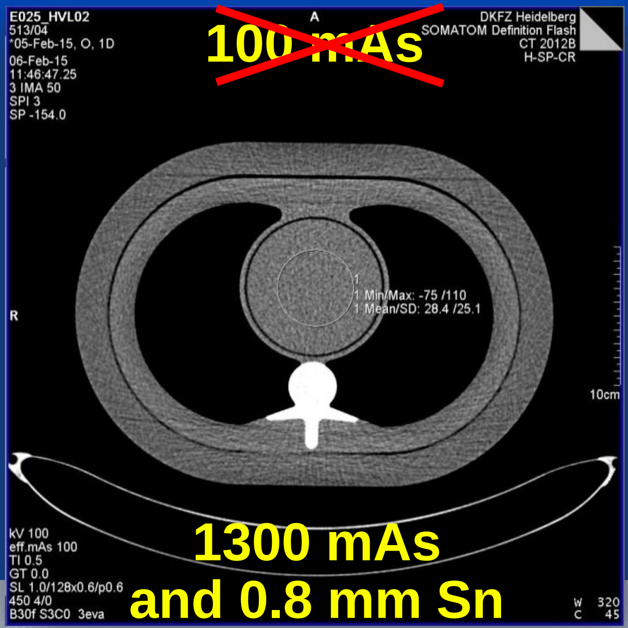


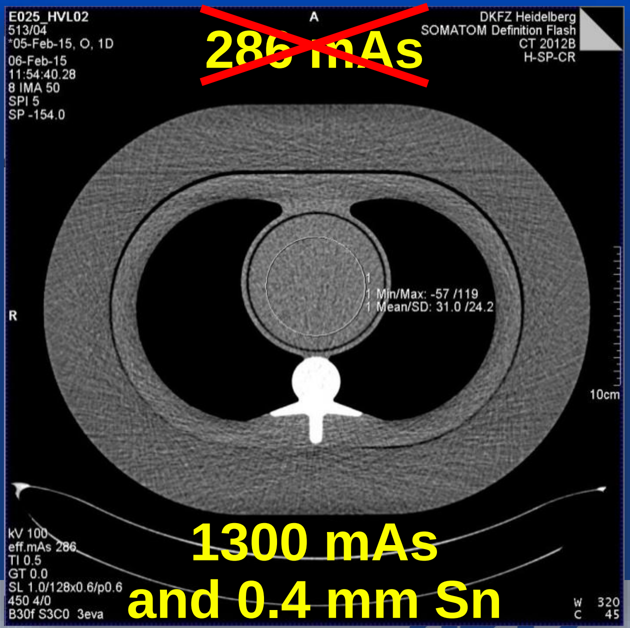

# Dynamic Bowtie Filters

# Bowtie Filter

- Also known as shaped filter or as form filter
- Static filter to optimize the intensity profile through a rotationally symmetric isocentered object $\mu(r)$ of typical shape, e.g. a disk
- Often optimized to either
  - be good for the detector, i.e. to yield a constant signal (e.g. energy-weighted intensity) at the detector,
  - or to be good for the patient[1], i.e. to yield the minimal patient dose at given image quality.

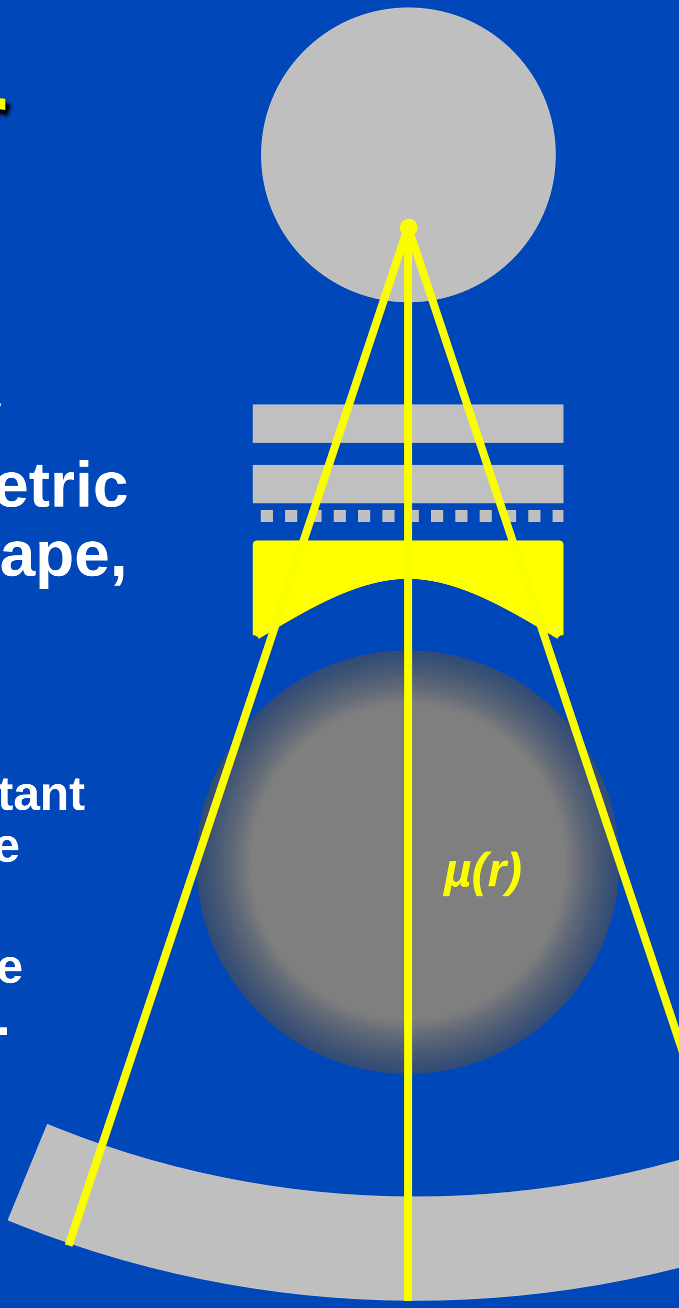


Figure not drawn to scale.

[1]Michael D. Harpen. A simple theorem relating noise and patient dose in computed tomography. Med. Phys. 26(11):2231-2234, November 1999

# Bowtie Filter

$$p(\xi) = \mathsf{R}\mu(r)$$

- **Good for the detector:**
  - **Radiation incident on the detector:** $I(\xi) = I_0(\xi)e^{-p(\xi)} = c$
  - **Radiation incident on the object:** $I_0(\xi) = c\, e^{p(\xi)}$
  - **Required form filter thickness:** $d(\xi) = d_0 - p(\xi)/\mu_{\text{bowtie}}$
- **Good for the patient:**
  - **Minimal noise at constant dose:** $\int d\xi \left(\sigma^2(\xi) + \lambda I_0(\xi)\right)$ **with** $\sigma^2(\xi) = \dfrac{e^{p(\xi)}}{I_0(\xi)}$
  - **Radiation incident on the object:** $I_0^2(\xi) = c\, e^{p(\xi)}$
  - **Required form filter thickness[1]:** $d(\xi) = d_0 - \frac{1}{2}p(\xi)/\mu_{\text{bowtie}}$

[1]Michael D. Harpen. A simple theorem relating noise and patient dose in computed tomography. Med. Phys. 26(11):2231-2234, November 1999

# Dynamic Bow Tie Filters

- Wedges[1]
- Fluid[2]
- Sheet-based[3]
- Multiple aperature devices[4]
- …

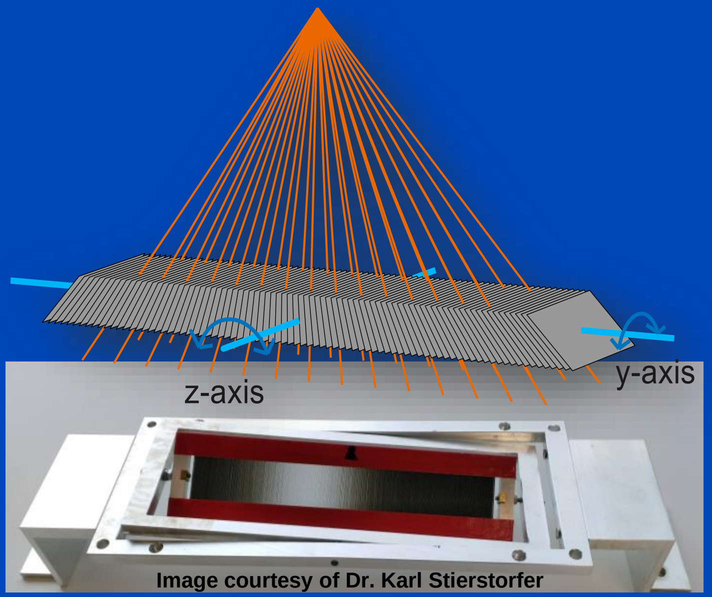


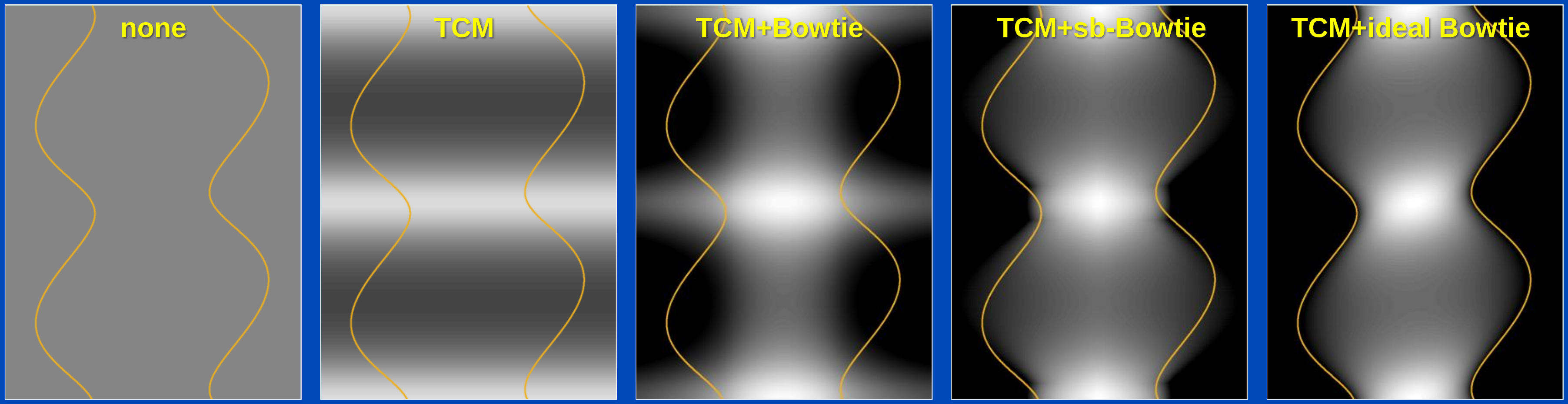


[1]Hsieh, Pelc. The Feasibility of a Piecewise-Linear Dynamic Bowtie Filter. MedPhys 2013
[2]Shunhavanich, Hsieh, Pelc. Fluid-filled Dynamic Bowtie Filter: Description and Comparison with other Modulators. MedPhys 2018
[3]Huck, Parodi, Stierstorfer. First Experimental Validation of a Novel Concept for Dynamic Beam Attenuation in CT. CT-Meeting 2018 and SPIE MI 2019
[4]Gang, Stayman et al. Dynamic Fluence Field Modulation in Computed Tomography using Multiple Aperture Devices. PMB 2019

# Risk-Specific TCM

# Patient Risk-Minimizing Tube Current Modulation

## 1. Coarse reconstruction from two scout views

– E.g. X. Ying, et al. X2CT-GAN: Reconstructing CT from biplanar x-rays with generative adversarial networks. CVPR 2019.

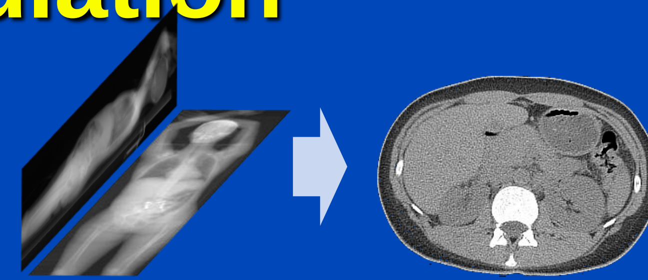

## 2. Segmentation of radiation-sensitive organs

– E.g. S. Chen, M. Kachelrieß et al., Automatic multi-organ segmentation in dual-energy CT (DECT) with dedicated 3D fully convolutional DECT networks. Med. Phys. 2019.

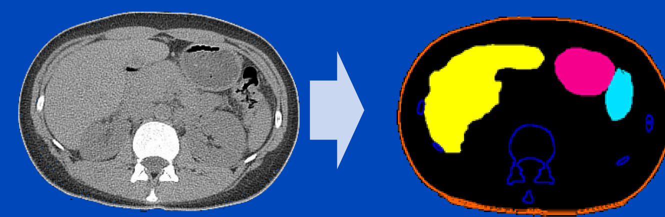

## 3. Calculation of the effective dose per view using the deep dose estimation (DDE)

– J. Maier, E. Eulig, S. Dorn, S. Sawall and M. Kachelrieß. Real-time patient-specific CT dose estimation using a deep convolutional neural network. IEEE Medical Imaging Conference Record, M-03-178: 3 pages, Nov. 2018.

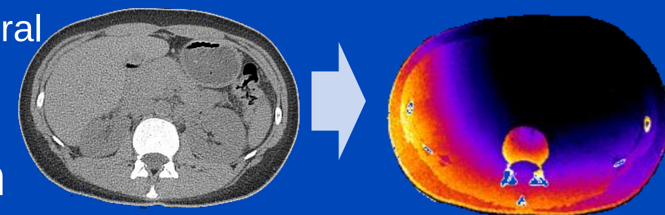

## 4. Determination of the tube current modulation curve that minimizes the radiation risk

– L. Klein, C. Liu, J. Steidel, L. Enzmann, M. Knaup, S. Sawall, A. Maier, M. Lell, J. Maier, and M. Kachelrieß. Patient-specific radiation risk-based tube current modulation for diagnostic CT. Med. Phys. 49(7):4391-4403, July 2022.

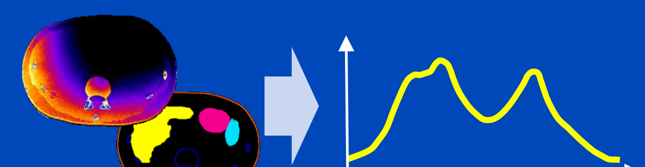


[1]L. Klein, C. Liu, J. Steidel, L. Enzmann, M. Knaup, S. Sawall, A. Maier, M. Lell, J. Maier, and M. Kachelrieß. Patient-specific radiation risk-based tube current modulation for diagnostic CT. Med. Phys. 49(7):4391-4403, July 2022.

dkfz.

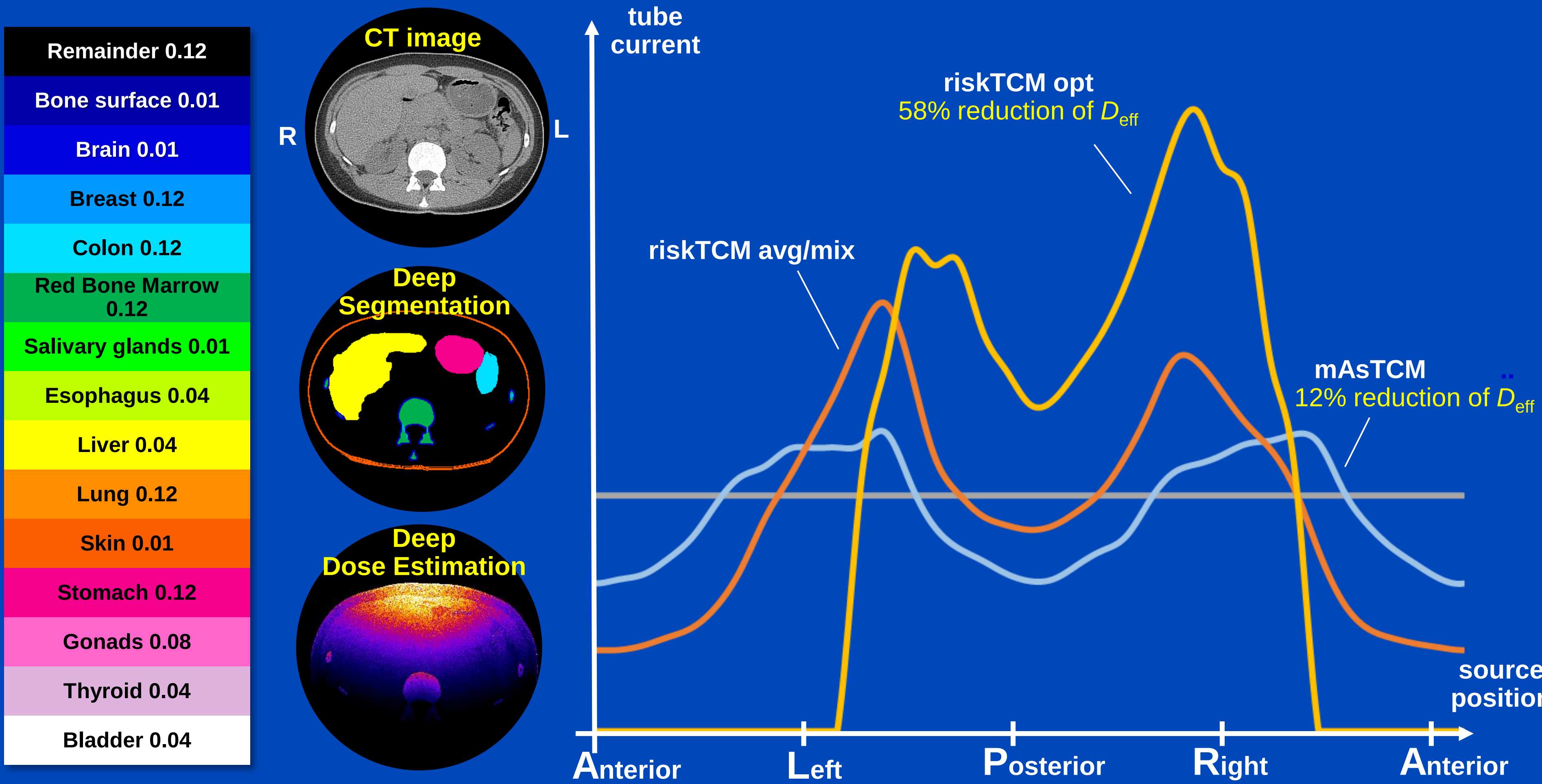


[1]L. Klein, C. Liu, J. Steidel, L. Enzmann, M. Knaup, S. Sawall, A. Maier, M. Lell, J. Maier, and M. Kachelrieß.
Patient-specific radiation risk-based tube current modulation for diagnostic CT. Med. Phys. 49(7):4391-4403, July 2022.

# Patient 03 - Neck

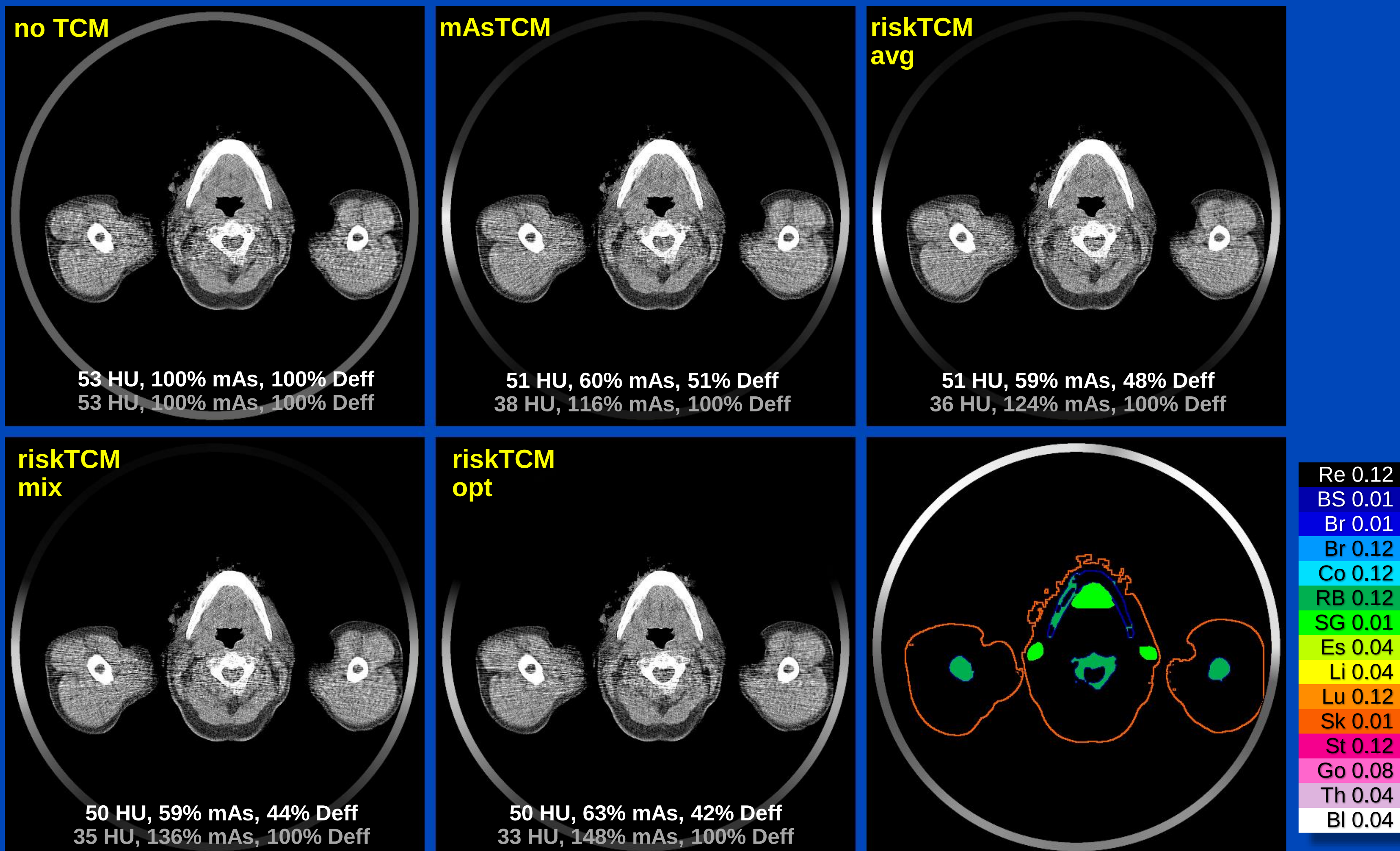


$C$ = 25 HU, $W$ = 400 HU

[1]L. Klein, C. Liu, J. Steidel, L. Enzmann, M. Knaup, S. Sawall, A. Maier, M. Lell, J. Maier, and M. Kachelrieß. Patient-specific radiation risk-based tube current modulation for diagnostic CT. Med. Phys. 49(7):4391-4403, July 2022.

# Patient 03 - Pelvis

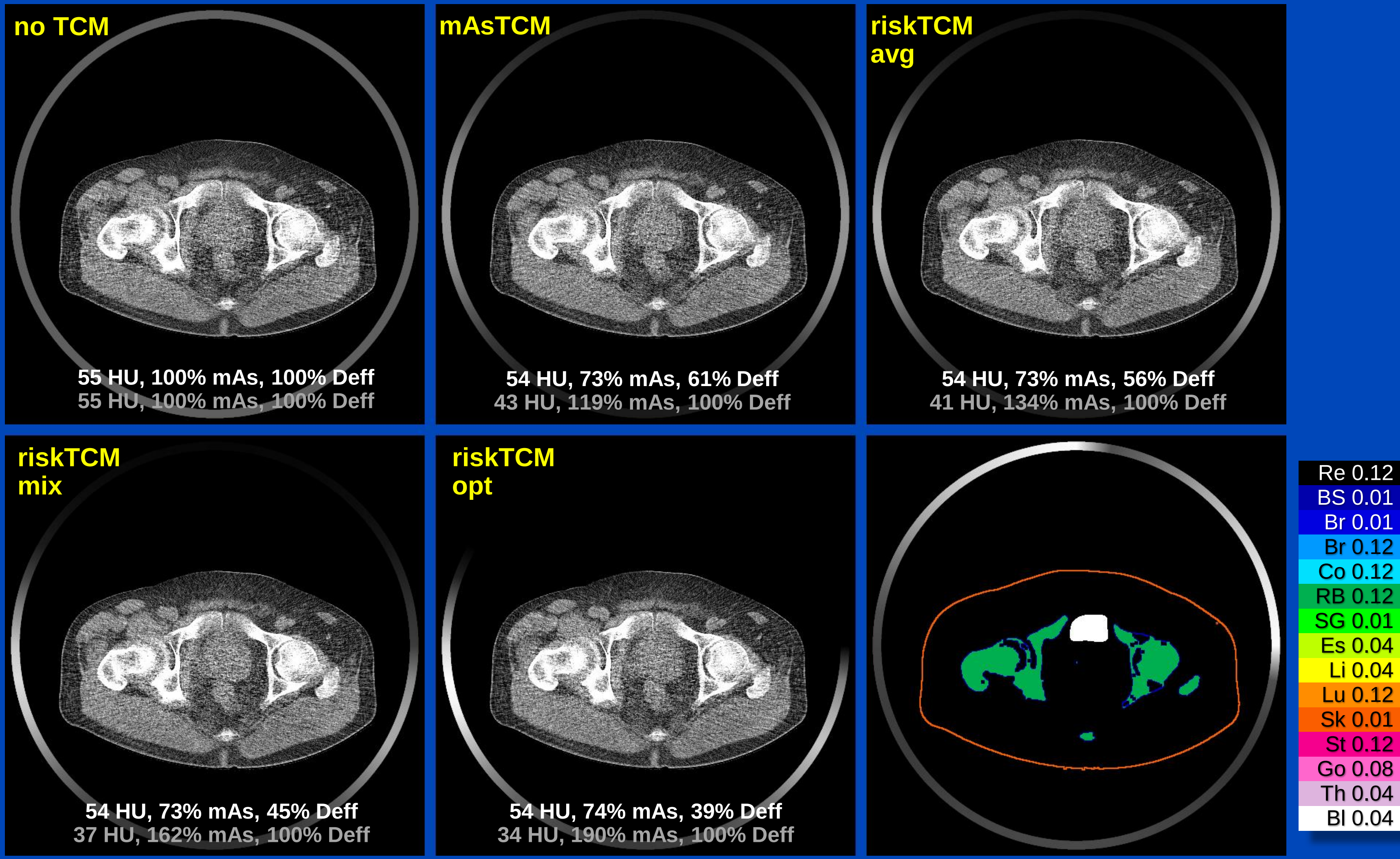


*C* = 25 HU, *W* = 400 HU

[1]L. Klein, C. Liu, J. Steidel, L. Enzmann, M. Knaup, S. Sawall, A. Maier, M. Lell, J. Maier, and M. Kachelrieß. Patient-specific radiation risk-based tube current modulation for diagnostic CT. Med. Phys. 49(7):4391-4403, July 2022.

# Patient 04 - Abdomen

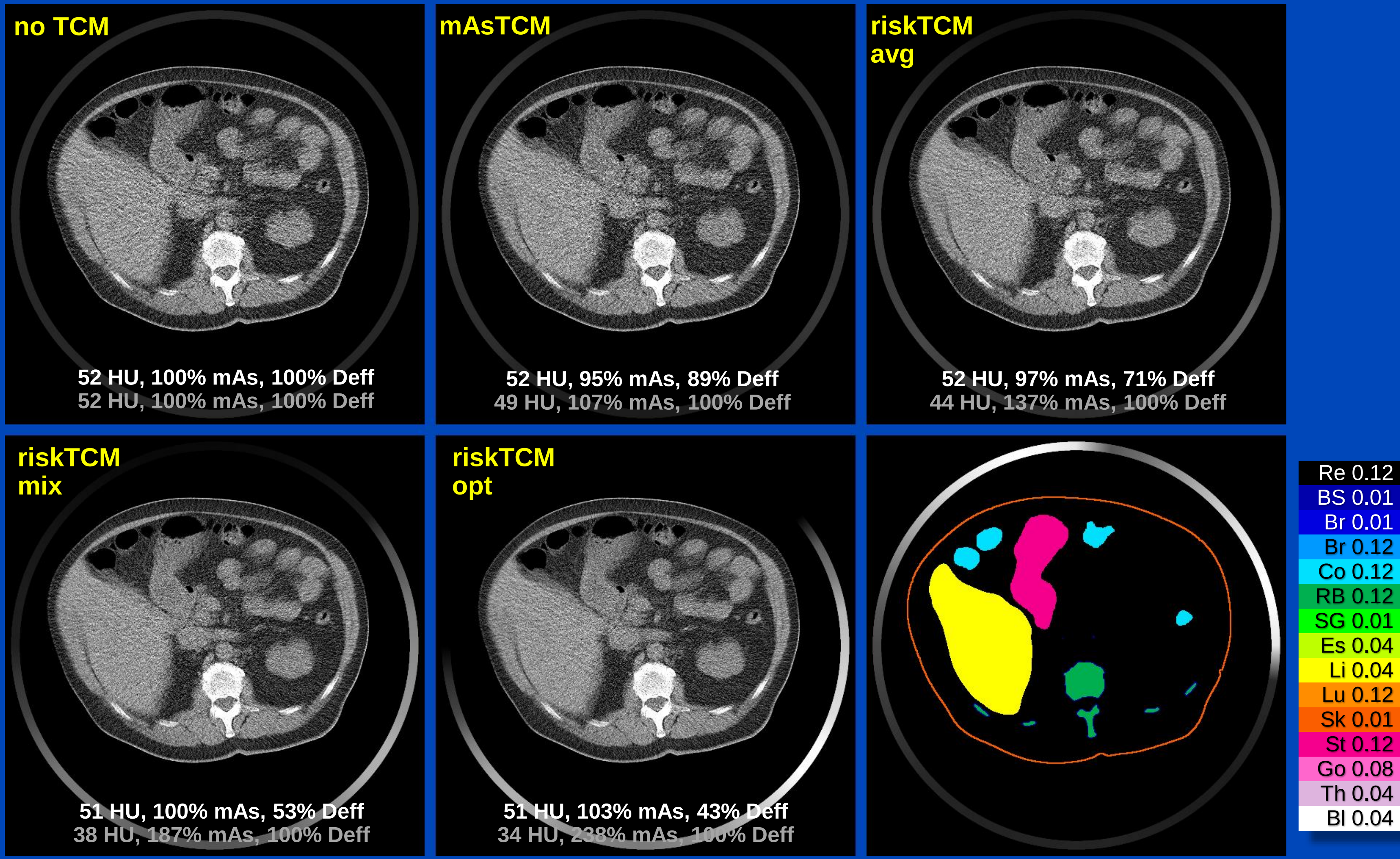


*C* = 25 HU, *W* = 400 HU

[1]L. Klein, C. Liu, J. Steidel, L. Enzmann, M. Knaup, S. Sawall, A. Maier, M. Lell, J. Maier, and M. Kachelrieß.
Patient-specific radiation risk-based tube current modulation for diagnostic CT. Med. Phys. 49(7):4391-4403, July 2022.

| | noTCM | mAsTCM | riskTCM |
|---|---|---|---|
| Head w Arms: | | | |
| 01 | 167% | 100% | 98% |
| 02 | 156% | 100% | 85% |
| 03 | 168% | 100% | 91% |
| 04 | 145% | 100% | 89% |
| Average | (159±11)% | 100% | (91±6)% |
| Head w/o Arms: | | | |
| 01 | 100% | 100% | 90% |
| 02 | 121% | 100% | 88% |
| 03 | 107% | 100% | 93% |
| 04 | 110% | 100% | 92% |
| Average | (110±9)% | 100% | (91±2)% |
| Thorax: | | | |
| 32no | 132% | 100% | 67% |
| 33ko | 112% | 100% | 80% |
| 40mm | 116% | 100% | 81% |
| 42mo | 115% | 100% | 75% |
| 54km | 112% | 100% | 80% |
| 66nm | 111% | 100% | 81% |
| 63mo | 115% | 100% | 76% |
| Average | (116±7)% | 100% | (77±5)% |
| Abdomen: | | | |
| 32no | 127% | 100% | 78% |
| 33ko | 102% | 100% | 90% |
| 40mm | 108% | 100% | 84% |
| 42mo | 115% | 100% | 75% |
| 54km | 103% | 100% | 75% |
| 66nm | 102% | 100% | 64% |
| 63mo | 110% | 100% | 69% |
| Average | (109±9)% | 100% | (77±9)% |
| Pelvis: | | | |
| 32no | 133% | 100% | 93% |
| 42mo | 135% | 100% | 81% |
| 63mo | 139% | 100% | 89% |
| Average | (136±2)% | 100% | (88±6)% |

[1]L. Klein, C. Liu, J. Steidel, L. Enzmann, M. Knaup, S. Sawall, A. Maier, M. Lell, J. Maier, and M. Kachelrieß.
Patient-specific radiation risk-based tube current modulation for diagnostic CT. Med. Phys. 49(7):4391-4403, July 2022.

# Conclusions on RiskTCM

- Risk-specific TCM minimizes the patient risk.
- With $D_{eff}$ as a risk model riskTCM can reduce risk by up to 30%, compared with the gold standard mAsTCM.
- Other risk models, in particular age-, weight- and sex-specific models, can be used with riskTCM as well.
- Note:
  - …
  - … good for the patient
  - detector flux equalizing TCM = good for the detector

**It is up to the vendors to take action!**

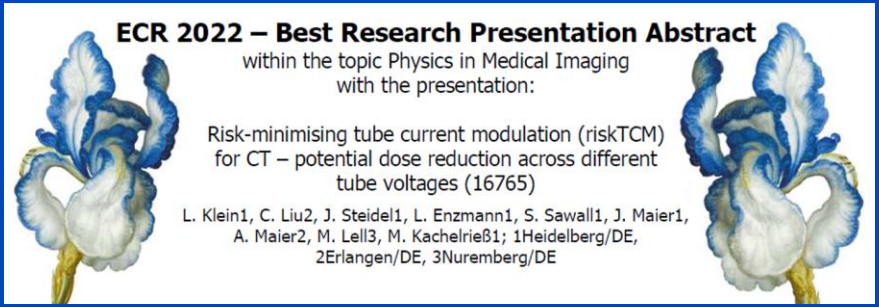


[1]L. Klein, C. Liu, J. Steidel, L. Enzmann, M. Knaup, S. Sawall, A. Maier, M. Lell, J. Maier, and M. Kachelrieß. Patient-specific radiation risk-based tube current modulation for diagnostic CT. Med. Phys. 49(7):4391-4403, July 2022.

# riskTCM vs. Breast-Specific TCM

- osTCM mimics X-Care (Siemens Healthineers)
- Reduces the tube current to 25% for the anterior 120°
- Higher tube current for the remaining 240°

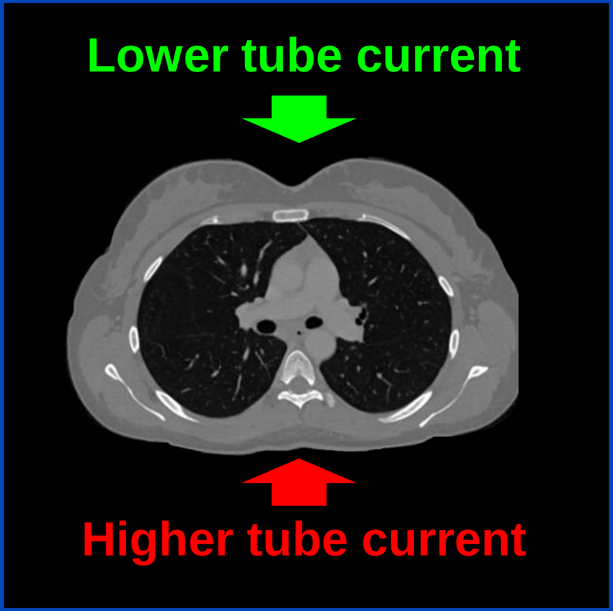


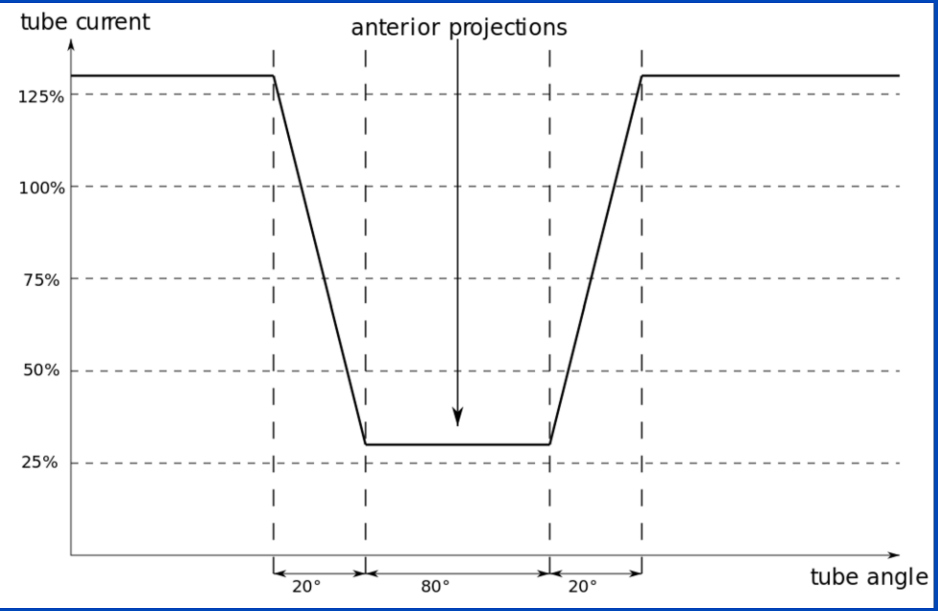


D. Ketelsen et al. Automated computed tomography dosesaving algorithm to protect radiosensitive tissues: estimation of radiation exposure and image quality considerations. Invest Radiol, 47(2):148–52, 2012

# Results

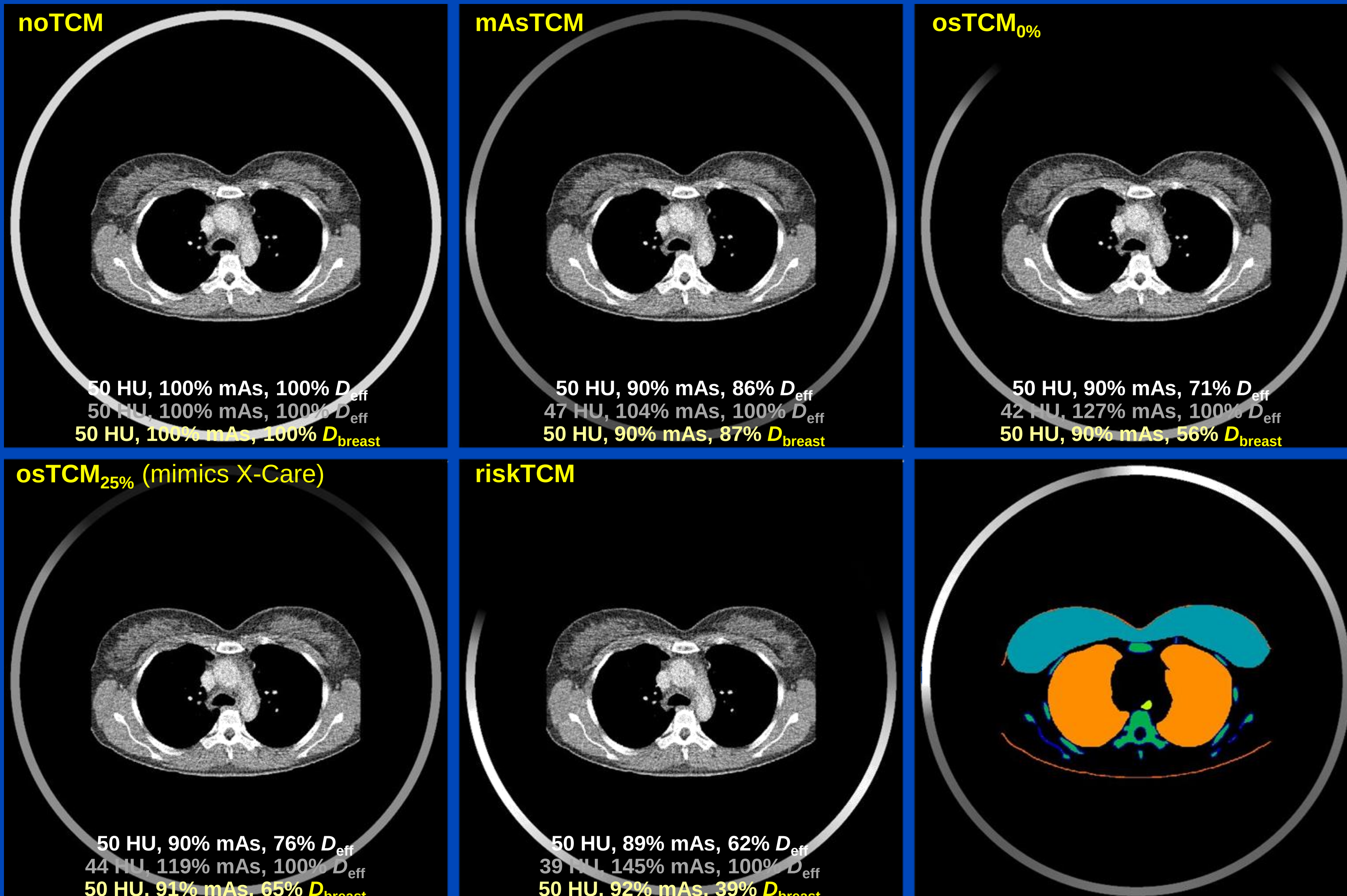


**Data courtesy of Prof. Lell, Nürnberg. $C$ = 25 HU, $W$ = 400 HU**

L. Klein, L. Enzmann, A. Byl, C. Liu, S. Sawall, A. Maier, J. Maier, M. Lell, and M. Kachelrieß.
Organ- vs. patient risk-specific TCM in thorax CT scans covering the female breast. CT Meeting 2022.

# Conclusions on RiskTCM

- Risk-specific TCM minimizes the patient risk.
- With $D_{eff}$ as a risk model riskTCM can reduce risk by up to 50% and more, compared with the gold standard mAsTCM.
- Other risk m… …ight- and sex-spec… …used with riskTCM as well.
- Note:
  - mAsTCM = good for the x-ray tube
  - riskTCM = good for the patient
  - detector flux equalizing TCM = good for the detector
- Compared with breast-specific TCM the riskTCM approach is 25% lower in dose.

**It is up to the vendors to take action!**

L. Klein, C. Liu, J. Steidel, L. Enzmann, M. Knaup, S. Sawall, A. Maier, M. Lell, J. Maier, and M. Kachelrieß.
Patient-specific radiation risk-based tube current modulation for diagnostic CT. Med. Phys. 49: in press, 2022.


Job opportunities through DKFZ’s international PhD or Postdoctoral Fellowship programs (www.dkfz.de), or directly through marc.kachelriess@dkfz.de.
Parts of the reconstruction software were provided by RayConStruct® GmbH, Nürnberg, Germany.
Thank You!